Distributed consensus control in vehicle platooning

Zegers, J.C.

Award date:
2015

Distributed Consensus Control in Vehicle Platooning

J.C. Zegers

DC 2015.029

Master Thesis

Coaches: dr.ir. E. Semsar-Kazerooni (TNO)
dr.ir. J. Ploeg (TNO)

Supervisors: prof.dr. H. Nijmeijer
prof.dr.ir. N. van de Wouw

Eindhoven University of Technology
Department of Mechanical Engineering
Dynamics & Control

TNO
Technical Sciences
Department of Integrated Vehicle Safety

Eindhoven, May, 2015

Summary

The interest in automation of vehicles is increasing over the past few years. By using Vehicle-to-Vehicle (V2V) and Vehicle-to-Infrastructure (V2I) communication, fully automated road vehicles can potentially reduce fuel consumption and emmission, improve traffic safety and increase road capacity. This will result in complex vehicular networks in which automated vehicles must be able to respond to other vehicles, change lanes, merge, etc.
Vehicles driving on a road can be interpreted as an interconnection of dynamical systems through an underlying communication/sensing network. Therefore, the vehicular network control problem seems to fit well within the proposed frameworks for distributed control of cooperative agents, e.g., consensus seeking, flocking, formation control, etc. In this thesis, a novel distributed consensus control approach for platooning of vehicles is proposed.
In the existing literature on the topic of distributed consensus control for vehicle platooning, unrealistic assumptions are made. For example, a simplistic vehicle model is used, or ideal communication, having unlimited range and zero latency, between the vehicles is assumed. Also, in many of the existing research, a constant spacing-policy between consecutive vehicles is assumed. However, in the scope of traffic throughput and safety, it is desired to have a spacing-policy depending on the vehicle's velocity. Another important property of an interconnected vehicle platoon (or string of vehicles) is disturbance attenuation, since it is undesired to amplify disturbances along the vehicle platoon. This property is named string stability and can be interpreted as a performance criterion, in addition to the normal stability property of a string of interconnected systems. In most research regarding distributed consensus control applied to vehicle platooning, the property of string stability is mostly ignored in the (performance) analysis of the proposed designs.
In this thesis, a literature survey, regarding the existing and relevant research on the topic of distributed consensus control in vehicle platooning is given. Based on this, a distributed consensus control approach, which covers the aforementioned properties, is developed. Thus, within the approach, a realistic model is used for modeling the longitudinal dynamics of a vehicle. A velocity-dependent inter-vehicle spacing policy is established by using a distributed control method in which only local information of other vehicles is used. Within this distributed control method, the interaction between the vehicles can be of bidirectional nature, depending on the chosen communication/interaction topology. Also, the string stability properties of the developed distributed consensus control approach are evaluated. Finally, the platoon coherence is assessed by introducing a constraint on the velocity of one of the vehicles in the platoon.

Acknowledgements

This thesis is the result of my graduation project in the Dynamics and Control group of the department of Mechanical Engineering at Eindhoven University of Technology (TU/e) in collaboration with the department of Integrated Vehicle Safety at TNO in Helmond. The result would not have been there without the help of many people. First of all, I would like to thank my supervising professors from TU/e, Henk Nijmeijer and Nathan van de Wouw, for giving me the opportunity to work on this thesis and for their support during the project. I would also like to thank my supervisors from TNO, Elham Semsar-Kazerooni and Jeroen Ploeg, for their enthusiasm, useful discussions and the careful reading and correction work.
Also, I would like to thank my parents for supporting me during my entire education. I am very grateful for their encouragement and interest. Furthermore, I would like to thank the fellow students with whom I collaborated during my entire education. Finally, I would like thank my girlfriend for her support, especially during my graduation project.

Contents

Nomenclature

Acronyms and abbreviations

CACC	Cooperative Adaptive Cruise Control
V2V	Vehicle-to-Vehicle
GPS	Global Positioning System

Roman symbols

A,$\mathcal{A}$	system matrix
a	acceleration
B,$\mathcal{B}$	input matrix (or vector); vector
C,$\mathcal{C}$	output matrix (or vector); constant
D	interaction matrix (or vector)
d	inter-vehicle distance
e	inter-vehicle distance error
f	index of faulty (or slow) vehicle
G	adjacency matrix
$\mathcal{G}$	transfer function
h	time gap
I	identity matrix
i,j	vehicle (or system) indices
K,k	control gain (vector)
L	Laplacian matrix; length
n	platoon length
P	pinning matrix
$\mathcal{P}$	transfer function
p	state vector
q	position
Q	vector

r	standstill distance
S	set of vehicles in a platoon
s	Laplace variable
T	similarity transformation matrix
t	time
U,u	lumped input vector; input; desired acceleration
v	velocity
w	constant; eigenvector of Laplacian
X,x	(lumped) state vector
y	output
z	controller state

Greek symbols

α	constant; class $\mathcal{K}$ function
β	constant; class $\mathcal{K}$ function
Γ	constant
γ	control gain
Δ	desired spacing-policy
δ	desired position
η	output
θ	communication delay
λ, μ	eigenvalue
ν	input
ξ	state vector; relative measurements
ρ	state vector
Σ	summation
σ	pole (vector)
τ	drive-line dynamics constant
ϕ	drive-line dynamics (or actuator) time delay
χ	state vector; lumped state vector

Subscripts

b	back
c,d	closed-loop
d,des	derivative; desired
e	equilibrium
f	faulty
H	(no meaning)
i,j	vehicle (or system) indices
lst	minimum

m	dimension
max	maximum
p	proportional
R,r	reduced
u	regarding desired acceleration
v	vehicle; velocity

Miscellaneous

$\mathcal{E}$	set of edges
$I_{(-1),n}$	$n \times n$ matrix, having ones on all entries of the first lower off-diagonal and zeros elsewhere
$I_{(1),n}$	$n \times n$ matrix, having ones on all entries of the first upper off-diagonal and zeros elsewhere
lim	limit
$\mathcal{L}_p$	signal class
$\hat{L}$	Laplacian L plus pinning constraint matrix
$\max\{x\}$	maximum of x
$\min\{x\}$	minimum of x
$\mathcal{N}$	neighbouring set
$\mathbb{N}$	set of positive integer numbers
$O_{n\times m}$	$n \times m$ zero matrix (or vector)
$\mathbb{R}^{n\times m}$	set of real $n \times m$ matrices
$\mathbb{R}^+$	set of positive real numbers
sup	supremum
$\mathcal{V}$	set of nodes
x^T	transpose of x
$\dot{x}$ ($\ddot{x}$, $\dddot{x}$)	(second or triple) time-derivative of x
$\lambda\{\cdot\}$,$\sigma\{\cdot\}$	eigenvalue/pole of
$\lvert\cdot\rvert$	absolute value; cardinality of a set
$\bar{\cdot}$	equilibrium; new input
$\hat{x}$	Laplace transform of x
$\{\cdot\}$	set of variables
$\lvert\lvert\cdot\rvert\rvert$	vector norm
$\lvert\lvert\cdot\rvert\rvert_{\mathcal{H}_\infty}$	$\mathcal{H}_\infty$ system norm
$\lvert\lvert\cdot\rvert\rvert_{\mathcal{L}_2}$	$\mathcal{L}_p$ signal norm, $p \in \{1, 2, \infty\}$
$\emptyset$	empty set
$\otimes$	Kronecker product

Chapter 1

Introduction

Recent developments in computation, sensing and communication technology have spurred an increasing interest in the development of automated highway systems. Potentially, automated vehicles can reduce traffic congestion, reduce overall exhaust emission and increase traffic safety. An example of such an automated highway system is Cooperative Adaptive Cruise Control (CACC), of which examples are presented in Ploeg et al. (2014a,b). In a CACC system, inter-vehicle data exchange through wireless Vehicle-to-Vehicle (V2V) communication, in addition to radar or lidar measurements, is used to control the longitudinal motion of vehicles in a platoon. A CACC system allows for small time gaps between two consecutive vehicles, such that an increase in traffic throughput can be realized. When vehicles cooperate in a platoon, the aerodynamic drag is reduced, especially for fleets of heavy-duty vehicles, thereby increasing fuel economy and reducing emissions (Ramakers et al., 2009). In general, in a CACC controlled platoon, as suggested in Ploeg et al. (2014a,b), the interaction between the vehicles in a platoon is of unidirectional nature, characterized by a look-ahead communication/sensing topology. In the remainder of this thesis, the CACC method as described in Ploeg et al. (2014b) is referred to as a conventional CACC method. As a result of this unidirectional nature, a platoon (as a whole) cannot respond to a possible (temporary) actuation fault occurring in one of the vehicles in the platoon. For example, a (temporary) saturation on velocity or acceleration. Hence, the platoon will break up if such an event occurs.
Inclusion of information of follower vehicles in the vehicle's motion controller could potentially improve the platoon coherence, such that it does not break up when such a vehicle fault occurs. Also, in the scope of maneuvering, e.g., merging into a platoon or splitting from a platoon, taking follower vehicles into account can be useful. As a result, the desired interaction between the vehicles in a platoon will be of bidirectional nature.

A platoon of vehicles can be interpreted as an interconnection of dynamic systems through an underlying communication/sensing network. Therefore, the platoon control problem seems to fit well within the proposed frameworks for distributed control of cooperative agents, e.g., consensus seeking (Olfati-Saber and Murray, 2004), flocking (Olfati-Saber, 2006), formation control (Gouvea et al., 2013), etc. However, the adaptation of the platoon control problem to match any of the above mentioned frameworks is not straightforward, as is explained below.
In some recent works (Bernardo et al., 2014; Montanaro et al., 2014; Zheng et al., 2014), attempts are made to fit the platoon control problem into a distributed consensus control framework, which is a decentralized control framework and is used in multi-agent networked systems. However, in most of the above mentioned research works, a constant distance spacing-policy between consecutive vehicles in the platoon is considered, which is not the most ideal spacing-policy in the scope of traffic throughput, safety and disturbance attenuation, as will be discussed later on. Another assumption that is made in some research works, is that a vehicle's dynamics can be represented by a simplistic model,

such as double integrator dynamics. However, such a model does not describe the dynamical behavior of a vehicle accurately. Also, in most research regarding distributed consensus control applied to vehicle platooning, string stability properties are mostly ignored in the (performance) analysis of the proposed designs. String stability (Middleton and Braslavsky, 2010; Ploeg et al., 2014a) can be seen as a performance criterion regarding input disturbance attenuation along the string of systems/vehicles, in addition to the normal stability property of a string of interconnected systems/vehicles.

1.1 Problem statement

The aim of this master thesis is to develop a distributed consensus control framework which covers many of the following desired properties in vehicle platooning. First, a realistic dynamical model must be used for modeling the longitudinal dynamics of a vehicle, thus representing an actual vehicle's dynamics. Second, the desired spacing-policy between two consecutive vehicles should be velocity-dependent. Third, due to limited or non-ideal communication channels, only local information can be exchanged between vehicles. Thus, as an example, the desired platoon cruising velocity v_{des} is only known to a (possible) leading vehicle and is not communicated to all other vehicles in the platoon. Finally, string stability properties of the designed framework must be evaluated to see how the disturbances acting on the platoon are influencing the platoon behavior. In addition, due to possible bidirectional interaction, one could improve a platoon's coherence such that it does not break up when a platoon member experiences a (possibly temporary) fault, e.g., saturation on velocity or acceleration.

1.2 Outline

This thesis is organised as follows. First, background information regarding distributed consensus control and the definition of a vehicle platoon is given in Chapter 2. Thereafter, an overview of the most relevant findings regarding distributed consensus control in multi-agent systems, and more specifically consensus control applied to vehicle platooning, is given in Chapter 3. In Chapter 4, the development of a distributed consensus control approach, which is the main result of this master thesis, is described. Hereafter, in Chapter 5, the platoon coherence is investigated in case the platoon involves a vehicle with a (temporary) constraint on the velocity. An additional control law is introduced to ensure coherence of the platoon. The string stability properties of the distributed consensus control approach are evaluated in Chapter 6. Finally, the conclusions and recommendations are presented in Chapter 7.

Chapter 2

Background and Preliminaries

In general, consensus control theory is applied to a group of dynamical systems (or agents) which interact. When all agents in the group agree on the value of the variable(s) of interest, they are said to have reached consensus. For example, when one single state of the state vector of a system is the variable of interest, all systems in a network reach consensus when this particular state of those coupled systems converge to a common value. A tool commonly used to analyse consensus control strategies is graph theory, in which network topologies, indicating potential interaction between neighbouring agents, are described by graphs. The algebraic properties of those graphs correspond to properties of the network topology it describes.
The principles of graph theory are briefly described in Section 2.1. Hereafter, the principles of a general distributed consensus control law, depending on the communication graph, for a group of identical linear systems are explained in Section 2.2. The longitudinal vehicle dynamics, represented by a third-order model, are defined in Section 2.3. Finally, in Section 2.4, a definition of a platoon of vehicles is given.

2.1 Graph theory

A graph consists of a node (or agent/system) set $\mathcal{V} = \{1, \cdots, n\}$, an edge set $\mathcal{E} \in \mathcal{V} \times \mathcal{V}$, and an adjacency matrix $G = [g_{ij}] \in \mathbb{R}^{n \times n}$ (Godsil and Royle, 2001). The adjacency matrix G of a graph is defined such that the elements g_{ij} describe the edges of the graph $\mathcal{E}$. As an example, for the network shown in Figure 2.1.a, the adjacency matrix is defined as

$$G = \begin{bmatrix} 0 & 1 & 0 \\ 1 & 0 & 1 \\ 0 & 1 & 0 \end{bmatrix}. \tag{2.1}$$

The adjacency matrix G has dimensions $n \times n$, where n is the number of systems involved. If a system j has a directed communication link to system i, then element g_{ij} is equal to one and system j is considered to be in the neighbouring set $\mathcal{N}_i$ of system i. And if a system j does not have a directed communication link to system i, then element g_{ij} is equal to zero and system j is not in the neighbouring set $\mathcal{N}_i$ of system i. Another example of an adjacency matrix, for the network shown in Figure 2.1.b, is defined as

$$G = \begin{bmatrix} 0 & 0 & 1 \\ 1 & 0 & 1 \\ 0 & 1 & 0 \end{bmatrix}. \tag{2.2}$$

Furthermore, the diagonal elements of the adjacency matrix are all equal to zero, which is obvious since a system does not communicate with itself. This could be verified by observing the adjacency matrices in (2.1) and (2.2) and the associated networks in Figure 2.1.
In an *undirected network*, all communication links between the systems are bidirectional which results in a symmetric adjacency matrix G. In a *directed network*, at least one communication link between a pair of systems is unidirectional instead of bidirectional which results in a non-symmetric adjacency matrix G (Godsil and Royle, 2001).

Another fundamental matrix in network or graph theory can be derived from the adjacency matrix G. This matrix is called the Laplacian matrix $L = [l_{ij}] \in \mathbb{R}^{n\times n}$ and is in general defined as

$$l_{ii} = \sum_{j=1, j\neq i}^{n} g_{ij} \quad \text{and} \quad l_{ij} = -g_{ij} \quad \forall i \neq j. \tag{2.3}$$

The Laplacian matrix L always satisfies the conditions

$$l_{ij} \leq 0 \quad \forall i \neq j \quad \text{and} \quad \sum_{j=1}^{n} l_{ij} = 0 \quad \forall\, i \in \mathcal{V}. \tag{2.4}$$

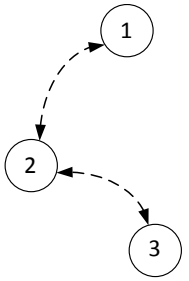

(a) undirected network which is connected.

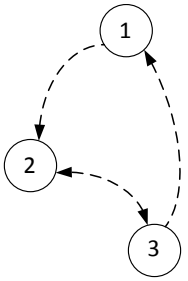

(b) directed network which is strongly connected.

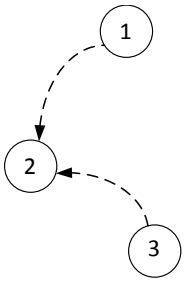

(c) directed network which is connected.

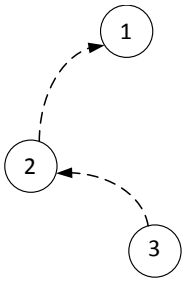

(d) directed network which contains a directed spanning tree.

Figure 2.1: Four different examples of a network consisting of three systems, having different communication topologies.

For the adjacency matrix given in (2.1), the Laplacian matrix is defined as

$$L = \begin{bmatrix} 1 & -1 & 0 \\ -1 & 2 & -1 \\ 0 & -1 & 1 \end{bmatrix}. \tag{2.5}$$

The Laplacian matrix L is a representation of the neighbouring sets $\mathcal{N}_i$ of all systems/agents i. Each row of the Laplacian matrix corresponds to the links towards one system in a graph. The amount of links that system i receives is indicated by the $(i,i)^{th}$ diagonal element of the Laplacian matrix. The off-diagonal elements of each i^{th} row indicate which systems are sending information to system i. The neighbouring set $\mathcal{N}_i$ of system i contains all systems j for which $l_{ij} = -1$. For example, given the Laplacian matrix L as in (2.5), the neighbouring sets for the three systems in the network would be defined as

$$\mathcal{N}_1 = \{2\}\,,\ \mathcal{N}_2 = \{1,3\}\,,\ \mathcal{N}_3 = \{2\}\,. \tag{2.6}$$

The Laplacian matrix L is of same dimensions as the adjacency matrix G. The Laplacian matrix L is by definition always positive semi-definite and has at least one eigenvalue equal to zero. This single, by definition, zero eigenvalue of the Laplacian matrix L is associated with the eigenvector of the Laplacian matrix L in the consensus (or equilibrium) state

$$w_r := \alpha[1,\ 1,\ \cdots,\ 1]^T, \tag{2.7}$$

with $\alpha \in \mathbb{R}$. An undirected network is called *connected* if there is a path between any distinct pair of systems via the communication links, possibly via other systems (Bondy and Murty, 2008; Ren and Beard, 2008). The undirected network in Figure 2.1.a is an example of a connected network. Indeed, from every system, there exists a path to each other system via the communication links. When an undirected network is connected, only one single eigenvalue of the Laplacian matrix L is equal to zero. For a directed network, a distinction is made between being connected and being strongly connected. A directed network is called *strongly connected* if there exists a path between any distinct pair of systems via the directed communication links. An example of a strongly connected directed network is shown in Figure 2.1.b. A directed network is called connected, if there exists a path between any distinct pair of systems when you replace all directed links in the graph by undirected links, an example is given in Figure 2.1.c. For a directed network which is strongly connected it holds that only one single eigenvalue of the Laplacian matrix L is equal to zero.
A directed network contains a so-called *directed spanning tree* if there is at least one system having a directed path, via the communication links of the network, to all other systems. This system is called a root. The networks in Figure 2.1.a,b,d are all examples of a network containing a directed spanning tree. Eigenvalue zero is a simple eigenvalue of Laplacian matrix L and all of the other eigenvalues of L have positive real parts if and only if a directed graph/network contains a directed spanning tree (Bondy and Murty, 2008; Ren and Beard, 2008). For a directed network, containing a directed spanning tree is a weaker condition than being strongly connected.

2.2 Distributed consensus control law

The most common continuous-time distributed consensus control law is designed for a group of agents having simple integrator dynamics (Lin et al., 2004; Olfati-Saber and Murray, 2004). Consider n identical systems having an m-dimensional state-space with single-integrator dynamics given by

$$\dot{q}_i(t) = u_i(t) \quad \forall i \in S_n, \tag{2.8}$$

with $q_i(t) \in \mathbb{R}^m$, $u_i(t) \in \mathbb{R}^m$ being, respectively, the position and input of agent i and $S_n = \{i \in \mathbb{N} \mid 1 \leq i \leq n\}$ being the set of all systems in a group of size $n \in \mathbb{N}$. A distributed consensus control law could be defined as

$$u_i(t) = -\sum_{j \in \mathcal{N}_i} (q_i(t) - q_j(t)) = -\sum_{j=1}^{n} g_{ij}(q_i(t) - q_j(t)) \quad \forall i \in S_n, \tag{2.9}$$

where $\mathcal{N}_i$ is the neighbouring set of agent i, g_{ij} is element (i, j) of the adjacency matrix G describing the interaction (or communication) topology. Note that in (2.9) two expressions are given for the same distributed control law. Suppose that the dimension of the state-space is one, i.e., $m = 1$. The closed-loop dynamics of (2.8) given distributed consensus control law (2.9) is written in matrix form as

$$\dot{q}(t) = -Lq(t), \tag{2.10}$$

where $q(t) = [q_1(t),\ \cdots,\ q_n(t)]^T$ and L is the Laplacian matrix describing the interaction (or communication) topology. Now if and only if the graph describing the network topology is designed such that it contains a directed spanning tree, i.e., the Laplacian matrix L has only one single eigenvalue equal to zero, the state $q_i(t)$ of each system will converge to a common consensus state q_e at steady state (Ren and Beard, 2008).

2.3 Longitudinal vehicle dynamics

In this section, the longitudinal vehicle dynamics are modeled. The longitudinal dynamics of a vehicle, as used for the design of the consensus framework in this thesis, are modeled as a linear third-order system:

$$\dot{p}_i(t) = Ap_i(t) + Bu_i(t) \quad \forall i \in S_n, \tag{2.11}$$

where

$$p_i(t) = \begin{bmatrix} q_i(t) \\ v_i(t) \\ a_i(t) \end{bmatrix},\ A = \begin{bmatrix} 0 & 1 & 0 \\ 0 & 0 & 1 \\ 0 & 0 & -\frac{1}{\tau} \end{bmatrix},\ B = \begin{bmatrix} 0 \\ 0 \\ \frac{1}{\tau} \end{bmatrix} \tag{2.12}$$

and where $S_n = \{i \in \mathbb{N} \mid 1 \leq i \leq n\}$ is the set of all vehicles in a platoon of length $n \in \mathbb{N}$, and $\tau > 0$ is a constant representing the vehicle drive-line dynamics. The states $q_i(t)$, $v_i(t)$ and $a_i(t)$ are position, velocity and acceleration, respectively. The input $u_i(t)$ is in fact the desired vehicle acceleration. First, it is assumed that the platoon is homogeneous which results in the constant τ being equal for each vehicle. In Naus et al. (2010); Ploeg et al. (2014b), it is shown that this model suits well for modeling of longitudinal vehicle dynamics. It is identified that a drive-line dynamics constant $\tau = 0.1$ suits well for the Toyota Prius, used by TNO for testing, and therefore this value is used in the remainder of this thesis. In fact, the full model also includes a drive-line dynamics time delay ϕ such that the full system model is defined as

$$\dot{p}_i(t) = Ap_i(t) + Bu_i(t - \phi), \quad \forall i \in S_n, \tag{2.13}$$

with matrix A and B being defined as in (2.12), but for sake of simplicity this time delay is ignored while designing the distributed consensus control law for the desired acceleration $u_i(t)$ of vehicle i. Later on, the influence of this drive-line dynamics time delay ϕ is taken into account in the analysis of the platoon's response.

2.4 Vehicle platoon

In this section, the definition of a platoon is given. A platoon is considered to be a string of vehicles having dynamics as defined in Section 2.3. Each vehicle in the string is assigned with an index increasing in upstream direction, as can be seen in Figure 2.2, where L_v is the vehicle length, and $q_i(t)$ and $v_i(t)$ are the position of the rear bumper and the velocity of vehicle i, respectively. The inter-vehicle distance between vehicle i and vehicle $i - 1$ is defined as

$$d_i(t) = q_{i-1}(t) - q_i(t) - L_v \quad \forall i \in S_n \backslash \{1\}\,. \tag{2.14}$$

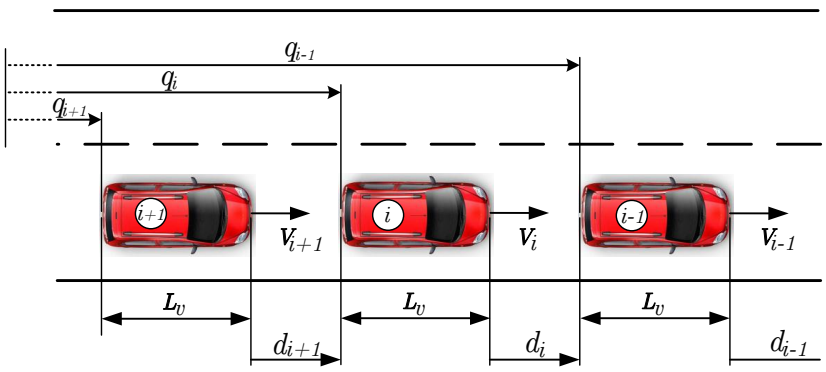

Figure 2.2: Schematic overview of a string of vehicles.

2.5 Summary

In this chapter, the general principles of graph theory and distributed consensus control are explained. Furthermore, the dynamical model describing the longitudinal vehicle dynamics is given and, in addition, the definition of a platoon of vehicles is introduced.

Chapter 3

Literature Survey

Distributed consensus control is a topic which is well-covered in literature. Many research projects are being executed on the topic of vehicle platooning as well. However, the application of distributed consensus control to vehicle platooning is a rather new topic which is only covered in several recent publications (Bernardo et al., 2014; Cao et al., 2013; Gowal et al., 2010; Iftekhar and Olfati-Saber, 2012; Montanaro et al., 2014; Zheng et al., 2014). This chapter gives a summary of the most relevant findings in literature regarding the design of a distributed consensus controllers for vehicle platooning.

The consensus algorithm from (2.9) is extended in various ways in the literature. For example, the single-integrator consensus control law is extended to double-integrator dynamics in Xie and Wang (2007) and Ren and Atkins (2007) and consensus is addressed with a time-varying reference state in Yang et al. (2008), Ren and Beard (2008) and Ren (2007). The most relevant extensions on distributed consensus control for single integrator dynamics are described in Section 3.1.
The dynamics of the motion of mechanical agents/systems in many cases can be modeled as a second-order system, and research is done on the application of distributed consensus control to non-holonomic mobile robots like unicycles or (kinematic) bicycle models. Such applications of a distributed consensus control approach are described in Iftekhar and Olfati-Saber (2012) and Gowal et al. (2010), both describing an approach in which non-holonomic mobile robots form a rigid formation using consensus control. In both publications, the agents/vehicles are modeled by a second-order model and a constant spacing-policy is assumed, and therefore not directly relevant for the distributed consensus framework pursued in this research, since a velocity-dependent (and thus state-dependent) spacing-policy is desired in vehicle platooning. In the scope of traffic throughput and safety, the desired spacing-policy in vehicle platooning is based on a time gap. In addition, in Swaroop and Hedrick (1999), it is shown that a constant spacing-policy performs less in terms of disturbance attenuation along the vehicle string in comparison with a time gap spacing-policy, i.e., a velocity dependent spacing-policy.
In Fax and Murray (2004), a framework for distributed consensus control for general linear systems is proposed. This consensus framework for general linear systems is discussed in Section 3.2. Since the longitudinal vehicle model, as presented in (2.3), is a third-order linear system, this framework seems to offer opportunities for application to vehicle platooning. However, the proposed method does not cover a velocity-dependent spacing-policy.

This brings us to the topic of the current thesis, namely distributed consensus control applied to vehicle platooning, which has received very little attention in literature. In the scope of traffic throughput and safety, the desired spacing-policy in vehicle platooning is based on a time gap h such that the desired inter-vehicle distance increases with increasing velocity, as also addressed in Ploeg et al. (2014b). Current literature on distributed consensus and formation control mainly focuses on a rigid formation, i.e., on a constant distance spacing-policy between agents. As a consequence, application of dis-

tributed consensus control to vehicle platooning, with a desired velocity-dependent spacing-policy, is not straightforward. This shortcoming on research on non-rigid formation control is explicitly stresses in Cao et al. (2013).
Relevant research regarding distributed consensus control in vehicle platooning is described in Section 3.3. In most publications, the vehicles are modeled as having double integrator dynamics, which is not a realistic model of a passenger vehicle. Furthermore, in most research, a constant spacing-policy between the vehicles in the platoon is considered. Consequently, none of the existing research does cover all the desired properties of the distributed control framework pursued in this master thesis.
Finally, in Section 3.4 and Section 3.5, a short description on the concept of, respectively, string stability and Cooperative Adaptive Cruise Control (CACC) is given.

3.1 Distributed consensus control for integrator dynamics

This section describes examples of distributed consensus control for systems having pure integrator dynamics. Distributed consensus control for systems modeled by higher-order integrator dynamics are described in Ren et al. (2006) and an example for a third-order integrator system including constant relative position state deviation is described in Section 3.1.1.
As was mentioned above, the desired spacing between vehicles in a platoon is not constant but velocity-dependent, and therefore the method described in Ren et al. (2006) is not directly applicable to vehicle platooning. In Ren (2007), an extension is made to the standard distributed consensus algorithm to be able to obtain a time-varying spacing policy between the agents which is described in Section 3.1.2.

3.1.1 Distributed consensus control for multiple-integrator dynamics

Consider n identical agents (or systems) with triple-integrator dynamics in an m-dimensional space given by

$$\begin{aligned} \dot{q}_i(t) &= v_i(t) \\ \dot{v}_i(t) &= a_i(t) \quad \forall i \in S_n, \\ \dot{a}_i(t) &= u_i(t) \end{aligned} \tag{3.1}$$

where $q_i(t) \in \mathbb{R}^m$, $v_i(t) \in \mathbb{R}^m$ and $a_i(t) \in \mathbb{R}^m$ are respectively, the position, velocity and acceleration of the i^{th} system, $u_i(t) \in \mathbb{R}^m$ is the control input, and $S_n = \{i \in \mathbb{N} \mid 1 \leq i \leq n\}$ is the set of all agents in a group of size $n \in \mathbb{N}$. Initially, all systems are at a different position $q_i(t=0)$ and move with different velocity $v_i(t=0)$ and acceleration $a_i(t=0)$. Suppose that it is desired that all agents move with similar velocity and acceleration and having a constant desired inter-agent spacing-policy. A distributed consensus control law for (3.1) having a constant desired spacing-policy Δ_{ij} is suggested in Ren et al. (2006) and is defined as

$$u_i = -\sum_{j \in \mathcal{N}_i} \left(\gamma_0 \left((q_i - q_j) - \Delta_{ij}\right) + \gamma_1 (v_i - v_j) + \gamma_2 (a_i - a_j)\right) \quad \forall i \in S_n, \tag{3.2}$$

where $\gamma_0, \gamma_1, \gamma_2$ are positive control gains (to be designed using Routh-Hurwitz criterion for a third-order polynomial) and Δ_{ij} is the desired constant spacing between vehicle i and vehicle j. Note that the time-argument is omitted in (3.2) for the sake of readability.
If the communication graph described by a Laplacian matrix L contains a directed spanning tree and the control gains are designed appropriately according to Routh-Hurwitz criterion, the control law in (3.2) results in the group of agents (3.1) having an asymptotically stable equilibrium. In this equilibrium (or consensus state) all n agents have a constant inter-agent spacing defined by Δ_{ij} and a common velocity $v_e(t)$ and common acceleration $a_e(t)$. The values of this common velocity $v_e(t)$ and common acceleration $a_e(t)$ are a result of the initial conditions, i.e., initial velocity and acceleration, of the agents in the platoon and are so-called consensus states. To drive these consensus states to desired equilibrium values, i.e., desired velocity and/or desired acceleration, a reference agent can be introduced which is described later on. The proof of the above mentioned distributed consensus protocol

can be found in Ren et al. (2006) and is too elaborate to show here.
Note that no information about absolute position is needed given this distributed control law (3.2). The actual position $q_i(t)$ is always used in combination with the actual position $q_j(t)$, such that only relative position information is required. This is an important consideration since it is known that global/absolute position information is not available in vehicle platooning due to low Global Positioning System (GPS) accuracy. Below it will become clear that some consensus protocols are not applicable in practice due to this limitation.

3.1.2 Time-varying relative position spacing

Above, a distributed consensus control protocol resulting in a constant relative spacing is suggested. However, in the scope of vehicle platooning, it is desired to have a velocity-dependent inter-vehicle distance. More specifically, the desired inter-vehicle distance between two consecutive vehicles depends on the velocity of the following vehicle, which will be explained in more detail when the control objective is defined.

As was mentioned above, the topic of time-varying desired relative positioning, i.e., non-rigid formation forming, is not well-covered in existing literature on distributed consensus control. In Ren (2007), a distributed consensus control law is suggested for a group of n first-order dynamical systems described by

$$\dot{q}_i(t) = u_i(t) \quad \forall i \in S_n, \tag{3.3}$$

where $q_i(t) \in \mathbb{R}^m$ is the position and $u_i(t) \in \mathbb{R}^m$ is the control input. The suggested control law is defined as

$$u_i(t) = \dot{\delta}_i(t) - \sum_{j \in \mathcal{N}_i} \gamma_0 \left((q_i(t) - q_j(t)) - \Delta_{ij}(t) \right) \quad \forall i \in S_n, \tag{3.4}$$

where γ_0 is a positive gain and

$$\Delta_{ij}(t) = \delta_i(t) - \delta_j(t) \; \forall i \neq j \tag{3.5}$$

denotes the desired time-varying separation between system i and system j. With (3.4) applied to (3.3), it can be shown that (Ren, 2007)

$$q_i(t) - q_j(t) \to \delta_i(t) - \delta_j(t) \quad \forall i \neq j, \text{ for } t \to \infty, \tag{3.6}$$

if and only if the information-exchange topology contains a directed spanning tree, i.e., the Laplacian matrix L has only one single eigenvalue zero. The proof of this is given as follows. With control law (3.4), the dynamics (3.3) can be written in matrix form as

$$\dot{\hat{q}}(t) = -\gamma_0 \left(L \otimes I_m \right) \hat{q}(t), \tag{3.7}$$

where $\hat{q}(t) = [\hat{q}_1^T(t), \; \cdots, \; \hat{q}_n^T(t)]$ with $\hat{q}_i(t) = q_i(t) - \delta_i(t)$, and $L = [l_{ij}] \in \mathbb{R}^{n \times n}$ being the Laplacian matrix, I_m being a $m \times m$ identity matrix, and $\otimes$ represents the Kronecker product. Note that these dynamics are of similar form as the dynamics in (2.9) (for $m = 1$), and thus asymptotic stability of the consensus state is proven.

A drawback of this control law is the necessity of knowledge about the time-derivative of the desired absolute position $\dot{\delta}_i(t)$, which is the desired absolute velocity. In vehicle platooning, it is assumed that the desired velocity is not known to all vehicles in the platoon, only to a leading vehicle.
Additionally, even if this information is available, it is not straightforward to extend the distributed control law in (3.4) to systems having dynamics of higher-order. Also, having a time-dependent spacing-policy is something different than having a velocity-dependent (or state-dependent) spacing-policy. The latter could lead to an even more complex proof of stability.

3.1.3 Behavior of a multi-agent system in presence of actuator faults

Another field of research regarding distributed consensus control for integrator dynamics is the behavior of the agents in a group in presence of actuator faults. An actuator fault can be seen as a saturation on the actuator input, which could be a saturation on an agent's velocity or acceleration, depending on the model of the agent. In Saboori et al. (2013), a distributed control law for a group of agents having first-order integrator dynamics as in (3.3) is defined. Also, an upper- and lower-bound on the control input $u_i(t)$ is defined. When such a bound on the control gain is reached during operation, i.e., saturation occurs, it is said that an actuator fault occurs. It is shown that the agents can reach consensus, on the position variable $q_i(t)$, even when some agents have partial actuation loss.
Furthermore, in Semsar-Kazerooni and Khorasani (2007), a distributed control approach to cope with actuator faults is suggested, but for agents having second-order integrator dynamics described by

$$\begin{aligned} \dot{q}_i(t) &= v_i(t) \\ \dot{v}_i(t) &= u_i(t) \end{aligned} \quad \forall i \in S_n, \tag{3.8}$$

where $q_i(t) \in \mathbb{R}^m$, $v_i(t) \in \mathbb{R}^m$ are respectively, the position and velocity, and $u_i(t) \in \mathbb{R}^m$ is the control input. A control law for $u_i(t)$, which is obtained by minimization of individual cost functions by using the available information from the neighboring sets $\mathcal{N}_i$, is defined as

$$\begin{aligned} u_i(t) &= \Gamma_i \left(v_i(t) - \frac{\sum_{j \in \mathcal{N}_i} v_j(t)}{|\mathcal{N}_i|} \right) \qquad \forall i \in \{ i \in S_n | i \neq 1 \} \\ u_1(t) &= \Gamma_1 \left(v_1(t) - \frac{\sum_{j \in \mathcal{N}_1} v_j(t)}{|\mathcal{N}_1|} \right) + \beta_1 (v_1(t) - v_d), \end{aligned} \tag{3.9}$$

where Γ_i and β_1 are obtained by solving a Riccati equation, where $|\mathcal{N}_i|$ is the cardinality of the neighbouring set $\mathcal{N}_i$, and where v_d is the desired group velocity. In normal operation, this control law (3.9) leads to the agents reaching consensus on their position $q_i(t)$ and velocity $v_i(t)$. In addition, it is shown that, given this distributed control law, if some agents fail to proceed in executing the distributed control law as defined in (3.9) due to actuator faults and instead a zero input is implemented by these agents, i.e., $u_i(t) = 0$, then the non-faulty agents will decrease their velocity in order to keep team cohesion. However, the non-faulty vehicles do not fully adapt their velocity to the saturated velocity of the faulty vehicle v_f, but will all reach an intermediate velocity, i.e., $v_f < v_i(t) < v_d$. This means that the group of agents does break up if the vehicle fault or saturation of velocity is not solved within a certain time.

3.2 Distributed consensus control for general linear systems

A direct extension of solutions of consensus problems for systems having single- or multiple-integrator dynamics, is to solve consensus problems for systems having general linear dynamics (Fax and Murray, 2004; Qu et al., 2008). This research is mainly devoted to finding feedback control laws such that consensus on the states (or at least a subset of them) can be achieved for a group of n general m^{th}-order linear systems as given by

$$\begin{aligned} \dot{x}_i(t) &= A x_i(t) + B u_i(t) \\ y_i(t) &= C x_i(t) \qquad\qquad \forall i \in S_n, \\ \xi_{ij}(t) &= D(x_i(t) - x_j(t)) \end{aligned} \tag{3.10}$$

where $x_i(t) \in \mathbb{R}^m$, $u_i(t) \in \mathbb{R}^p$ are the system state vector and control input, respectively, $y_i(t) \in \mathbb{R}^k$ represent the internal state measurements, and $\xi_{ij}(t) \in \mathbb{R}^l$ represents the external state measurements relative to other systems.
The well-studied single-integrator kinematics and multiple-integrator dynamics are special cases of

(3.10) for a proper choice of matrices A, B, C and D.
A distributed controller proposed in Fax and Murray (2004) is defined as

$$\begin{aligned} \dot{z}_i(t) &= K_A z_i(t) + K_B y_i(t) + K_C \textstyle\sum_{j\in\mathcal{N}_i} \xi_{ij}(t) \\ u_i(t) &= K_D z_i(t) + K_E y_i(t) + K_F \textstyle\sum_{j\in\mathcal{N}_i} \xi_{ij}(t) \end{aligned} \quad \forall i \in S_n, \tag{3.11}$$

which maps the internal state measurements $y_i(t)$, and relative measurements $\xi_{ij}(t)$ to control input $u_i(t)$ and has internal states $z_i(t) \in \mathbb{R}^c$.
As for the longitudinal vehicle dynamics model as given in Section 2.3, such a distributed consensus control law for general linear systems seems to fit well. However, the velocity-dependent spacing-policy, which is desired in vehicle platooning, does not directly fit into the framework as proposed in the literature. The control framework (3.11) does allow for a time-varying vehicle agent/system formation, but it does not allow for the case where the desired formation shape directly depends on internal system states or measurements such as velocity.
The time-varying spacing-policy between the agents is established by defining a time-varying offset function $d_{ij}(t) \in \mathbb{R}^m$ for each pair of agents (i, j). This offset function $d_{ij}(t)$ is added to the relative (position-)state measurement, such that

$$lim_{t\to\infty}\xi_{ij}(t) = d_{ij}(t) \quad \forall i \neq j. \tag{3.12}$$

Only for a (uni-directional) single vehicle look-ahead structure in the communication topology of the distributed control term in (3.11), a velocity-dependent spacing-policy is covered by the distributed control framework in Fax and Murray (2004). In this case, a vehicle i only regulates its distance to its preceding vehicle $i-1$. Thus the controller of vehicle i only needs the actual velocity $v_i(t)$ of vehicle i itself to establish a velocity-dependent spacing. Suppose that the state vector $x_i(t)$ and matrices A and B of the linear system in (3.10) are defined as in the longitudinal vehicle dynamics model in Section 2.3. Furthermore, suppose that the output matrix C is defined such that the velocity $v_i(t)$ is an observable state. Then, the velocity-term of the velocity-dependent spacing-policy can be embedded in the controller (3.11) through the second term on the right-hand side of the relation for $u_i(t)$ or the relation for $\dot{z}_i(t)$ in (3.11).

For a vehicle i, the desired distance to a following vehicle $i+1$ depends on the velocity of this following vehicle $v_{i+1}(t)$, which cannot be embedded in the distributed controller given in (3.11).

3.3 Distributed consensus control in vehicle platooning

As was mentioned in the introduction of this chapter, the current literature on distributed consensus control applied to vehicle platooning is rather limited and only addresses longitudinal platoon control. In Le et al. (2012), a platoon control method for adjusting the distance between vehicles based on a constraint function is proposed. Within the proposed method, the inter-vehicle distances are vehicle-dependent and are defined by a vehicle-dependent weighting factor, but this does not suit well with the velocity-dependent spacing policy pursued by this master thesis research. Furthermore, the research only describes vehicle coordination in cyber-space (or discrete-time) and actual vehicle dynamics are not considered.
Although there are some very recent works where distributed consensus control is applied to platooning of vehicles, these methods still lack certain desired properties. For example, in Bernardo et al. (2014) the vehicles in the platoon are modeled as having double-integrator dynamics in longitudinal direction, which is not a realistic assumption for a passenger car. A spacing-policy involving a time gap h_{ij} is applied in the distributed consensus control law. However, this spacing policy is defined as

$$d_{des,ij} = h_{ij} v_0 \quad \forall i \neq j, \tag{3.13}$$

where $d_{des,ij}$ is the desired distance between vehicle i and vehicle j, h_{ij} is a constant desired time gap and v_0 is constant desired platoon velocity. Since the time gap h_{ij} and the desired platoon velocity v_0

are both assumed to be constant, the spacing-policy $d_{des,ij}$ is actually not velocity-dependent but constant. Also, in this approach, it is assumed that all vehicles in the platoon have knowledge about the desired platoon cruise velocity. In the framework to be designed, it is assumed that only a (possible) leading vehicle has information about the desired platoon cruise velocity and all other vehicles in the platoon do not.

Also in Zheng et al. (2014), a distributed consensus control law is applied to vehicle platooning, however with a constant spacing policy assumption. Vehicles are modeled as a third-order linear system similarly as defined in (2.11) and (2.12). The proposed distributed control law is of similar form as the control law which is given in (3.2) and is defined as

$$u_i(t) = -\sum_{j \in \mathcal{N}_i} (k_1(q_i(t) - q_j(t) - d_{des,ij}) + k_2(v_i(t) - v_j(t)) + k_3(a_i(t) - a_j(t))) \quad \forall i \in S_n, \tag{3.14}$$

where k_1, k_2 and k_3 are control gains, $d_{des,ij}$ is the desired constant spacing between vehicle i and vehicle j, and where $q_i(t)$, $v_i(t)$ and $a_i(t)$ are defined as in (2.11) and (2.12). It is assumed that there is a leading vehicle having a constant velocity, and tracking errors of each vehicle are defined with respect to this leading vehicle having constant velocity. The tracking errors of all vehicles in the platoon are lumped into one vector. The behavior of the distributed consensus controlled platoon is assessed by analyzing the asymptotic stability of the closed-loop platoon error dynamics. It is shown that the error dynamics are asymptotically stable for a proper design for both the control gains $k^T = [k_1,\ k_2,\ k_3]$ and the communication topology of the distributed controller.

Another example of application of a distributed controller to longitudinal platoon control is proposed in Montanaro et al. (2014). A velocity-dependent spacing policy is realized which is defined as

$$d_{des,i}(t) = r_i + h_i v_i(t) \quad \forall i \in S_n, \tag{3.15}$$

where $d_{des,i}(t)$ is the desired inter-vehicle distance between the i^{th} and the preceding $(i-1)^{th}$ vehicle, with r_i being the required standstill distance and h_i is desired time gap. To the best of the author's knowledge, this is the only research in which a velocity-dependent spacing policy is established in a distributed consensus control framework applied to vehicle platooning. In this proposed framework, vehicles are modeled as double-integrator dynamics and thus not (directly) applicable to the problem defined in this master thesis.

3.4 String stability

String stability is another important property of interconnected systems, which is mostly ignored in research work on application of distributed consensus control to vehicle platooning. A platoon of vehicles is said to be string stable when disturbances acting on the platoon are being attenuated (preferably in in both upstream direction as well as downstream direction), which is of course desired in real on-road implementation. A more extended and specific definition of string stability will be given in Chapter 6.
If the coupling between the controlled vehicles in a platoon is uni-directional and if each neighbouring set $\mathcal{N}_i$ for each vehicle i only contains one vehicle, i.e., the dynamics of a vehicle only depends on its predecessor (or following) vehicle, a transfer function between the motion of a vehicle with respect to its preceding (or following) vehicle can easily be established and string stability can be evaluated. This is due to the fact that the transfer function is the same for each pair of predecessor- and following vehicles (in a homogeneous platoon).
However, when the control coupling between the vehicles in a platoon is bidirectional and/or the neighbouring sets $\mathcal{N}_i$ contain more than one vehicle, i.e., the dynamics of a vehicle depends on more than one other vehicle, the assessment of string stability is not so straightforward. In Bernardo et al. (2014), string stability of a distributed consensus controlled platoon is being assessed, but indeed only for a communication topology resulting in an uni-directionally coupled platoon involving the direct preceding vehicle only. String stability will be further considered in Chapter 6.

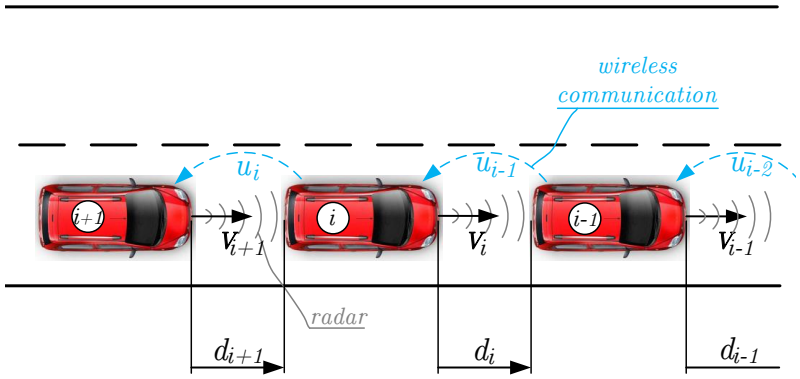

Figure 3.1: Schematic overview of conventional CACC controlled platoon. The distance to a preceding vehicle $d_i(t)$ is measured using radar and the desired acceleration of a preceding vehicle $u_{i-1}(t)$ is obtained through wireless communication.

3.5 Cooperative Adaptive Cruise Control (CACC)

An example of a uni-directionally coupled platoon, which is developed by TNO and TU/e, is proposed and examined in Ploeg et al. (2014b). Vehicles in a platoon are modeled as in (2.13). String stability of a platoon controlled using the proposed CACC method, is evaluated. Within this framework, a controller of a vehicle i uses the inter-vehicle distance to its preceding vehicle $d_i(t)$ and feed-forward information of its preceding vehicle $i-1$ to improve string stability properties of the platoon. Also, the influence of the time gap h and a communication delay θ, involved with communication of the feed-forward information, on the string stability property is investigated. Figure 3.1 shows an illustrative example of such a CACC system. Vehicle i measures its distance with respect to its preceding vehicle $i-1$ (using radar) and it receives feed-forward information of its preceding vehicle in terms of $u_{i-1}(t)$ (via wireless communication), which is in fact the actual input (or desired acceleration) applied to vehicle $i-1$.

3.6 Summary

In summary, standard consensus algorithms normally guarantee agreement of a team of agents (or systems) on some common state, without taking group formation into consideration. In vehicle platooning, however, the spacing-policy (or desired formation) between two consecutive vehicles is velocity-dependent, and therefore some extensions are necessary.
According to the literature, some extensions are made to be able to have a (time-varying) formation between the agents in a group. However, except for Montanaro et al. (2014), all proposed methods in the existing literature do not allow for this desired formation to depend on states of the agents in the group, e.g. an agent's velocity.
Also, in most research on distributed consensus control in vehicle platooning, vehicles are modeled as having second-order (integrator) dynamics, which is also the case for Montanaro et al. (2014). This is not a realistic representation of an actual road vehicle since drive-line dynamics cannot simply be neglected. Furthermore, in some suggested consensus frameworks, it is assumed that information about the desired group velocity and information about global position is available to all agents, which are not realistic assumptions in the scope of vehicle platooning.
Finally, it is found that the use of feed-forward of the desired acceleration of a preceding vehicle can improve string stability properties. However, analysis of string stability seems to become more complex when the distributed control of a platoon is of a bidirectional nature.

In this master thesis, it is aimed to develop a distributed consensus control framework which covers many of the desired properties in vehicle platooning. First, the longitudinal dynamics of a vehicle must be modeled by the third-order linear system as given in Section 2.3 since this is a realistic representation of actual longitudinal vehicle dynamics. Second, a velocity-dependent spacing-policy must be accomplished by the distributed controller, where the desired gap from a vehicle i to vehicle $i-1$ depends on the velocity of vehicle i. Third, due to limited or non-ideal communication channels, only local information can be exchanged between vehicles. Thus, as an example, the desired platoon cruising velocity v_{des} is only known to a (possible) leading vehicle and is not communicated to all other vehicles in the platoon. Finally, string stability properties of the designed framework must be evaluated since disturbances acting on the platoon should be attenuated.

Chapter 4

Distributed Consensus Control Framework

In this chapter, a distributed controller for single-lane platooning is designed. The method is based on defining distance errors and their derivatives as system states. The introduction of a pinning constraint (Wang et al., 2010) guarantees that all errors go to zero at steady state. In Zheng et al. (2014), a similar approach is applied, however for a platoon having constant inter-vehicle spacing-policy. In addition to a velocity-dependent spacing-policy, the second key difference with respect to the method developed in Zheng et al. (2014) is the use of feed-forward of the desired acceleration. This feed-forward is incorporated by introduction of a controller having internal dynamics. With this feed-forward, it is aimed to improve string stability properties of the controlled platoon, which will be evaluated later on.
First, the platoon control objective is given in Section 4.1. Hereafter, in Section 4.2, the definition of an error state vector is given. Also, a control filter, having a new (to be defined) input, is introduced, and the resulting platoon dynamics are given. In Section 4.3, a distributed control law for this new input is developed. Furthermore, conditions for asymptotic stability of the resulting closed-loop platoon dynamics are formalised in a theorem. Section 4.4 describes two examples of communication topologies for the distributed control law for the new input of the control filter. Finally, simulation results are given in Section 4.5 to illustrate the closed-loop platoon response for the developed distributed control approach.

4.1 Platoon control objective

The control objective of the single lane platoon is to track a certain desired velocity v_{des} while maintaining a formation governed by a velocity-dependent spacing-policy between any two consecutive vehicles. The spacing-policy is defined as

$$d_{des,i}(t) = r + hv_i(t) \quad \forall i \in S_n, \tag{4.1}$$

where $d_{des,i}(t)$ is the desired distance from vehicle i to its preceding vehicle $i-1$, $v_i(t)$ is the velocity of vehicle i, constants r and h represent a standstill distance and time gap, respectively, and $S_n = \{i \in \mathbb{N} \mid 1 \leq i \leq n\}$ is the set of all vehicles in a platoon of size $n \in \mathbb{N}$. A homogeneous platoon is assumed such that standstill distance r and time gap h are the same for each vehicle in the platoon. Given spacing-policy (4.1) and by using the definition of a vehicle platoon as shown in Figure 2.4, the tracking error of each vehicle is defined as

$$e_i(t) = q_{i-1}(t) - q_i(t) - (L_v + r + hv_i(t)) \quad \forall i \in S_n, \tag{4.2}$$

with $q_i(t)$ being the rear-bumper position of vehicle i and L_v being the vehicle length. The vehicle following objective can be defined as

$$lim_{t\to\infty} e_i(t) = 0 \quad \forall i \in S_n. \tag{4.3}$$

In addition, the internal platoon dynamics must be asymptotically stable.
Since the first vehicle of the platoon does not have a preceding vehicle, a virtual reference vehicle is defined. The dynamics of the virtual reference vehicle are similar to the third-order dynamics of the actual vehicles in the platoon and are described by

$$\dot{p}_0(t) = Ap_0(t) + Bu_0(t), \tag{4.4}$$

where

$$p_0(t) = \begin{bmatrix} q_0(t) \\ v_0(t) \\ a_0(t) \end{bmatrix}, A = \begin{bmatrix} 0 & 1 & 0 \\ 0 & 0 & 1 \\ 0 & 0 & -\frac{1}{\tau} \end{bmatrix} \text{ and } B = \begin{bmatrix} 0 \\ 0 \\ \frac{1}{\tau} \end{bmatrix}. \tag{4.5}$$

For $u_0(t) = 0$, the constant velocity equilibrium of the virtual reference vehicle is defined as

$$lim_{t\to\infty} p_0(t) = [\bar{q}_0(t),\ \bar{v}_0,\ 0]^T, \tag{4.6}$$

where $\bar{v}_0$ is a constant velocity depending on the initial state of (4.4). As one can see in (4.2), the virtual reference vehicle state vector $p_0(t)$ is only used in determining the error of the first vehicle $e_1(t)$. For now, it is assumed that the virtual reference vehicle is uncontrolled and has a constant velocity defined by

$$\bar{v}_0 \equiv v_{des}, \tag{4.7}$$

which can be achieved by taking

$$p_0(0) = [\bar{q}_0(0),\ \bar{v}_{des},\ 0]^T. \tag{4.8}$$

This means that when the controlled platoon satisfies the objective defined in (4.3) it also satisfies

$$lim_{t\to\infty} v_i(t) = v_{des} \quad \forall i \in S_n. \tag{4.9}$$

The main control objective for single-lane platooning as defined in (4.3) and (4.9) is also established by conventional (uni-directional) CACC (Ploeg et al., 2014b). However, inclusion of looking-back in the communication topology is a means to realize a certain objective such as improved platoon coherence, as explained in Chapter 1.
Note that, in practice, this virtual reference vehicle is a vehicle model which runs on software of the first vehicle in the platoon.

4.2 State definition

Suppose we have a platoon of n vehicles described by the dynamics (2.11) and (2.12). The inter-vehicle distance error state of vehicle i is defined as

$$e_i(t) = d_i(t) - (r + hv_i(t)) = q_{i-1}(t) - q_i(t) - (r + hv_i(t)), \tag{4.10}$$

which is in fact the error of the inter-vehicle distance between vehicle i and vehicle $i-1$ as defined in (4.2), but with the assumption that the vehicle length L_v is equal to zero. This simplification does not influence stability properties since the vehicle length L_v is constant. For now, some of the time arguments are omitted for the sake of readability. The first and second time-derivatives of $e_i(t)$ can be obtained by differentiation of (4.10) with respect to time:

$$\dot{e}_i = v_{i-1} - v_i - ha_i, \tag{4.11}$$

and by using the relation in (2.11) and (2.12) for $\dot{a}_i(t)$:

$$\ddot{e}_i = a_{i-1} - a_i - h(-\frac{1}{\tau}a_i + \frac{1}{\tau}u_i) = a_{i-1} + \frac{h-\tau}{\tau}a_i - \frac{h}{\tau}u_i. \tag{4.12}$$

The error state vector for vehicle i is defined as

$$x_i = \begin{bmatrix} e_i \\ \dot{e}_i \\ \ddot{e}_i \end{bmatrix}. \tag{4.13}$$

Note that this error state vector $x_i(t)$ is the error state vector belonging to vehicle i, but actually also depends on the vehicle states of vehicle $i-1$, in terms of q_{i-1}, v_{i-1} and a_{i-1}. The time-derivative of the third state of $x_i(t)$ is derived as

$$\begin{aligned} \dddot{e}_i &= -\frac{1}{\tau}a_{i-1} + \frac{1}{\tau}u_{i-1} + \frac{h-\tau}{\tau}\left(-\frac{1}{\tau}a_i + \frac{1}{\tau}u_i\right) - \frac{h}{\tau}\dot{u}_i \\ &= -\frac{1}{\tau}\ddot{e}_i + \frac{1}{\tau}u_{i-1} - \frac{1}{\tau}u_i - \frac{h}{\tau}\dot{u}_i \\ &= -\frac{1}{\tau}\ddot{e}_i + \frac{1}{\tau}\bar{u}_i, \end{aligned} \tag{4.14}$$

where $\bar{u}_i$ is a new input defined as

$$\bar{u}_i := u_{i-1} - u_i - h\dot{u}_i, \tag{4.15}$$

which can be rewritten as the filter

$$\dot{u}_i = -\frac{1}{h}u_i + \frac{1}{h}\left(u_{i-1} - \bar{u}_i\right). \tag{4.16}$$

This dynamic control law determines the desired acceleration $u_i(t)$ for each vehicle i, based on the new input $\bar{u}_i(t)$ and the desired acceleration $u_{i-1}(t)$ of the preceding vehicle. It can be observed that this is a stable filter since it has a pole at $-\frac{1}{h}$ with $h > 0$. As was mentioned above, it can be observed that the desired acceleration of the preceding vehicle $u_{i-1}(t)$ appears in the relation for $\dot{u}_i(t)$. To be able to apply this in practice, the desired acceleration of a preceding vehicle is obtained through wireless communication. This $u_{i-1}(t)$-term in the controller defined in (4.16) is from now on referred to as the feed-forward term. In Ploeg et al. (2014b), it is shown that the use of this feed-forward-term $u_{i-1}(t)$ can positively contribute to the string stability properties of a platoon and therefore from now on it is assumed that the feed-forward-term $u_{i-1}(t)$ is always available for vehicle i.
A distributed consensus control law for the new input $\bar{u}_i(t)$ in (4.16) will be defined below. The error-dynamics for vehicle i can now be expressed as

$$\dot{x}_i(t) = Ax_i(t) + B\bar{u}_i(t), \tag{4.17}$$

where $x_i(t)$ is defined as in (4.13) and

$$A = \begin{bmatrix} 0 & 1 & 0 \\ 0 & 0 & 1 \\ 0 & 0 & -\frac{1}{\tau} \end{bmatrix}, B = \begin{bmatrix} 0 \\ 0 \\ \frac{1}{\tau} \end{bmatrix}. \tag{4.18}$$

The dynamics of the entire platoon is now described by

$$\left[\begin{array}{c} \dot{x}_i(t) \\ \hline \dot{u}_i(t) \end{array}\right] = \left[\begin{array}{c|c} A & O_{3\times 1} \\ \hline O_{1\times 3} & -\frac{1}{h} \end{array}\right] \left[\begin{array}{c} x_i(t) \\ \hline u_i(t) \end{array}\right] + \left[\begin{array}{c} B \\ \hline -\frac{1}{h} \end{array}\right] \bar{u}_i(t) + \left[\begin{array}{c} O_{3\times 1} \\ \hline \frac{1}{h} \end{array}\right] u_{i-1}(t) \quad \forall i \in S_n, \tag{4.19}$$

where vector $O_{1\times 3} = [0,\ 0,\ 0]$ and $O_{3\times 1} = O_{1\times 3}^T$. A distributed consensus control law for $\bar{u}_i(t)$ will be defined below. The virtual reference vehicle as defined in (4.4) and (4.5) is embedded in the error state of the first vehicle $x_1(t)$. Therefore, (4.19) also, implicitly, includes the virtual reference vehicle dynamics. After implementing the distributed control for $\bar{u}_i(t)$, the only external input to the platoon is the desired acceleration of the virtual reference vehicle $u_0(t)$.

4.3 Distributed control law and closed-loop platoon dynamics

The following distributed control law is suggested for the input $\bar{u}_i(t)$ in (4.19)

$$\bar{u}_i(t) = -\sum_{j \in \mathcal{N}_i} k^T \left(x_i(t) - x_j(t) \right) \quad \forall i \in S_n, \tag{4.20}$$

where the positive controller gain vector k is defined as $k^T = [k_1,\ k_2,\ k_3]$, the neighbouring sets $\mathcal{N}_i\ \forall i \in S_n$ are defined by an arbitrary communication topology which is described by a Laplacian matrix L.
Let a lumped state vector $X(t)$ being defined as

$$X^T(t) = [x_1^T(t),\ x_2^T(t),\ \cdots,\ x_n^T(t)] \tag{4.21}$$

and a lumped vector $U(t)$ of the desired acceleration $u_i(t)$ being defined as

$$U(t) = [u_1(t),\ u_2(t),\ \cdots,\ u_n(t)]^T. \tag{4.22}$$

Substitution of expression (4.20) into (4.19), results in the following closed-loop platoon dynamics

$$\left[\begin{array}{c} \dot{X}(t) \\ \hline \dot{U}(t) \end{array}\right] = \left[\begin{array}{c|c} I_n \otimes A - L \otimes Bk^T & O_{3n\times n} \\ \hline L \otimes \frac{k^T}{h} & \frac{1}{h}(I_{(-1),n} - I_n) \end{array}\right] \left[\begin{array}{c} X(t) \\ \hline U(t) \end{array}\right] + \left[\begin{array}{c} O_{3n\times 1} \\ \hline B_u \end{array}\right] u_0(t), \tag{4.23}$$

where $\otimes$ denotes the Kronecker product, matrix I_n is an $n \times n$ identity matrix, matrix $I_{(-1),n}$ is an $n \times n$ matrix defined as

$$I_{(-1),n} = \begin{bmatrix} 0 & \cdots & \cdots & \cdots & 0 \\ 1 & \ddots & \ddots & \ddots & \vdots \\ 0 & \ddots & \ddots & \ddots & \vdots \\ \vdots & \ddots & \ddots & \ddots & \vdots \\ 0 & \cdots & 0 & 1 & 0 \end{bmatrix} \tag{4.24}$$

and $B_u \in \mathbb{R}^{n\times 1}$ being defined as

$$B_u = \left[\frac{1}{h},\ 0,\ \cdots,\ 0\right]^T. \tag{4.25}$$

Furthermore, all entries of $3n \times 1$ vector $O_{3n\times 1}$ and $3n \times n$ matrix $O_{3n\times n}$ are equal to zero.

Due to the lower block triangular structure of (4.23), stability can be analysed by analyzing stability of the block-diagonal subsystems. First, the subsystem regarding the lumped error state vector $X(t)$ is isolated

$$\dot{X}(t) = A_c X(t) = \left(I_n \otimes A - L \otimes Bk^T\right) X(t). \tag{4.26}$$

It is known that (A, B) is controllable. Now suppose that the communication topology described by the Laplacian matrix L contains a directed spanning tree, i.e., the Laplacian matrix L is positive-definite having only one single zero eigenvalue, and the controller gain vector k are designed appropriately, such that the dynamics (4.26) is asymptotically stable. Which controller gain vector k satisfies this assumption will become clear below.
Based on consensus theory for higher-order systems (Ren et al., 2006), it is known that in this case, a common consensus state vector $x_e(t)$ exists, which is also an asymptotically stable equilibrium. Thus it is know that all state vectors converge to this common consensus state vector, i.e.,

$$lim_{t\to\infty} x_i(t) = x_e(t) \quad \forall i \in S_n. \tag{4.27}$$

A formal proof of this is not given here since this result is not used as such. Below a more formal proof will be given for a specific case of common consensus state vector $x_e(t)$, namely the zero vector. Second, the subsystem of (4.23) regarding state vector $U(t)$ is isolated

$$\dot{U}(t) = \left(L \otimes \frac{k^T}{h}\right) X(t) + \frac{1}{h}\left(I_{(-1),n} - I_n\right) U(t). \tag{4.28}$$

Hereby, it is assumed that the external input $u_0(t)$ equals zero. As was defined in (2.4), the rowsum of the Laplacian matrix L is by definition equal to zero. By using this result and the result of (4.27), it is known that the first term on the right hand-side of (4.28) is equal to zero in steady state. It can easily be seen that the matrix in the last term on the right hand-side of (4.28) has only one single eigenvalue with algebraic multiplicity n, i.e.,

$$\lambda_i \left\{ \frac{1}{h}\left(I_{(-1),n} - I_n\right) \right\} = -\frac{1}{h} \quad \forall i \in S_n, \tag{4.29}$$

and therefore the platoon dynamics have an asymptotically stable equilibrium.
At this point, the consensus state vector $x_e(t)$ in this equilibrium is not necessarily the desired consensus state equilibrium. The state vector $x_i(t)$ contains the inter-vehicle distance error $e_i(t)$ and its first and second time-derivative, which are of course desired to be zero. Therefore, the zero vector

$$\bar{x}_e = [0,\ 0,\ 0]^T \tag{4.30}$$

is the desired consensus state equilibrium. To ensure that the consensus state vector $x_e(t)$ equals the desired consensus state vector as defined in (4.30), a pinning constraint is introduced. This pinning constraint can be defined by a $n \times n$ pinning matrix

$$P = \begin{bmatrix} p_{11} & 0 & \cdots & 0 \\ 0 & p_{22} & \ddots & \vdots \\ \vdots & \ddots & \ddots & 0 \\ 0 & \dots & 0 & p_{nn} \end{bmatrix}. \tag{4.31}$$

All pinning elements p_{ii} are equal to zero, except for one vehicle i it holds that $p_{ii} = 1$. In general, this pinning constraint will be applied to the first or the last vehicle in the platoon. By this addition of a pinning constraint, the distributed control law for $\bar{u}_i(t)$ is defined as

$$\bar{u}_i(t) = -\sum_{j \in \mathcal{N}_i} [k^T(x_i(t) - x_j(t))] - p_{ii} k^T x_i(t) \quad \forall i \in S_n. \tag{4.32}$$

Note that the controller gain vector k is the same for the distributed term as for the pinning constraint term, which is designed as such to have uniformity. In principle, these controller gains could be designed differently, but in the remainder of this thesis these are assumed to be the same, as shown in (4.32).
Substitution of this new definition for the distributed control law (4.32) into (4.19) results in the following closed-loop platoon dynamics

$$\left[\begin{array}{c} \dot{X}(t) \\ \hline \dot{U}(t) \end{array}\right] = \left[\begin{array}{c|c} I_n \otimes A - \hat{L} \otimes Bk^T & O_{3n\times n} \\ \hline \hat{L} \otimes \frac{k^T}{h} & \frac{1}{h}(I_{(-1),n} - I_n) \end{array}\right] \left[\begin{array}{c} X(t) \\ \hline U(t) \end{array}\right] + \left[\begin{array}{c} O_{3n\times 1} \\ \hline B_u \end{array}\right] u_0(t), \tag{4.33}$$

with matrix $\hat{L} = L + P$ being an $n \times n$ matrix, where L is the Laplacian matrix and P is the pinning matrix.
Due to the lower block triangular structure, asymptotic stability of the equilibrium of (4.33) can be assessed by evaluation of the eigenvalues of the individual diagonal block matrices. As was shown in (4.29), all eigenvalues of the right-lower block matrix of (4.33) are in the left-half plane. What

remains is to show under which conditions the eigenvalues of the left-upper block matrix in (4.33) are in the left-half plane, i.e the dynamics of the subsystem regarding lumped error state vector $X(t)$ is asymptotically stable. The dynamics of this subsystem is given by

$$\dot{X}(t) = A_d X(t) = \left(I_n \otimes A - \hat{L} \otimes Bk^T \right) X(t). \tag{4.34}$$

Now conditions on the controller gain vector k, depending on the chosen communication topology described by the Laplacian matrix L, are derived by using ***Lemma 4.1*** and the Routh-Hurwitz stability theorem (Hurwitz, 1964).

Lemma 4.1: *The origin is an asymptotically stable equilibrium of the dynamics in* (4.34) *if and only if all matrices*

$$A - \lambda_i Bk^T \quad \forall i \in S_n \tag{4.35}$$

are Hurwitz, where λ_i *is the* i^{th} *eigenvalue of the square* $n \times n$ *matrix* $\hat{L}$*.*

By using Schur triangulation (Horn and Johnson, 1988), a proof of the above stated ***Lemma 4.1*** is derived and shown in Appendix A. In Fax and Murray (2004), a theorem of asymptotic stability of similarly interconnected system dynamics is also found, but is less elaborate.

Theorem 4.1: *The closed-loop platoon dynamics* (4.33)*, with the communication topology defined by* $\hat{L} = L + P$*, with* $\lambda_i \in \mathbb{R}^+$*, where* λ_i *is the* i^{th} *eigenvalue of matrix* $\hat{L}$*, have an asymptotically stable equilibrium (for* $lim_{t\to\infty} u_0(t) = 0$*) if and only if the controller gain vector* $k^T = [k_1,\ k_2,\ k_3]$ *of the controller defined by* (4.16) *and* (4.32) *satisfies*

$$\begin{cases} k_1 > 0 \\ k_2 > \frac{k_1 \tau}{min\{\lambda_i k_3 + 1\}} \\ k_3 > -\frac{1}{max\{\lambda_i\}} \end{cases} \quad \forall i \in S_n. \tag{4.36}$$

Proof: It directly follows from (4.33) that the origin is an equilibrium of the lumped state vector $X(t)$, and thus corresponds to the desired consensus equilibrium state $x_e(t)$ in (4.30). Asymptotic stability of this equilibrium can be evaluated by using ***Lemma 4.1***. The characteristic polynomial of matrix (4.35) is given by

$$|\mu I_3 - \left(A - \lambda_i Bk^T\right)| = \mu^3 + \frac{\lambda_i k_3 + 1}{\tau}\mu^2 + \frac{\lambda_i k_2}{\tau}\mu + \frac{\lambda_i k_1}{\tau}, \tag{4.37}$$

where I_3 is a 3×3 identity matrix and μ is an eigenvalue of matrix (4.35). By using the fact that the eigenvalues of matrix $\hat{L}$ are positive and real, i.e.,

$$\lambda_i \in \mathbb{R}^+ \quad \forall i \in S_n, \tag{4.38}$$

and $\tau > 0$, the following conditions on the controller gain vector k are derived for asymptotic stability (Zheng et al., 2014)

$$\begin{cases} k_1 > 0 \\ k_2 > \frac{k_1 \tau}{\lambda_i k_3 + 1} \\ k_3 > -\frac{1}{\lambda_i} \end{cases} \quad \forall i \in S_n. \tag{4.39}$$

This result, in addition to the result in (4.29), proves asymptotic stability of the platoon dynamics (4.33). Hence, ***Theorem 4.1*** is proven.

As was mentioned above, the Laplacian matrix L of a communication topology which contains a directed spanning tree is positive semi-definite having one single eigenvalue being equal to zero. From now on, it is assumed that the communication topology, defined by the Laplacian matrix L, indeed

contains a directed spanning tree. Then, by using the Geršgorin Disk Criterion, it can be derived that all eigenvalues of matrix $\hat{L} = L + P$ are located in the open right-half plane (Zheng et al., 2014). If, in addition, the communication topology is of a certain type, as further explained hereafter, it is known that the eigenvalues of matrix $\hat{L}$ are real, thus satisfying (4.38).
Examples of communication topologies which result in the eigenvalues of $\hat{L}$ being real are:

- The communication topology of the platoon described by Laplacian matrix L is undirected and connected (Godsil and Royle, 2001). An example of such a topology was shown in Figure 2.1.a.
- Vehicles in the platoon are of look-ahead type, i.e., each vehicle i uses the state (vector) $x_j(t)$ of w preceding vehicles, where w is a positive constant. This is an example of a directed network containing a directed spanning tree, of which an example was shown in Figure 2.1.d, for $w = 1$.

Remark 4.1: *For conventional CACC as described in Ploeg et al. (2014b), a similar filter as in* (4.16) *is applied for* $u_i(t)$*, however with*

$$\bar{u}_i(t) = -k^T x_i(t) \quad \forall i \in S_n. \tag{4.40}$$

Note that in the scope of the consensus framework described in this chapter, this would mean that there are no communication links for the error states $x_i(t)$ *at all. Only the desired acceleration* $u_{i-1}(t)$ *of vehicle* $i-1$ *is communicated to its following vehicle* i*. The entire closed-loop platoon dynamics can then be described by* (4.33) *with matrix* $\hat{L}$ *being replaced by an* $n \times n$ *identity matrix.*
The eigenvalues of the identity matrix satisfy the condition in (4.38)*, thus by replacing* $\hat{L}$ *by the identity matrix,* ***Theorem 4.1*** *can also be applied for conventional CACC. The identity matrix has only one eigenvalue equal to one, with algebraic multiplicity* n*, which means that the conditions in* (4.36) *result in*

$$\begin{cases} k_1 > 0 \\ k_2 > k_1\tau/(k_3+1) \\ k_3 > -1 \end{cases}. \tag{4.41}$$

This corresponds to the conditions on the controller gain vector $k^T = [k_1,\ k_2,\ k_3]$ *which guarantee asymptotically stable platoon error dynamics for conventional CACC, as derived in Ploeg et al. (2014b).*

The result of the origin being an asymptotically stable equilibrium of (4.33), and thus the error state vector $x_i(t)$ converging to zero for every vehicle i, can be expressed as

$$lim_{t\to\infty} x_i(t) = lim_{t\to\infty} \begin{bmatrix} q_{i-1}(t) - q_i(t) - (r + hv_i(t)) \\ v_{i-1}(t) - v_i(t) - ha_i(t) \\ a_{i-1}(t) + \frac{h-\tau}{\tau} a_i(t) - \frac{h}{\tau} u_i(t) \end{bmatrix} = \begin{bmatrix} 0 \\ 0 \\ 0 \end{bmatrix} \quad \forall i \in S_n. \tag{4.42}$$

Note that the origin being an asymptotically stable equilibrium of (4.33) implies that the vehicle following objective in (4.3) is achieved.
From (4.33), it directly follows that, for $u_0(t) = 0$, the origin is the equilibrium of the $U(t)$ dynamics. Thus it is known that

$$lim_{t\to\infty} u_i(t) = 0 \quad \forall i \in S_n. \tag{4.43}$$

As a result, according to (2.11) and (2.12), the vehicle acceleration $a_i(t)$ also converges to zero, i.e.,

$$lim_{t\to\infty} a_i(t) = 0 \quad \forall i \in S_n. \tag{4.44}$$

By using (4.42), (4.43) and (4.44), one can state that

$$lim_{t\to\infty} \begin{bmatrix} e_i(t) \\ \dot{e}_i(t) \end{bmatrix} = lim_{t\to\infty} \begin{bmatrix} q_{i-1}(t) - q_i(t) - (r + hv_i(t)) \\ v_{i-1}(t) - v_i(t) \end{bmatrix} = \begin{bmatrix} 0 \\ 0 \end{bmatrix} \quad \forall i \in S_n. \tag{4.45}$$

From (4.45), it can be observed that the velocity difference between vehicle $i-1$ and vehicle i converges to zero. This in turn implies that the velocity difference between each vehicle i and the virtual reference vehicle converges to zero, i.e.,

$$lim_{t\to\infty} \left(v_0(t) - v_i(t)\right) = 0 \quad \forall i \in S_n. \tag{4.46}$$

As was stated in (4.7), the velocity of the virtual reference vehicle $v_0(t)$ is defined to be equivalent to the desired platoon velocity v_{des}. Then, it is established that the velocity $v_i(t)$ of every vehicle i converges to this desired velocity v_{des}. Hence, the control objective (4.9) is achieved.

4.4 Communication topologies

For conventional CACC, the desired acceleration $u_{i-1}(t)$ of vehicle $i-1$ is communicated to the following vehicle i, as was explained in Section 3.5 and schematically shown in Figure 3.1. Similarly, in the distributed consensus control approach described above, this desired acceleration $u_{i-1}(t)$ is also used in the controller of the following vehicle vehicle i, as can be seen in (4.19).
For the distributed consensus control approach, in addition, a distributed consensus control law is designed for the input $\bar{u}_i(t)$. As was mentioned above, this distributed control law has a communication topology which can be described by a Laplacian matrix L, and in addition, a pinning constraint described by a pinning matrix P. In this section, two communication topologies and corresponding Laplacian matrices, which are treated later, are now shown to give some insight.

Suppose the communication topology, described by the Laplacian matrix, is defined by the Laplacian matrix

$$L_1 = \begin{bmatrix} 1 & -1 & 0 & \dots & 0 \\ -1 & 2 & -1 & \ddots & \vdots \\ 0 & \ddots & \ddots & \ddots & 0 \\ \vdots & \ddots & -1 & 2 & -1 \\ 0 & \dots & 0 & -1 & 1 \end{bmatrix}. \tag{4.47}$$

The corresponding communication topology would look like as depicted in Figure 4.1, indicated by the green arrows. The blue arrows indicate the communication of the desired acceleration $u_{i-1}(t)$ as explained above. When comparing Figure 4.1 and Figure 3.1, one can see this similarity in communication of this desired acceleration $u_{i-1}(t)$ between conventional CACC and the designed distributed consensus control approach.
When the communication topology of the distributed consensus controller for $\bar{u}_i(t)$ is defined by Laplacian matrix L_1, the neighbouring sets $\mathcal{N}_i$ for the vehicles in the platoon would be defined as

$$\mathcal{N}_1 = \{2\}, \quad \mathcal{N}_i = \{i-1, i+1\} \ \forall i \in \{i \in S_n | 1 < i < n\} \quad \text{and} \quad \mathcal{N}_n = \{n-1\}. \tag{4.48}$$

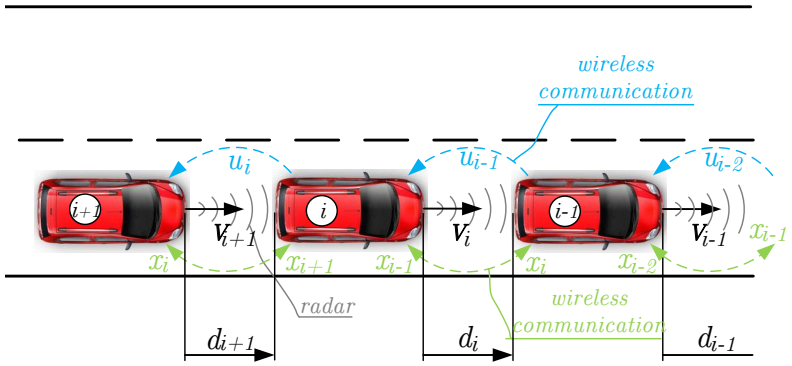

Figure 4.1: Schematic overview of communication topology for feed-forward control (blue) and communication topology for distributed consensus control given Laplacian matrix L_1 (green).

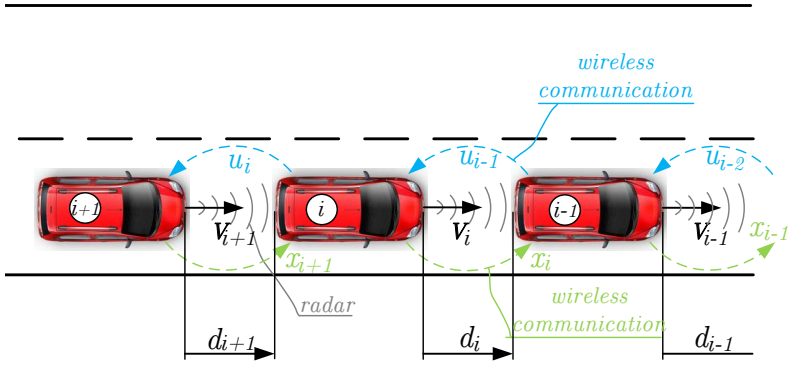

Figure 4.2: Schematic overview of communication topology for feed-forward control (blue) and communication topology for distributed consensus control given Laplacian matrix L_2 (green).

Note that this neighbouring set $\mathcal{N}_i$ describes the set of vehicles of which the error state vectors $x_j(t)$ are used in the distributed controller for $\bar{u}_i(t)$ of vehicle i.
The communication topology described by Laplacian matrix L_1 is referred to as *Topology 1*. Given this topology, each vehicle i receives the error state vector of its follower $x_{i+1}(t)$ and the error state vector of its preceding vehicle $x_{i-1}(t)$, unless it is the first or last vehicle in the platoon since those vehicles have no (actual) preceding or following vehicle, respectively.

Another possible communication topology is defined by Laplacian matrix

$$L_2 = \begin{bmatrix} 1 & -1 & 0 & \cdots & 0 \\ 0 & 1 & -1 & \ddots & \vdots \\ \vdots & \ddots & \ddots & \ddots & 0 \\ \vdots & \ddots & 0 & 1 & -1 \\ 0 & \cdots & 0 & 0 & 0 \end{bmatrix}. \tag{4.49}$$

The neighbouring sets, given Laplacian matrix L_2, are defined as

$$\mathcal{N}_i = \{i+1\} \ \forall i \in \{i \in S_n | 1 \leq i < n\} \quad \text{and} \quad \mathcal{N}_n = \emptyset. \tag{4.50}$$

The communication topology described by the Laplacian L_2 is referred to as *Topology 2*. For this communication topology, the controller of each vehicle uses the error state vector of its following vehicle $x_{i+1}(t)$, in addition to its own error state vector $x_i(t)$. Except for the last vehicle which receives no error state vector of any vehicle, since it has no following vehicle. Also, the controller of each vehicle i uses the desired acceleration $u_{i-1}(t)$ of its preceding vehicle, as was mentioned before. This communication topology is schematically presented in Figure 4.2.
The communication topologies described above are just two possible communication topologies for the distributed controller for $\bar{u}_i(t)$, but there are various communication topologies for the distributed control which, in combination with appropriately designed controller gains k, result in asymptotically stable platoon dynamics (4.33).

4.5 Simulation results

The consensus controller as designed in Section 4.3 is simulated using MATLAB. The simulation results of a platoon having size $n = 10$ vehicles are shown and analysed below. Each vehicle, modeled

Table 4.1: Eigenvalues of matrix $\hat{L} = L + P$ given *Topology 1 and 2*.

λ_i ***Topology 1***	λ_i ***Topology 2***
0.0223	1
0.1981	1
0.5339	1
1.0000	1
1.5550	1
2.1495	1
2.7307	1
3.2470	1
3.6525	1
3.9111	1

as defined in (2.11) and (2.12), is controlled using the controller as defined by (4.16) and (4.32). First, the communication topology is chosen according to *Topology 1*, which is defined in Section 4.4. Additionally, only the first vehicle in the platoon is subjected to the pinning constraint, i.e.,

$$\begin{cases} p_{11} = 1 \\ p_{ii} = 0 \quad \forall i \in \{i \in S_n | i \neq 1\}. \end{cases} \tag{4.51}$$

Given *Topology 1*, the neighbouring sets $\mathcal{N}_i$ are defined as in (4.48). Each vehicle uses its own error state vector $x_i(t)$, obtained by radar measurements, and the error states of its preceding and following vehicle $x_{i+1}(t)$ and $x_{i-1}(t)$, respectively, obtained via wireless communication. Note that the first and the last vehicle in the platoon only use the error state vector of its following or preceding vehicle, respectively. In addition, the desired acceleration of a preceding vehicle $u_{i-1}(t)$ is also obtained by a vehicle i via wireless communication.
Given *Topology 1* and pinning constraint (4.51), the resulting closed-loop platoon dynamics are defined as in (4.33) with matrix $\hat{L} = L + P$, where Laplacian matrix L is defined as L_1 in (4.47) and the elements of pinning matrix P are defined as in (4.51).

The eigenvalues of matrix $\hat{L}$ representing this topology are shown in the left column of Table 4.1. All eigenvalues of matrix $\hat{L}$ satisfy the conditions defined in (4.38), and therefore the conditions on the controller gain vector $k = [k_1,\ k_2,\ k_3]$ stated in **Theorem 4.1** in (4.36) do guarantee asymptotic closed-loop platoon stability.

For *Topology 1*, upper and lower bounds on the smallest eigenvalue of $\hat{L}$ can be defined as (Zheng et al., 2014)

$$\frac{1}{n^2} \leq \min_{i \in S_n} \{\lambda_i\} \leq \frac{\pi^2}{n^2}. \tag{4.52}$$

Note that the smallest eigenvalue of $\hat{L}$ converges to zero as the platoon length n increases. As a result, according to the characteristic polynomial as given in (4.37), the minimum eigenvalue of matrix $A - \lambda_i B k^T$ converges to zero, i.e.,

$$lim_{n \to \infty} \sigma_{lst} \left\{ A - \min_{i \in S_n} \{\lambda_i\} B k^T \right\} = 0, \tag{4.53}$$

where $\sigma_{lst}\{W\}$ is the minimum eigenvalue of matrix W. This leads to the origin becoming a marginally stable equilibrium of the closed-loop platoon error system (4.34), as the platoon length

n goes to infinity. In practice, each platoon has a finite length such that a larger platoon length n will only result in an expontially slower transient response.

Next, asymptotic stability of the entire platoon dynamics, for both *Topology 1* as well as *Topology 2*, is verified by time-simulations. The controller gain vector, for the simulated platoon, is designed to be $k^T = [0.2,\ 1.0,\ 0]$, such that the conditions in (4.36) are satisfied.
Note that controller gain k_3 is designed to be $k_3 = 0$ for all controllers described in this thesis. This design is due to the fact that, in the scope of practical implementation, it is not feasible to apply feedback of the jerk due to measurement noise. In theory, controller gain k_3 can have any value as long as the conditions in (4.36) are satisfied.
The drive-line dynamics constant is $\tau = 0.1$. The desired standstill distance and time gap are set to $r = 2$ m and $h = 0.6$ s. The initial position, velocity and acceleration of all vehicles i are perturbed, i.e., the platoon is not in steady state at $t = 0$ s. The initial velocity of all vehicles in the platoon slighly differs and the average initial platoon velocity is chosen as

$$\sum_{i=1}^{n} \frac{v_i(0)}{n} = 17m/s. \tag{4.54}$$

The initial velocity of the virtual reference vehicle $v_0(t)$ is set to the desired velocity $v_{des} = 22$ m/s, i.e., $v_0(0) = v_{des}$. The velocity of the virtual reference vehicle $v_0(t)$ does not change because $u_0(t) = 0$ and $a_0(0) = 0$ is chosen. The resulting platoon response is shown in Figure 4.3. It can be observed that the vehicle velocity $v_i(t)$ starts at approximately 17 m/s and converges to 22 m/s for each vehicle i. For the first six vehicles, the overshoot on velocity increases, which is undesired behavior. However, it can be observed that for vehicle $i = 7$ to $i = 10$ the overshoot on velocity decreases, which is desired. Furthermore, the vehicle acceleration $a_i(t)$ and desired acceleration $u_i(t)$ both converge to zero for each vehicle i. And, in addition, a decreasing trend in the maximum amplitude of the acceleration $a_i(t)$ and the desired acceleration $u_i(t)$ in upstream direction can be observed. This indicates that a fast acceleration executed in the front of the platoon attenuates in upstream direction, which is desired behavior. One can also observe that the inter-vehicle distance error $e_i(t)$ converges to zero, thus illustrating that the origin is indeed a asymptotically stable equilibrium of (4.33).

Another topology which seems to offer nice properties is the single vehicle look-back communication topology for the distributed consensus controller for $\bar{u}_i(t)$. This topology is referred to as *Topology 2* in Section 4.4 and is represented by Laplacian matrix L_2 in (4.49). Note that notion of look-back only relates to the distributed controller for $\bar{u}_i(t)$, which means that vehicle $i + 1$ is the only vehicle in the neighbouring set $\mathcal{N}_i$ of vehicle i.
The first nice property for *Topology 2* is the fact that the minimum eigenvalue does not converge to be marginally stable for increasing platoon length n, as is shown in Table 4.1. And secondly, this topology seems to have a structure which is usefull for improving a platoons coherence, but this will become clear in Chapter 5.
Given this control topology, a vehicle i thus receives the desired acceleration of the preceding vehicle $u_{i-1}(t)$ and the error state vector $x_{i+1}(t)$ of its following vehicle, both via a communication network. The controller of vehicle i uses this information received via the communication network in addition to its own state vector $x_i(t)$ (determined using radar measurements). Additionally, only the last vehicle in the platoon is subjected to the pinning constraint, i.e.,

$$\begin{cases} p_{ii} = 0 & \forall i \in \{i \in S_n | i \neq n\} \\ p_{nn} = 1. \end{cases} \tag{4.55}$$

The fact that the last vehicle is subjected to the pinning constraint can be understood by having a look at the Laplacian matrix for *Topology 2* in (4.49). All entries of the last row of the Laplacian matrix L_2 are zero since the vehicle $i = n$ has no following vehicle to receive an error state vector $x_{n+1}(t)$ from. In fact, given that the last vehicle is subjected to the pinning constraint, the last vehicle $i = n$ is controlled by a conventional CACC controller as described in Ploeg et al. (2014b). As a result of this and

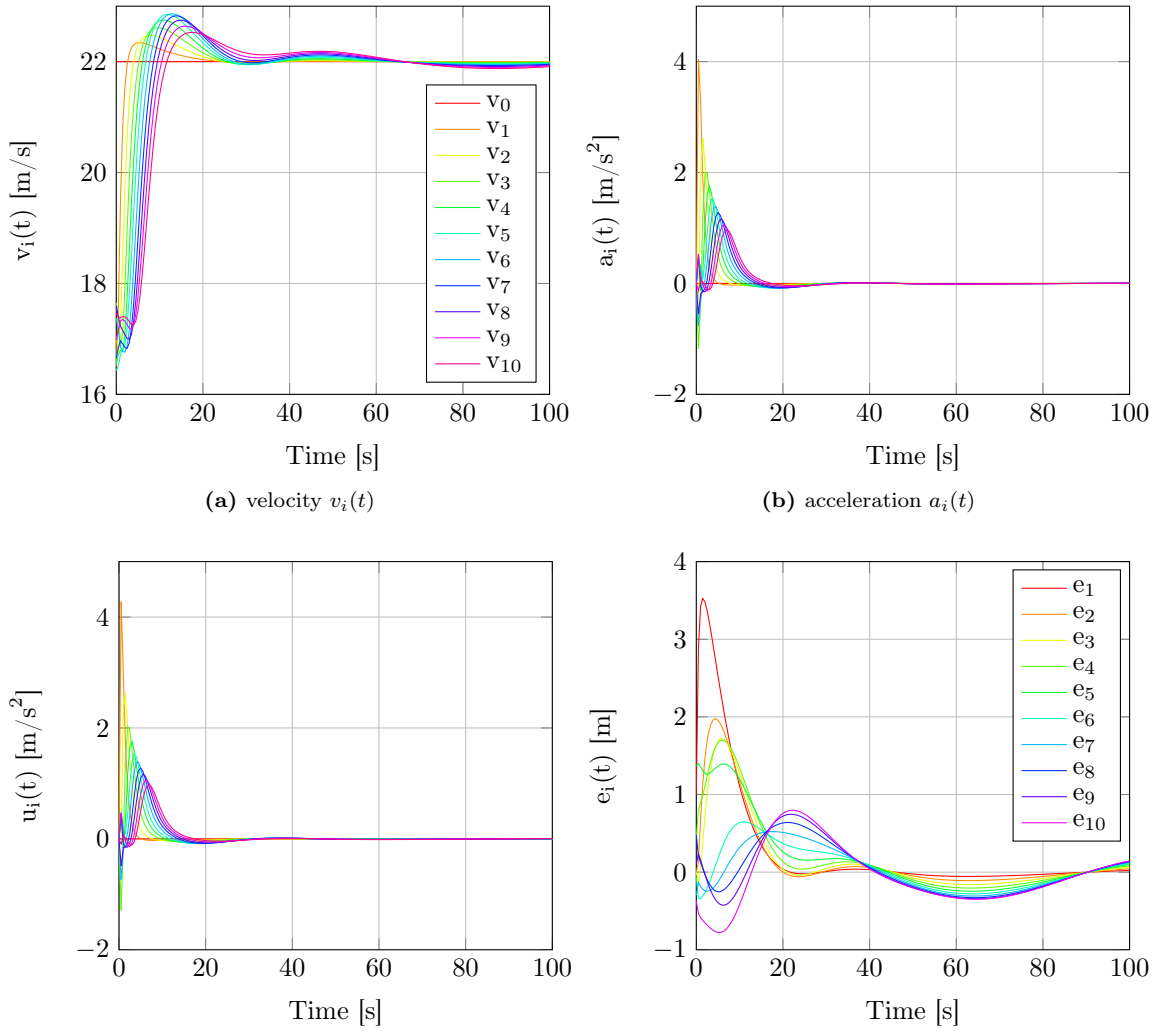

(a) velocity $v_i(t)$

(b) acceleration $a_i(t)$

(c) desired acceleration $u_i(t)$

(d) inter-vehicle distance error $e_i(t)$

Figure 4.3: The velocity $v_i(t)$, acceleration $a_i(t)$, desired acceleration $u_i(t)$ and inter-vehicle longitudinal distance error $e_i(t)$ of each vehicle i versus time. The legend shown in the velocity plot also applies for the acceleration $a_i(t)$ and desired acceleration $u_i(t)$. Distributed controller with *Topology 1* and controller gain vector $k^T = [0.2,\ 1.0,\ 0]$.

the single vehicle look-back topology in the distributed consensus controller (4.32), the origin is an asymptotically stable equilibrium of the error dynamics of each vehicle i, under the assumption that the control gains are designed appropriately.
Topology 2 is also very intuitive, since the controller of each vehicle i uses the difference of the inter-vehicle distance error of the i^{th} vehicle $e_i(t)$ and the inter-vehicle distance error of the vehicle directly behind, i.e., $e_{i+1}(t)$. Therefore each vehicle i individually regulates its position to the center of the distance gap between its preceding and following vehicle and, due to the last vehicle regulating its inter-vehicle distance error $e_n(t)$ to zero, all inter-vehicle distance errors $e_i(t)$ converge to zero.

As was mentioned above, for *Topology 2*, the eigenvalues of matrix $\hat{L}$ are displayed in the second column of Table 4.1. All eigenvalues λ_i of matrix $\hat{L}$ are equal to 1 and do not depend on the platoon length n, as is the case for *Topology 1*. For *Topology 1*, all eigenvalues λ_i change with changing platoon

length n.
Due to all eigenvalues λ_i of matrix $\hat{L}$ being equal to 1, for *Topology 2*, the conditions on the controller gain vector k guaranteeing asymptotic closed-loop stability are similar as for conventional CACC as defined in (4.41). As was mentioned before, *Topology 2* also offers opportunities for design of a control law for the virtual reference vehicle to improve the platoon coherence, as will be explained in Chapter 5.

Figure 4.4 shows the platoon response given *Topology 2* for the distributed consensus controller. The initial conditions, standstill distance r, time gap h and controller gain vector k are the same as described above for the simulation with *Topology 1*. The controller gain vector $k^T = [0.2,\ 1.0,\ 0]$ satisfies the conditions in (4.36). It can again be observed that the vehicle velocity $v_i(t)$ converges to the desired velocity $v_{des} = 22$ m/s, the vehicles acceleration $a_i(t)$ and desired acceleration $u_i(t)$ converge

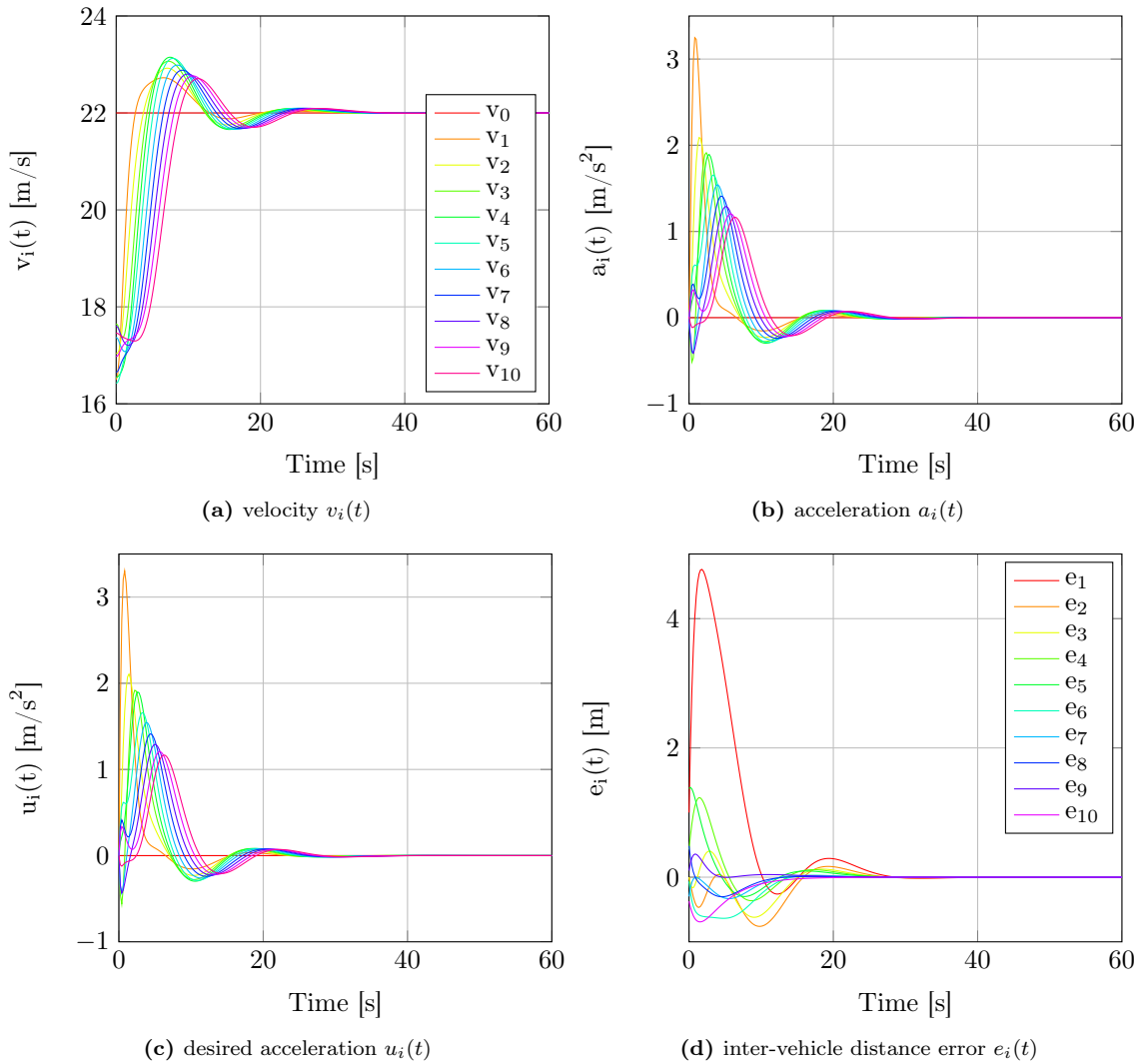

(a) velocity $v_i(t)$

(b) acceleration $a_i(t)$

(c) desired acceleration $u_i(t)$

(d) inter-vehicle distance error $e_i(t)$

Figure 4.4: The velocity $v_i(t)$, acceleration $a_i(t)$, desired acceleration $u_i(t)$ and inter-vehicle longitudinal distance error $e_i(t)$ of each vehicle i versus time. The legend shown in the velocity plot also applies for the acceleration $a_i(t)$ and desired acceleration $u_i(t)$. Distributed controller with *Topology 2* and controller gain vector $k^T = [0.2,\ 1.0,\ 0]$.

to zero for each vehicle i. The inter-vehicle distance error $e_i(t)$ also converges to zero for each vehicle i. It can be observed that the inter-vehicle distance error of the first vehicle $e_1(t)$ has a large initial increase. This is due to the fact that the initial velocity of the virtual reference vehicle is much higher than the platoon velocity. This inter-vehicle distance error $e_1(t)$ is a virtual distance error and therefore not relevant in the sense of a possible collision or increased road usage.

When comparing both platoon responses for *Topology 1* and *Topology 2*, it can be observed that both platoon responses are quite similar. However, one can see that for *Topology 2*, the damping of the inter-vehicle distance errors $e_i(t)$ is much better since all inter-vehicle distance errors are approximately zero after 30 seconds. In comparison, for *Topology 1*, the inter-vehicle distance errors $e_i(t)$ are still oscillating after 100 seconds.
This difference in convergence rate originates from the algebraic connectivity of the communication graph (Olfati-Saber and Murray, 2004). The algebraic connectivity of a graph is the second smallest eigenvalue of the Laplacian matrix L. As can be seen by comparing the eigenvalues in Table 4.1, the second smallest eigenvalue is smaller for *Topology 1*, resulting in a lower convergence rate. Note that in Table 4.1, the eigenvalues of matrix $\hat{L}$ are displayed, but these are of comparable order as the eigenvalues of the Laplacian matrix L.

4.5.1 Controller gain $k_1 = 0$ for first vehicle

In the control framework described above, homogeneity is assumed for the controller gains k and therefore the inter-vehicle distance error of the first vehicle $e_1(t)$ is also controlled to zero, according to the first control objective, which is defined in (4.3). However, as was mentioned above, the inter-vehicle distance error of the first vehicle $e_1(t)$ is a virtual distance error and therefore not physically relevant in the sense that it must converge to zero. The time-derivative of this inter-vehicle distance error of the first vehicle $\dot{e}_1(t)$, however, is relevant, since it is desired to drive this time-derivative of the inter-vehicle distance error $\dot{e}_1(t)$ to zero, such that the velocity of the first vehicle converges to the velocity of the virtual reference vehicle, i.e., the second control objective (4.9) is satisfied.

For practical implementation, controlling this virtual inter-vehicle distance error $e_1(t)$ to zero can indeed be undesired. Suppose that the position of the virtual reference vehicle is a kilometer in front of the first vehicle in the platoon. The first vehicle then tries to close this virtual gap which is not necessary. It is only desired to drive the velocity of the first vehicle to the velocity of the virtual reference vehicle.
Given *Topology 2*, described by Laplacian matrix L_2, and the pinning constraint defined in (4.55), the control gain k_1 of the controller of the first vehicle in the platoon can be set equal to zero. As a result, the (virtual) inter-vehicle distance error $e_1(t)$ of the first vehicle will not converge to zero. Given this fact, the platoon equilibrium is defined as

$$lim_{t\to\infty} X(t) = \left[\bar{e}_1,\ O_{1\times 2},\ O_{1\times 3},\ \cdots,\ O_{1\times 3}\right]^T, \tag{4.56}$$

where scalar $\bar{e}_1$ is an equilibrium value depending on the initial conditions, and vectors $O_{1\times 2}$ and $O_{1\times 3}$ have all zero elements.
The simulation for *Topology 2*, of which the simulation results where shown in Figure 4.4, is repeated, with the only difference being the control gain k_1 for the first vehicle, which is defined as $k_1 = 0$, and the initial inter-vehicle distance error for the first vehicle is defined as $e_1(0) = 25$ m. Setting the control gain k_1 to zero for the first vehicle can only be done when vehicle $i = 1$ is not present in the neighbouring set $\mathcal{N}_i$ of any other vehicle i in the platoon, and the communication graph described by the Laplacian matrix L contains a directed spanning tree with vehicle $i \neq 1$, which is subjected to the pinning constraint, being the root of this directed spanning tree. If the communication graph described by the Laplacian matrix L satisfies the aforementioned conditions, setting the control gain $k_1 = 0$ to zero for vehicle $i = 1$ only leads to one eigenmode of the error dynamics to become marginally stable, i.e., eigenvalue equal to zero. This eigenmode is only associated with virtual inter-vehicle distance error $e_1(t)$.

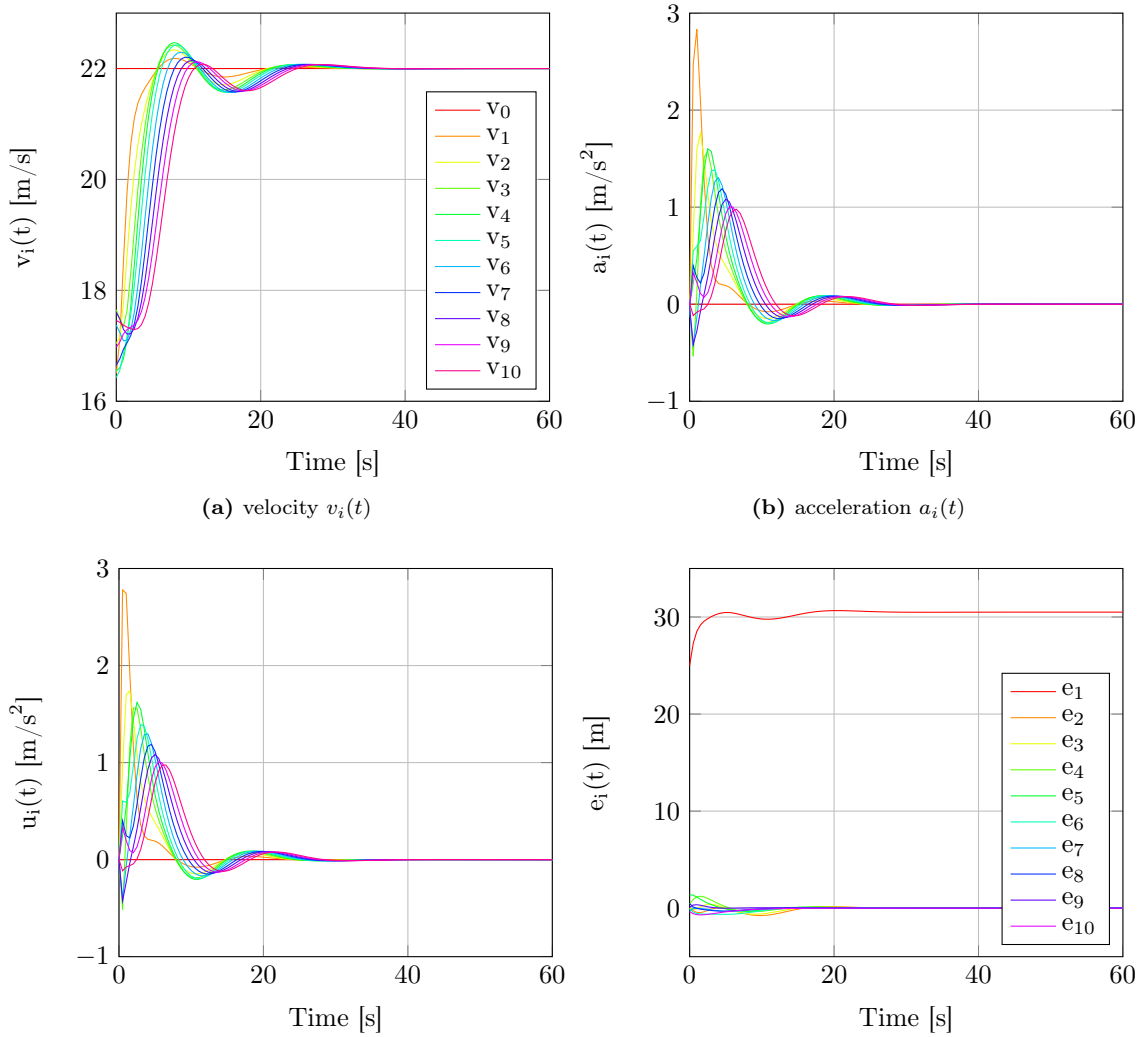

(a) velocity $v_i(t)$

(b) acceleration $a_i(t)$

(c) desired acceleration $u_i(t)$

(d) inter-vehicle distance error $e_i(t)$

Figure 4.5: The velocity $v_i(t)$, acceleration $a_i(t)$, desired acceleration $u_i(t)$ and inter-vehicle longitudinal distance error $e_i(t)$ of each vehicle i versus time. The legend shown in the velocity plot also applies for the acceleration $a_i(t)$ and desired acceleration $u_i(t)$. Distributed controller with *Topology 2* and the controller gain vector being $k^T = [0.2,\ 1.0,\ 0]$ for vehicle $i \in \{i \in S_n | i \neq 1\}$, and being $k^T = [0,\ 1.0,\ 0]$ for vehicle $i = 1$.

In the case of *Topology 2* in combination with the pinning constraint (4.55), the last vehicle $i = n$ is subjected to the pinning constraint and this last vehicle is the root of a directed spanning tree in the communication topology. Also, vehicle $i = 1$ is not present in the neighbouring set $\mathcal{N}_i$ of any other vehicle in the platoon, such that all abovementioned controller conditions are satisfied and thus k_1 can be set to zero for vehicle $i = 1$.
The results for this simulation are shown in Figure 4.5. It can be observed that, indeed the inter-vehicle distance error of the first vehicle does not converge to zero, but all other inter-vehicle distance errors do. Furthermore, the velocity of the vehicles in the platoon converges to the desired velocity $v_0(t) = v_{des} = 22$ m/s. It can be seen that the large initial (virtual) inter-vehicle distance error $e_1(0)$ does not really affect the platoon response. If the control gain k_1 is defined similar as for the rest of

the vehicles in the platoon, this large initial (virtual) inter-vehicle distance error $e_1(0)$ would result in a larger acceleration for the first vehicle and as a result for all vehicles in the platoon. Furthermore, as was mentioned above, in many situations it would not make sense to regulate this inter-vehicle distance error with respect to a virtual reference vehicle to zero, since only a certain platoon cruising velocity is desired.
Note that this is only a practical solution. Thus in the remainder of this thesis, homogeneity is assumed such that the controller gain vector k is the same for all vehicle in the platoon, including the first vehicle $i = 1$.

4.5.2 Drive-line dynamics delay ϕ and communication delay θ

As was already mentioned in Section 2.3, the full model of the longitudinal vehicle dynamics also contains a drive-line dynamics time delay ϕ. It is known that for the TNO Prius test vehicles this drive-line dynamics time delay can be best approximated by $\phi = 0.2$ s (Ploeg et al., 2014a).
All information which is transferred via a communication network suffers from communication delay. Therefore, also a communication delay θ is introduced of which it is known that this communication delay can be best approximated by $\theta = 0.02$ s for the TNO wireless communication equipment (Ploeg et al., 2014a). Both the drive-line dynamics delay and communication delay are modeled using a third-order Padé approximation yielding a sufficiently accurate phase and magnitude approximation in the frequency interval of interest (Ploeg et al., 2014a). It is not straightforward to analyse the influence of these delays on the position of the poles of the closed-loop platoon (error-)dynamics as presented in (4.33). Amongst others, this is due the fact that the actuator delay ϕ is a delay between the desired acceleration $u_i(t)$ and the acceleration $a_i(t)$ and thus is a delay in the second time-derivative of the inter-vehicle distance error state $\ddot{e}_i(t)$, as can be seen in (4.12). To verify the influence of these delays on the platoon's stability, simulations including these delays are executed. Given this drive-line dynamics delay ϕ, the full vehicle model is described by

$$\dot{p}_i(t) = Ap_i(t) + Bu_i(t-\phi), \quad \forall i \in S_n, \tag{4.57}$$

where

$$p_i(t) = \begin{bmatrix} q_i(t) \\ v_i(t) \\ a_i(t) \end{bmatrix}, A = \begin{bmatrix} 0 & 1 & 0 \\ 0 & 0 & 1 \\ 0 & 0 & -\frac{1}{\tau} \end{bmatrix}, B = \begin{bmatrix} 0 \\ 0 \\ \frac{1}{\tau} \end{bmatrix}. \tag{4.58}$$

The full general controller model, including communication delay θ, is described by

$$\dot{u}_i(t) = -\frac{1}{h}u_i(t) + \frac{1}{h}\left(u_{i-1}(t-\theta) + \sum_{j \in \mathcal{N}_i} [k^T(x_i(t) - x_j(t-\theta))] + p_{ii}k^T x_i(t) \right). \tag{4.59}$$

The controller gain vector $k^T = [0.2,\ 1.0,\ 0]$ and platoon parameters, such as time gap $h = 0.6$ s and standstill distance $r = 2$ m, are the same as for the simulations described above. *Topology 2* is used for the distributed controller.
The platoon response is shown in Figure 4.6. When comparing the platoon responses in Figure 4.6 with the platoon responses in Figure 4.4, one can see that the responses are quite similar. The transients are slightly different, but the vehicle platoon arives at steady state after approximately $t = 30$ s for both situations. Thus it seems that the introduction of the drive-line dynamics delay $\phi = 0.2$ s and the communication delay $\theta = 0.02$ s does not lead to unstable closed-loop platoon dynamics.
A significant increase of the values of these delays will lead to unstable platoon behavior. For example, suppose that the actuator delay is defined as $\phi = 0.2$ seconds. It is numerically determined that the platoon dynamics becomes unstable when the communication delay θ is larger than 0.38 seconds.
Now, on the other hand, suppose that the communication delay is defined as $\theta = 0.02$ seconds. It is numerically determined that the platoon dynamics becomes unstable for a actuator delay ϕ which is larger than 0.70 seconds.
For the TNO Toyota Pruis fleet, it is known that these delays are approximately $\phi = 0.2$ and $\theta = 0.02$

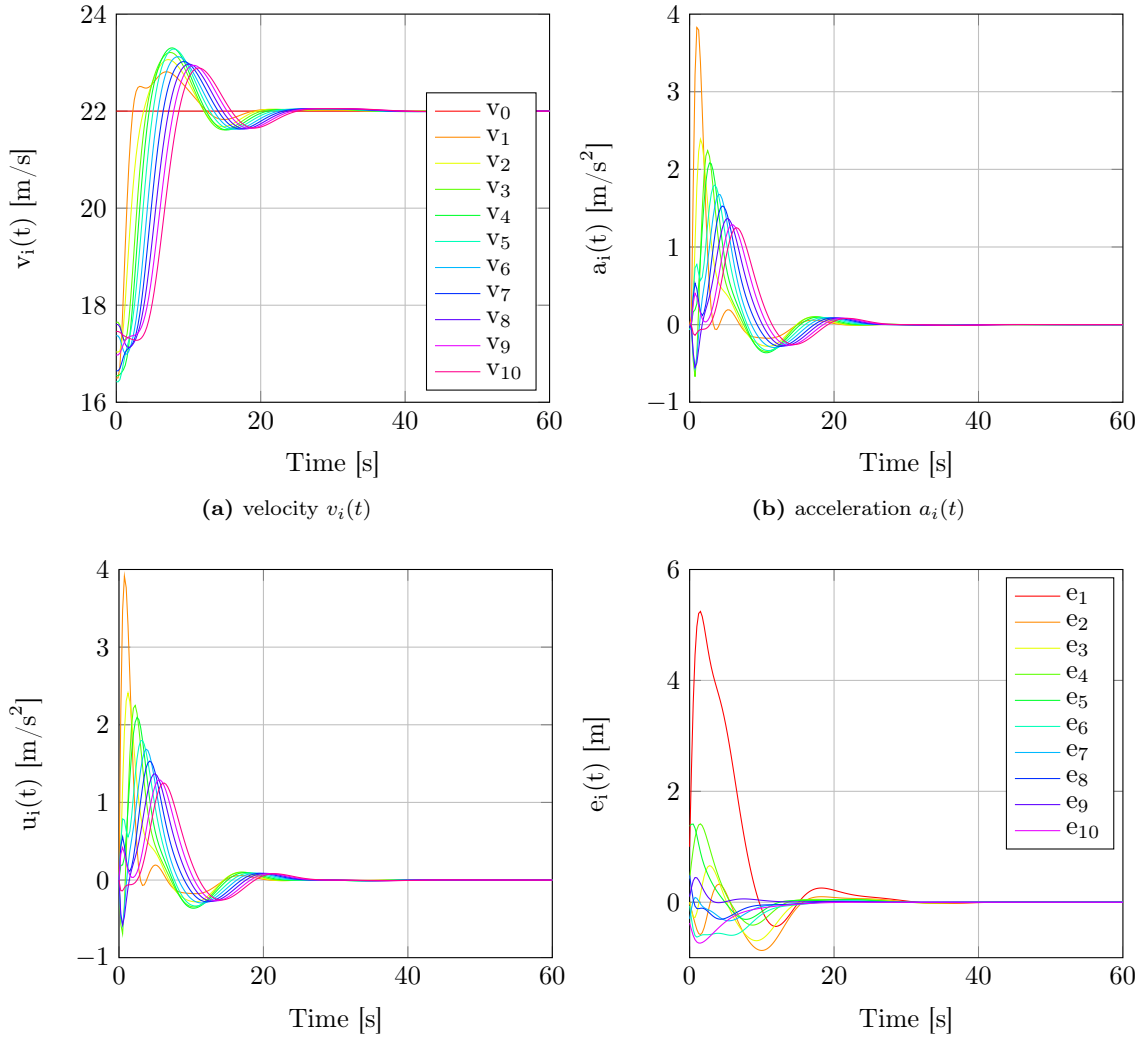

(a) velocity $v_i(t)$

(b) acceleration $a_i(t)$

(c) desired acceleration $u_i(t)$

(d) inter-vehicle distance error $e_i(t)$

Figure 4.6: The velocity $v_i(t)$, acceleration $a_i(t)$, desired acceleration $u_i(t)$ and inter-vehicle longitudinal distance error $e_i(t)$ of each vehicle i versus time. The legend shown in the velocity plot also applies for the acceleration $a_i(t)$ and desired acceleration $u_i(t)$. Distributed controller with *Topology 2* and controller gain vector $k^T = [0.2,\ 1.0,\ 0]$. Drive-line dynamics delay and communication delay are $\phi = 0.2$ s and $\theta = 0.02$ s, respectively.

seconds, thus a slight increase of the network latency θ or actuator delay ϕ does not lead to instability of the platoon.

4.6 Summary

In this chapter, the development of a distributed consensus control strategy for longitudinal vehicle platooning is presented. Conditions on the controller gain vector k, depending on the chosen communication topology defined by a Laplacian matrix L and guarenteeing closed-loop stability of the platoon dynamics, are derived. The conditions for stability are formulated in a general fashion such that these are valid for various communication topologies. Feedforward of the desired acceleration of the pre-

ceding vehicle is included, with the aim of a positive contribution to the string stability properties of the platoon. The analytical result is verified using time simulations for two different topologies for the distributed control input $\bar{u}_i(t)$. Communication *Topology 1* is defined such that a vehicle i uses the error state vector $x_{i-1}(t)$ of its predecessor and the error state vector $x_{i+1}(t)$ of its following vehicle, in addition to its own error state vector $x_i(t)$. Communication *Topology 2* is defined such that a vehicle i uses the error state vector $x_{i+1}(t)$ of its following vehicle, in addition to its own error state vector $x_i(t)$. It is found that for *Topology 2*, for similar controller gains, the convergence of the inter-vehicle distance error $e_i(t)$ is much faster than for *Topology 1*. Furthermore, *Topology 2* leaves the possibility for setting the control gain k_1 of the first vehicle equal to zero, which makes more sense in practice. Also, it is analysed that the influence of the drive-line dynamics delay $\phi = 0.2$ s and the communication delay $\theta = 0.02$ s do not compromise stability.

Chapter 5

Platoon Coherence

In the framework designed in the previous chapter, the vehicles in the platoon can respond to the dynamics of preceding as well as following vehicles, depending on the chosen communication topology. One of the possible functionalities that could arise from inclusion of look-back in the communication topology is that a platoon can adapt to (temporary) limited functionality of one of its vehicle members in the platoon. For example, the maximum velocity v_{max} (and/or maximum acceleration a_{max}) of a heavily loaded truck, in a platoon of trucks, can be slightly lower than the velocity (and/or acceleration) of the leading, less loaded, truck. In conventional CACC, with only look-ahead sensing and communication, this would result in the platoon to break up.
The controller structure which is used in this chapter is as described in Section 4.3, such that the desired acceleration input $u_i(t)$ applied to each vehicle is determined using the controller defined by (4.16) and (4.32). The platoon responses for both *Topology 1* as well as *Topology 2*, which were both introduced in Section 4.4, are analysed in this chapter.
In Section 5.1, it is shown that when the virtual reference vehicle is uncontrolled, i.e., having a constant velocity

$$v_0(t) \equiv v_{des} > v_{max}, \tag{5.1}$$

the steady-state solution of the platoon is not an equilibrium when there is a vehicle in the platoon which has a maximum velocity of v_{max}. Similar as for conventional CACC, this results in the platoon to break up. To enhance platoon behavior such that the platoon stays coherent in case a velocity saturation occurs in one of the vehicles, in Section 5.2, a control law for the virtual reference vehicle is designed. As a result of this additional control law, the platoon automatically adapts its velocity, such that the platoon does not break up in the case of a present faulty (or slow) vehicle. Thereafter, in Section 5.3 and Section 5.4, additional conditions for asymptotic closed-loop platoon stability, for a vehicle platoon subject to this designed controller for the virtual reference vehicle, are given. In Section 5.5, for *Topology 2*, using time-simulations it is shown that the platoon indeed adapts its velocity to a vehicle (temporarily) having a lower maximum velocity. Finally, in Section 5.6, the steady-state response for *Topology 1* is evaluated.

5.1 Platoon steady state

Suppose the topology of the distributed consensus controller is designed to be as *Topology 2* as described in Section 4.5, i.e., the neighbouring sets $\mathcal{N}_i$ are defined as

$$\mathcal{N}_i = \{i+1\} \ \forall i \in \{i \in S_n | 1 \leq i < n\} \quad \text{and} \quad \mathcal{N}_n = \emptyset, \tag{5.2}$$

and the pinning constraint being defined as

$$\begin{cases} p_{ii} = 0 & \forall i \in \{i \in S_n | i \neq n\} \\ p_{nn} = 1. \end{cases} \tag{5.3}$$

Given this, the relation for the control of the vehicles in the platoon is defined as

$$\begin{cases} \dot{u}_i(t) = -\frac{1}{h}u_i(t) + \frac{1}{h}u_{i-1}(t) + \frac{1}{h}k^T(x_i(t) - x_{i+1}(t)) & \forall i \in \{i \in S_n | i \neq n\} \\ \dot{u}_n(t) = -\frac{1}{h}u_n(t) + \frac{1}{h}u_{n-1}(t) + \frac{1}{h}k^T x_n(t). \end{cases} \tag{5.4}$$

Given this control structure, the resulting closed-loop platoon dynamics can be expressed as defined in (4.33) with matrix $\hat{L} = L_2 + P$ being defined as

$$\hat{L} = \begin{bmatrix} 1 & -1 & 0 & \cdots & 0 \\ 0 & 1 & -1 & \ddots & \vdots \\ \vdots & \ddots & \ddots & \ddots & 0 \\ \vdots & \ddots & \ddots & 1 & -1 \\ 0 & \cdots & \cdots & 0 & 1 \end{bmatrix}. \tag{5.5}$$

In Chapter 4, it is shown that the distributed control law as defined in (5.4) results in asymptotically stable closed-loop platoon dynamics (4.33) when the controller gain vector $k^T = [k_1,\ k_2,\ k_3]$ is designed appropriately according to ***Theorem 4.1*** for a homogeneous platoon. Next, a faulty (or slow) vehicle is introduced, similar as done in Semsar-Kazerooni and Khorasani (2007), and the platoon dynamics after introducing this slow vehicle are analysed.
Now suppose that the maximum velocity of the f^{th} vehicle ($i = f$) in the platoon is defined as v_{max} such that

$$v_f(t) \leq v_{max} \quad \forall t. \tag{5.6}$$

Some additional definitions are given to model this saturation on the velocity of vehicle $i = f$ correctly. When vehicle $i = f$ reaches its maximum velocity, i.e., $v_f(t) = v_{max}$, then by definition, the acceleration $a_f(t)$ and desired acceleration $u_f(t)$ are equal to zero, i.e., $a_f(t) = 0$ and $u_f(t) = 0$. Only when $\dot{u}_f(t)$ resulting from the relation

$$\dot{u}_f(t) = -\frac{1}{h}u_f(t) + \frac{1}{h}u_{f-1}(t) + \frac{1}{h}k^T(x_f(t) - x_{f+1}(t)) \tag{5.7}$$

becomes negative, then $u_f(t) \neq 0$ and $u_f(t)$ is again determined using relation (5.7). This can be seen as a kind of switching between two modes. With *Mode* 1 being normal platoon operation with continuous dynamics as treated in Chapter 4, and *Mode* 2 being the fixed velocity for vehicle f and normal operation with continuous dynamics for all other vehicles in the platoon.

For the analytical derivation of the steady state, it is assumed that when vehicle f goes in saturation, i.e., switches from *Mode* 1 to *Mode* 2, it stays in *Mode* 2. This assumption ensures that no switching back and forth between the two modes occurs. As a result of the velocity of vehicle f being saturated and the particular (single vehicle look-back) structure of *Topology 2*, the platoon dynamics can be divided into two subgroups. The first group contains all vehicles which drive behind the saturated vehicle, i.e., all vehicles $i \in \{i \in S_n | i > f\}$, and the second group contains all vehicles in front of the saturated vehicle and the saturated vehicle itself, i.e., all vehicles $i \in \{i \in S_n | i \leq f\}$.
As can be seen in (5.4), for this particular topology (5.2) for the distributed controller in combination with the pinning constraint (5.3), the last vehicle $i = n$ in the platoon is controlled using conventional CACC as presented in Ploeg et al. (2014b). This means that the origin is an asymptotically stable equilibrium of the error state vector $x_n(t)$ of vehicle $i = n$, under the condition of a properly designed controller gain vector k according to the conditions in (4.41).

Theorem 5.1: *The closed-loop platoon dynamics* (4.33)*, with the communication topology defined by* $\hat{L} = L + P$ *as in* (5.5)*, do not have an asymptotically stable equilibrium in the reachable subspace if* $v_0(t)$ *and* $v_f(t) \leq v_{max}$ *satisfy* (5.1)*.*

Proof: First, the dynamics of the vehicles behind vehicle $i = f$ are evaluated, i.e., the vehicles $i \in \{i \in S_n | i > f\}$. Let $X_b(t)$ and $U_b(t)$ be a lumped error state vector and lumped desired acceleration vector, respectively, which are defined as

$$X_b^T(t) = [x_{f+1}^T(t),\ \cdots,\ x_n^T(t)]\,, \quad U_b(t) = [u_{f+1}(t),\ \cdots,\ u_n(t)]^T. \tag{5.8}$$

Thus $X_b(t) \in \mathbb{R}^{3g\times 1}$ and $U_b(t) \in \mathbb{R}^{g\times 1}$, where $g = n - f$, contain the states of all vehicles $i \in \{i \in S_n | i > f\}$. The dynamics of this subsystem of the platoon can be described by

$$\left[\frac{\dot{X}_b(t)}{\dot{U}_b(t)}\right] = \left[\begin{array}{c|c} I_g \otimes A - \hat{L}_b \otimes Bk^T & O_{3g\times g} \\ \hline \hat{L}_b \otimes \frac{k^T}{h} & \frac{1}{h}(I_{(-1),g} - I_g) \end{array}\right] \left[\frac{X_b(t)}{U_b(t)}\right] + \left[\frac{O_{3g\times 1}}{B_b}\right] u_f(t), \tag{5.9}$$

with $\hat{L}_b \in \mathbb{R}^{g\times g}$ being a sub-matrix of matrix $\hat{L}$ as defined in (5.5), i.e.,

$$\hat{L}_b = \begin{bmatrix} 1 & -1 & 0 & \cdots & 0 \\ 0 & 1 & -1 & \ddots & \vdots \\ \vdots & \ddots & \ddots & \ddots & 0 \\ \vdots & \ddots & \ddots & 1 & -1 \\ 0 & \cdots & \cdots & 0 & 1 \end{bmatrix}, \tag{5.10}$$

and where $B_b \in \mathbb{R}^{g\times 1}$ is defined as

$$B_b = \left[\frac{1}{h},\ 0,\ \cdots,\ 0\right]^T. \tag{5.11}$$

When vehicle $i = f$ is in saturation, it holds that $u_f(t) = 0$. In Chapter 4, it is already shown that the origin is an asymptotically stable equilibrium of a system having a structure as in (5.9), under the condition that the controller gain vector k is designed properly. Thus for the vehicles behind the saturated vehicle it still holds that

$$lim_{t\to\infty} x_i(t) = \begin{bmatrix} 0 \\ 0 \\ 0 \end{bmatrix} \quad \forall i \in \{i \in S_n | i > f\}\,. \tag{5.12}$$

Thus the inter-vehicle distance errors $e_i(t)$ of all vehicles behind vehicle $i = f$ converge to zero. Hence, for this particular topology, the stability properties of the interconnected vehicles $i \in \{i \in S_n | i > f\}$ are identical to those of a platoon without a saturated vehicle.

Second, an equilibrium analysis is executed to evaluate what happens for the inter-vehicle distance error states of the saturated vehicle $i = f$ and all vehicles in front of this vehicle, i.e., the vehicles $i \in \{i \in S_n | i \leq f\}$. In an equilibrium, all time-derivatives of a system are equal to zero. For the second time-derivative of $e_i(t)$, this equilibrium can be expressed as

$$\ddot{e}_i(t) = a_{i-1}(t) + \frac{h-\tau}{\tau} a_i(t) - \frac{h}{\tau} u_i(t) = 0 \quad \forall i \in \{i \in S_n | i \leq f\}\,. \tag{5.13}$$

As was stated above, the (desired) acceleration of vehicle $i = f$ is equal to zero when it is in saturation, i.e., $u_f(t) = 0$ and $a_f(t) = 0$. Also, it is assumed that there are no restrictions (or saturations) on

the vehicle acceleration $a_i(t)$ or on the desired acceleration $u_i(t)$. Therefore, equilibrium (5.13) is an equilibrium in the reachable subspace. By using this, and the known relation between the desired acceleration $u_i(t)$ and the actual acceleration $a_i(t)$ (2.11), it can be derived that the acceleration $a_i(t)$ and desired acceleration $u_i(t)$ are equal to zero for each vehicle $i \in \{i \in S_n | i \leq f\}$ when (5.13) holds. For the first time-derivative of $e_i(t)$, the equilibrium can be expressed as

$$\dot{e}_i(t) = v_{i-1}(t) - v_i(t) - ha_i(t) = 0 \quad \forall i \in \{i \in S_n | i \leq f\}. \tag{5.14}$$

As was mentioned above, vehicle acceleration $a_i(t)$ is equal to zero for each vehicle i when the platoon is in steady state. Employing this, the equilibrium in (5.14) results in

$$\begin{aligned} \dot{e}_1(t) &= v_0(t) - v_1(t) \;\; = 0 \\ \dot{e}_i(t) &= v_{i-1}(t) - v_i(t) = 0 \qquad \forall i \in \{i \in S_n | 1 < i < f\}. \\ \dot{e}_f(t) &= v_{f-1}(t) - v_f(t) = 0 \end{aligned} \tag{5.15}$$

It is assumed that the velocity of the virtual reference vehicle $v_0(t) \equiv v_{des}$ and the velocity of the f^{th} vehicle in saturation $v_f(t) = v_{max}$ satisfy (5.1), and therefore the equilibrium in (5.15) cannot be reached. As a result, the platoon dynamics do not have an equilibrium. The inter-vehicle distance error $e_i(t)$ keeps increasing for the vehicles $i \in \{i \in S_n | i \leq f\}$, even when the platoon is partially at steady state, i.e., acceleration is zero. Hence, ***Theorem 5.1*** is proven.

5.1.1 Simulation results

In this section, the platoon response for two different topologies is analysed, namely for *Topology 1* an *Topology 2*, with the presence of a saturated (or faulty) vehicle, as introduced above.
A platoon of size $n = 10$ vehicles, the longitudinal dynamics of which are modeled as in Section 2.3 (with actuator delay $\phi = 0$ s), is simulated. The desired standstill distance and time gap are $r = 2$ m and $h = 0.6$ s, respectively. First, the platoon response is shown where communication *Topology 2* in combination with the pinning constraint in (5.3) is used for the distributed controller. Given this, the control input applied to the vehicles in the platoon is as expressed in (5.4). The controller gain vector is designed to be $k^T = [0.1,\ 1.2,\ 0]$. These controller gains satisfy the conditions in ***Theorem 4.1***. The desired platoon velocity is set equal to $v_{des} = 25$ m/s. The virtual reference vehicle is uncontrolled, i.e., $u_0(t) = 0$, such that the velocity of the virtual reference vehicle is constant $v_0(t) = v_{des} = 25$ m/s. During the entire simulation, the fifth vehicle ($f = 5$) in the platoon has a maximum velocity $v_{max} = 24$ m/s. The platoon response is shown in Figure 5.1. At $t = 0$ s, all vehicles in the platoon have a velocity around 20 m/s and all vehicles have a slightly different nonzero initial acceleration. Also, one can observe that the initial inter-vehicle distance error $e_i(t)$ is non-zero for all vehicles.
It can be observed that, starting at $t = 0$ s, the velocity of the vehicles in the platoon increases. At $t \approx 7$ s, vehicle $i = 5$ reaches its maximum velocity $v_{max} = 24$ m/s and it stays at this maximum velocity. As a result, the velocity of all vehicles in the platoon do not converge to a common velocity, i.e., the platoon does not reach an equilibrium. It can be observed that, only the velocity of the vehicles behind the saturated vehicle converge to v_{max}, as was predicted in Section 5.1. Also, the inter-vehicle distance error $e_i(t)$ converges to zero for those vehicles. This corresponds to the origin being an asymptotically stable equilibrium for the vehicles behind vehicle $i = f$, as given in (5.12).
When observing the response of the inter-vehicle distance error $e_i(t)$, one can also see that the inter-vehicle distances $d_i(t)$ keep increasing in time for the vehicles in front of the saturated vehicle, i.e., $\dot{e}_i(t)$ is positive in steady state, which can be verified in Figure 5.1d. This is a result of the absence of an equilibrium in the reachable subspace, as mentioned above. However, in Figure 5.1c, it can be observed that the inter-vehicle distance errors $e_i(t)$ do converge to a common (increasing) value for all vehicles $i \in \{i \in S_n | i \leq f\}$. Thus the vehicles $i \in \{i \in S_n | i \leq f\}$ reach consensus on the inter-vehicle distance error $e_i(t)$, but due to the influence of the faulty vehicle, this consensus value is not zero for those vehicles.

Second, the simulation as described above is repeated, but now communication *Topology 1* in combination with the pinning constraint (4.51) is used for the distributed controller. The controller applied

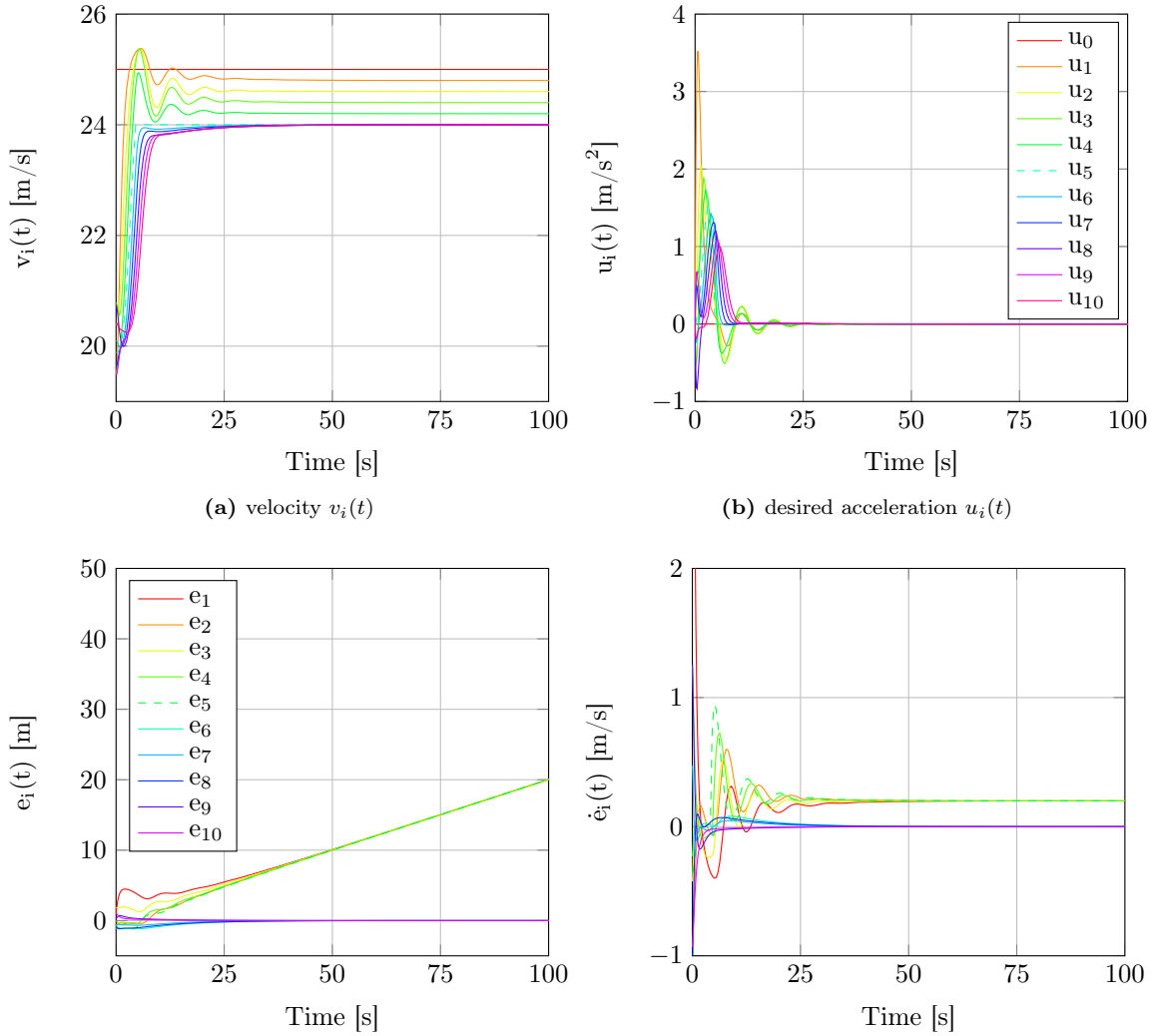

(a) velocity $v_i(t)$

(b) desired acceleration $u_i(t)$

(c) inter-vehicle distance error $e_i(t)$

(d) time-derivative of the inter-vehicle distance error $\dot{e}_i(t)$

Figure 5.1: The velocity $v_i(t)$, desired acceleration $u_i(t)$, inter-vehicle distance error $e_i(t)$ and its time-derivative $\dot{e}_i$ of each vehicle i versus time. The legend shown in the desired acceleration plot also applies to the velocity $v_i(t)$ and the legend shown for the inter-vehicle distance error $e_i(t)$ also applies to its time-derivative $\dot{e}_i(t)$. The communication topology is chosen as *Topology 2* in combination with the pinning constraint (4.55). Vehicle $i = 5$ (indicated with dashed line) goes in saturation at $t \approx 7$ seconds.

to the vehicles in the platoon is then defined as

$$\begin{cases} \dot{u}_1(t) = -\frac{1}{h}u_1(t) + \frac{1}{h}u_0(t) + \frac{1}{h}k^T(2x_1(t) - x_2(t)) \\ \dot{u}_i(t) = -\frac{1}{h}u_i(t) + \frac{1}{h}u_{i-1}(t) + \frac{1}{h}k^T(2x_i(t) - x_{i-1}(t) - x_{i+1}(t)) \;\; \forall i \in \{i \in S_n | 1 < i < n\} \\ \dot{u}_n(t) = -\frac{1}{h}u_n(t) + \frac{1}{h}u_{n-1}(t) + \frac{1}{h}k^T(x_n(t) - x_{n-1}(t)). \end{cases} \quad (5.16)$$

The platoon response, with this distributed controller applied to it, is shown in Figure 5.2. Again, starting from $t = 0$ s, the velocity of the vehicles in the platoon starts to increase. At $t \approx 7$ s, vehicle $i = 5$ reaches its maximum velocity v_{max}. It can be observed that, for all vehicles $i \in S_n$, the velocity

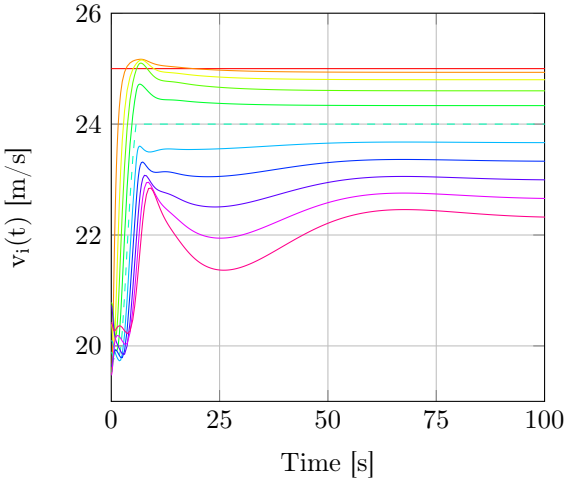

(a) velocity $v_i(t)$

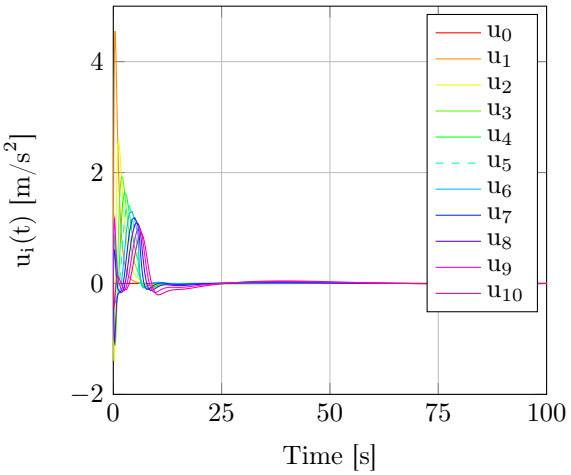

(b) desired acceleration $u_i(t)$

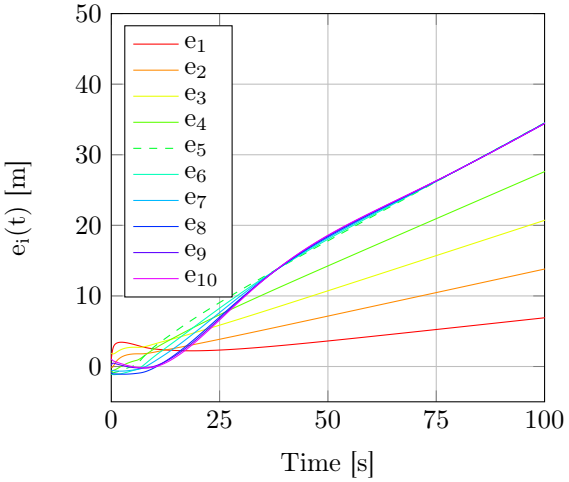

(c) inter-vehicle distance error $e_i(t)$

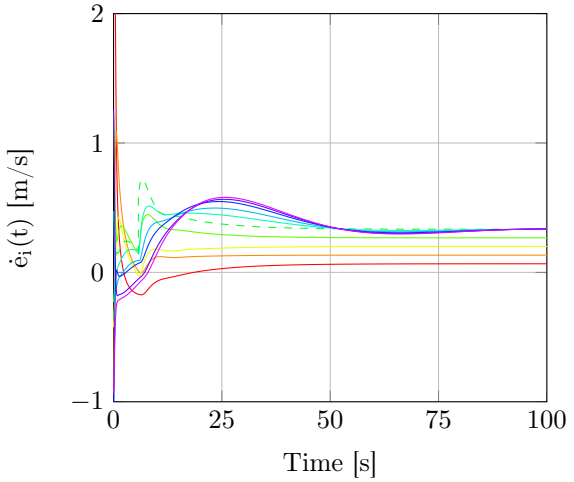

(d) time-derivative of the inter-vehicle distance error $\dot{e}_i(t)$

Figure 5.2: The velocity $v_i(t)$, desired acceleration $u_i(t)$, inter-vehicle distance error $e_i(t)$ and its time-derivative $\dot{e}_i(t)$ of each vehicle i versus time. The legend shown in the desired acceleration plot also applies to the velocity $v_i(t)$ and the legend shown for the inter-vehicle distance error $e_i(t)$ also applies to its time-derivative $\dot{e}_i(t)$. The communication topology is chosen as *Topology 1* in combination with the pinning constraint (4.51). Vehicle $i = 5$ (indicated with dashed line) goes in saturation at $t \approx 7$ seconds.

$v_i(t)$ converges to a different velocity. For the vehicles in front of the saturated (or faulty) vehicle, the velocity converges to an intermediate velocity, i.e., in between the desired velocity $v_{des} = 25$ m/s and the maximum velocity $v_{max} = 24$ m/s of vehicle $i = f$. For the vehicles behind the saturated vehicle, the steady-state velocity converges to a velocity lower than v_{max}.
As can be observed in Figure 5.2c, similar as for *Topology 2*, the inter-vehicle distance error $e_i(t)$ for the vehicles $i \in \{i \in S_n | i \leq f\}$ keeps increasing, such that the entire platoon does not end up in an equilibrium. Furthermore, it can be seen that, for *Topology 1*, even for the vehicles behind the saturated vehicle, i.e., the vehicles $i \in \{i \in S_n | i > f\}$, the inter-vehicle distance $d_i(t)$ increases.

Now, we aim to derive an additional control law for the dynamics of the virtual reference vehicle, which

is previously assumed to have a constant velocity, such that the inter-vehicle distance error $e_1(t)$ of the first vehicle goes to zero. As a result, the inter-vehicle distance errors of all vehicles $i \in S_n$ go to zero. This control law for the virtual reference vehicle has two objectives. On the one hand, it must aim to drive the platoon velocity to a desired velocity v_{des}. On the other hand, it should ensure that the platoon does not brake-up when there is a vehicle in the platoon having a maximum velocity v_{max} which is lower than the desired velocity v_{des}.
After analysing the platoon response for various topologies, it is found that *Topology 2*, in combination with pinning constraint (4.55), offers opportunities for the design of a control law for the input to the virtual reference vehicle $u_0(t)$, such that the platoon can automatically adapt its velocity to the slowest vehicle in the platoon, as will be explained below.

5.2 Closed-loop virtual reference vehicle

As was mentioned above, the aim for the design of a controller for the virtual reference vehicle is to prevent the platoon from breaking up, even when there is a f^{th} vehicle in the platoon which has a maximum velocity $v_{max} < v_{des}$, i.e., to guarantee that the platoon has an asymptotically stable equilibrium. The only input to the platoon is the desired acceleration of the virtual reference vehicle $u_0(t)$ and therefore a control law is designed for this input $u_0(t)$. To arrive at a stable equilibrium, the following control law is proposed for the virtual reference vehicle

$$\dot{u}_0(t) = -\frac{1}{h}u_0(t) + \frac{k_v}{h}(v_{des} - v_0(t)) - \frac{k_0^T}{h}x_1(t), \tag{5.17}$$

where $k_v > 0$ is the velocity control gain, $k_0^T = [k_p,\ k_d,\ 0]$ are proportional and derivative error controller gains, and $x_1(t)$ is the error state vector of vehicle $i = 1$. One can observe that again a low-pass filter is used having a pole at $-\frac{1}{h}$, to have some relaxation effect, such that the desired acceleration of the virtual reference vehicle changes less rapidly. The purpose of the velocity control term in (5.17) is to drive the velocity of the virtual reference vehicle $v_0(t)$ to the desired platoon velocity v_{des}. The error control term in (5.17) aims to drive the inter-vehicle distance error $e_1(t)$ to zero, since it has a negative contribution to the desired acceleration of the virtual reference vehicle.
Given the control law for the virtual reference vehicle in (5.17), the velocity of the virtual reference vehicle $v_0(t)$ is not fixed anymore, i.e., $v_0(t) \not\equiv v_{des}$. As a result, the equilibrium in (5.15) may be in the reachable subspace. According to (5.15), when vehicle $i = f$ is in saturation, in this equilibrium it should hold that

$$v_0(t) = v_{max}, \tag{5.18}$$

which is the case, as will become clear below.

As was mentioned above, the platoon dynamics, given a vehicle having a maximum velocity, can be divided into two modes which both must have an asymptotically stable equilibrium (or desired steady state). The first mode is when vehicle $i = f$ is not in saturation. This mode is named *Mode 1*. The second mode is when vehicle $i = f$ is in saturation, this mode is named *Mode 2*. For analytical derivation of stability of the equilibrium, it is assumed that when vehicle $i = f$ arrives at its maximum velocity, i.e., $v_f(t) = v_{max}$, the velocity of vehicle $i = f$ stays at this maximum velocity. By this, it is assumed that switching back and forth between the two modes does not occur. For this, it is required that v_{des} is separated away from v_{max}. Note that the analysis of stability, when allowing unlimited switching between the two modes, is beyond the scope of this master thesis.

5.3 Stability in *Mode 1*

In this section, asymptotic platoon stability, given control law (5.17) for the virtual reference vehicle, in *Mode 1* is assessed. An additional condition for asymptotic platoon stability is derived in Subsection 5.3.1. Also, the poles of the platoon dynamics are analysed, which is described in Subsection 5.3.2.

5.3.1 Steady state

Below a representation of the entire platoon dynamics is given. This representation is based on the platoon dynamics (4.33) and in addition the dynamics of the controlled virtual reference vehicle (4.4) is added.

$$\left[\begin{array}{c|c|c|c} \dot{X}(t) \\ \hline \dot{U}(t) \\ \hline \dot{u}_0(t) \\ \hline \dot{p}_0(t) \end{array}\right] = \left[\begin{array}{c|c|c|c} I_n \otimes A - \hat{L} \otimes Bk^T & O_{3n\times n} & O_{3n\times 1} & O_{3n\times 3} \\ \hline \hat{L} \otimes \frac{k^T}{h} & \frac{1}{h}(I_{(-1),n} - I_n) & B_u & O_{n\times 3} \\ \hline B_u^T \otimes -k_0^T & O_{1\times n} & -\frac{1}{h} & [0,\ -\frac{k_v}{h},\ 0] \\ \hline O_{3\times 3n} & O_{3\times n} & B & A \end{array}\right] \left[\begin{array}{c} X(t) \\ \hline U(t) \\ \hline u_0(t) \\ \hline p_0(t) \end{array}\right] + \cdots$$

$$\left[\begin{array}{c} O_{3n\times 1} \\ \hline O_{n\times 1} \\ \hline \frac{k_v}{h} \\ \hline O_{3\times 1} \end{array}\right] v_{des}, \tag{5.19}$$

with matrix A and vector B is as in (2.12), I_n being an $n \times n$ identity matrix, $I_{(-1),n}$ being an $n \times n$ matrix having ones on the first lower off-diagonal and zeros elsewhere, and where matrix $\hat{L} \in \mathbb{R}^{n\times n}$ is as in (5.5) and vector $B_u \in \mathbb{R}^{n\times 1}$ is as in (4.25).
As can be seen from the dynamical representation in (5.19), the closed-loop error dynamics, i.e., the $X(t)$-dynamics, is asymptotically stable under the conditions of ***Theorem 4.1***, thus

$$lim_{t\to\infty} X(t) = O_{3n\times 1}. \tag{5.20}$$

From the entire platoon dynamics (5.19), it can be seen that only the error state vector $X(t)$ acts as an input to the dynamics of the virtual reference vehicle, i.e., the dynamics regarding the state vector $p_0(t)$ and state $u_0(t)$. These dynamics are defined as follows

$$\left[\begin{array}{c} \dot{p}_0(t) \\ \dot{u}_0(t) \end{array}\right] = \left[\begin{array}{c} \dot{q}_0(t) \\ \hline \dot{v}_0(t) \\ \dot{a}_0(t) \\ \dot{u}_0(t) \end{array}\right] = \left[\begin{array}{c|ccc} 0 & 0 & 1 & 0 \\ \hline 0 & 0 & 0 & 1 \\ 0 & 0 & -\frac{1}{\tau} & \frac{1}{\tau} \\ 0 & -\frac{k_v}{h} & 0 & -\frac{1}{h} \end{array}\right] \left[\begin{array}{c} q_0(t) \\ \hline v_0(t) \\ a_0(t) \\ u_0(t) \end{array}\right] + \left[\begin{array}{c} 0 \\ \hline 0 \\ 0 \\ B_u^T \otimes -k_0^T \end{array}\right] X(t) + \left[\begin{array}{c} 0 \\ \hline 0 \\ 0 \\ \frac{k_v}{h} \end{array}\right] v_{des}, \tag{5.21}$$

where $p_0(t)$ and $u_0(t)$ are reordered to obtain a different structure. Since it is known that the origin is an asymptotically stable equilibrium of the dynamics of the lumped error state vector $X(t)$, asymptotic stability of the virtual reference vehicle dynamics can be assessed by evaluating the poles of the subsystem matrix. The steady state of this subsystem, i.e., dynamics of the virtual reference vehicle, is given by

$$lim_{t\to\infty} \begin{bmatrix} p_0(t) \\ u_0(t) \end{bmatrix} = \begin{bmatrix} \bar{q}_0(t) \\ v_{des} \\ 0 \\ 0 \end{bmatrix}, \tag{5.22}$$

where $\bar{q}_0(t)$ is the position of the virtual reference vehicle in steady state. What remains is to check under which conditions this steady state is asymptotically stable. One pole of the subsystem is equal to 0, which is associated with the position state $q_0(t)$. The stability of the steady-state solution can be assessed by evaluating the poles of the subsystem of (5.21) regarding the states $v_0(t)$, $a_0(t)$ and $u_0(t)$ The characteristic polynomial of the system matrix of this subsystem is defined as

$$\lambda^3 + \left(\frac{1}{\tau} + \frac{1}{h}\right)\lambda^2 + \frac{1}{h\tau}\lambda + \frac{k_v}{h\tau} = 0. \tag{5.23}$$

Using Routh-Hurwitz stability criterion (Hurwitz, 1964) it is determined that the subsystem has an asymptotically stable equilibrium under the condition that the velocity control gain satisfies the following condition

$$k_v < \left(\frac{1}{\tau} + \frac{1}{h}\right). \tag{5.24}$$

And as a result, the steady state in (5.22) is stable.
What remains is to check the stability of the subsystem of (5.19) regarding the control inputs in $U(t)$, i.e, the subsystem

$$\dot{U}(t) = \frac{1}{h}\left(I_{(-1),n} - I_n\right)U(t) + \hat{L} \otimes \frac{k^T}{h} X(t) + B_u u_0(t). \tag{5.25}$$

Again, it is known that all inputs of this subsystem converge to zero, i.e., $X(t)$ and $u_0(t)$ converge to zero. Furthermore, matrix $\frac{1}{h}\left(I_{(-1),n} - I_n\right)$ is a Hurwitz matrix having one eigenvalue

$$\lambda_1 = -\frac{1}{h}, \tag{5.26}$$

with algebraic multiplicity n. Using this result, it is known that the origin is an asymptotically stable equilibrium of the $U(t)$-dynamics, thus

$$lim_{t\to\infty} U(t) = O_{n\times 1}. \tag{5.27}$$

Thus when condition (4.36) of ***Theorem 4.1*** and condition (5.24) are satisfied, it is shown that the steady state of the entire platoon dynamics (5.19) is asymptotically stable in *Mode 1*, regardless of the platoon length n. Note that this is called a steady state and not an equilibrium since the state $q_0(t)$ is not constant in this steady state of the platoon dynamics.

5.3.2 Analysis of closed-loop poles depending on platoon length

Let the poles of the entire platoon dynamics in (5.19), with matrix $\hat{L}$ being defined as in (5.5), be stacked in the vector $\sigma = [\sigma_i] \in \mathbb{R}^{4(n+1)\times 1}$. Figure 5.3 shows the closed-loop poles of the entire platoon dynamics (5.19) for different platoon lengths, namely $n = 4$, $n = 9$ and $n = 12$ vehicles. As expected, it can be observed that, for all three different platoon lengths, all poles lie in the closed left half-plane. It can be seen that for all three platoon lengths, only one pole lies exactly on the imaginary axis. This is the pole at zero, which is associated with position state $q_0(t)$ of the virtual reference vehicle. Also, three other fixed poles, i.e., not shifting when changing the platoon length, regarding the dynamics of the virtual reference vehicle can be observed, namely $\{-10.02,\ -1.54,\ -0.11\} \in \sigma$. These four poles, regarding the dynamics of the virtual reference vehicle, are equal to the eigenvalues of the system matrix in (5.21). Furthermore, n fixed poles at $-\frac{1}{h} = -1.67$ can be observed in the pole plot. These poles are related to the controller dynamics $u_i(t)\ \forall i \in S_n$. The aforementioned poles of the entire platoon dynamics (5.19) are all fixed and do not shift with changing platoon length. However, there are $3n$ poles which are influenced by the platoon length. For a platoon of length $n = 4$ vehicles, by approximation, the poles $\{-8.90,\ -0.83,\ -0.27\} \in \sigma$ can be observed, all having a multiplicity of $n = 4$. By approximation it is meant that the poles actually do have an imaginary part, but this is negligible. Those three poles are (by approximation) equal to the eigenvalues of the matrix in (4.35), with $\lambda_i = 1\ \forall i \in S_n$, which are the eigenvalues of matrix $\hat{L}$ in (5.5).
When increasing the platoon length, it can be seen that also pairs of complex conjugate poles start to appear, i.e., the imaginary part increases and the poles shift from the real axis into the complex plane. Note that when the platoon length increases, the number of poles of the entire platoon dynamics also increases. As a result of an increasing number of poles having an increasing imaginary part magnitude, oscillations during transient behavior will also amplify by a platoon length increase. For large platoon lengths n, this could lead to large oscillations in the platoon.
This is a drawback which does not appear in a conventional one-vehicle look ahead CACC approach. In the conventional CACC approach, the poles do not shift at all by changing the platoon length n, which is logical since each vehicle only depends on its predecessor. Thus the interaction between each pair of predecessor-follower vehicle is the same.

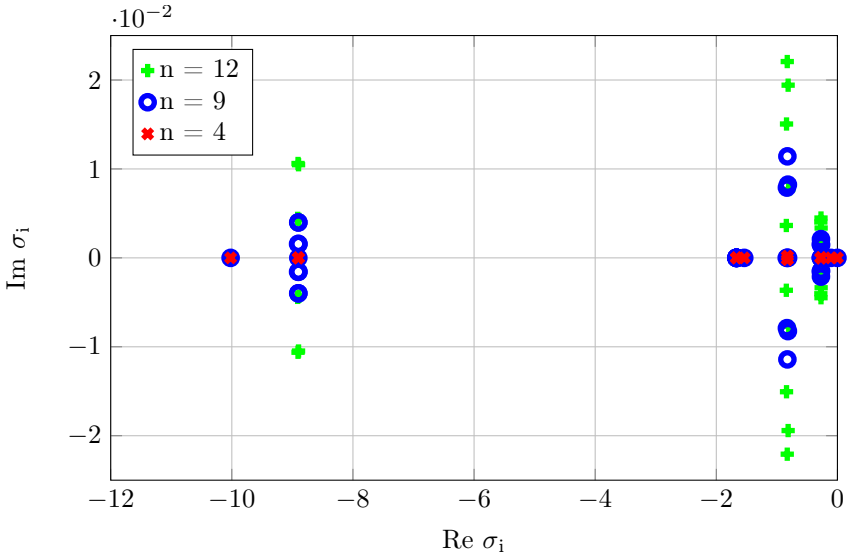

Figure 5.3: The poles of platoon dynamics (5.19), with matrix $\hat{L}$ being defined as in (5.5), for three different platoon lengths, namely $n = 4$, $n = 9$, and $n = 12$ vehicles. The controller gain vector is designed to be $k^T = [0.2,\ 1.0,\ 0]$, $k_v = 0.1$ and $k_0^T = [0.05,\ 1.0,\ 0]$. The desired time gap $h = 0.6$ s.

5.4 Stability in *Mode 2*

In this section, first, the steady state of the platoon dynamics in *Mode 2* is evaluated in Subsection 5.4.1. Hereafter, in Subsection 5.4.2, asymptotic stability of this steady state is assessed using a pole analysis.

5.4.1 Steady state

In *Mode 2*, the velocity of vehicle $i = f$ is constant, i.e., $v_f(t) = v_{max}$. As was shown in Section 5.1, for *Topology 2*, the origin is an asymptotically stable equilibrium of the dynamics (5.9) of all $n - f$ vehicles behind vehicle $i = f$. Thus, for assessment of stability, it can be assumed that vehicle $i = f$ is the last vehicle in a platoon, i.e. $f = n$. Below the dynamics of such platoon is evaluated.

In *Mode 2* the velocity $v_f(t)$ is constant, thus the acceleration and desired acceleration of vehicle $i = f$ satisfy: $a_f(t) = 0$, $u_f(t) = 0$ and $\dot{u}_f(t) = 0$.
Since the velocity of the f^{th} vehicle is now fixed, it can be seen as a constant input to the entire platoon. In the previous section, the platoon dynamics was represented by error state vectors $x_i(t) = [e_i(t),\ \dot{e}_i(t),\ \ddot{e}_i(t)]^T\ \forall i \in S_n$, controller state $u_i(t)\ \forall i \in S_n$, and the states of the virtual reference vehicle $p_0(t)$ and $u_0(t)$. However, to be able to write the velocity v_{max} of vehicle $i = f$ as a fixed input to the platoon, the entire platoon dynamics must be represented in a different way. In this new representation of the platoon dynamics, the vehicles' states are defined to be the inter-vehicle distance error $e_i(t)$, the vehicle velocity $v_i(t)$ and acceleration $a_i(t)$, instead of the error states $e_i(t)$, $\dot{e}_i(t)$ and $\ddot{e}_i(t)$. Given this state definition, the dynamics of a single (uncontrolled) vehicle i is defined as follows

$$\dot{\chi}_i(t) = A_1\chi_i(t) + A_2\chi_{i-1}(t) + Bu_i(t) \quad \forall i \in S_n, \tag{5.28}$$

where

$$\chi_i(t) = \begin{bmatrix} e_i(t) \\ v_i(t) \\ a_i(t) \end{bmatrix}, A_1 = \begin{bmatrix} 0 & -1 & -h \\ 0 & 0 & 1 \\ 0 & 0 & -\frac{1}{\tau} \end{bmatrix}, A_2 = \begin{bmatrix} 0 & 1 & 0 \\ 0 & 0 & 0 \\ 0 & 0 & 0 \end{bmatrix}, B = \begin{bmatrix} 0 \\ 0 \\ \frac{1}{\tau} \end{bmatrix} \tag{5.29}$$

and $u_i(t)$ is the desired acceleration of vehicle i. Again the states of the vehicles in the platoon can be stacked in a lumped state vector. Let $\chi(t)$ and $U(t)$ be the lumped state vectors being defined as

$$\chi^T(t) = [\chi_1^T(t),\ \cdots,\ \chi_f^T(t)], \quad U(t) = [u_1(t),\ \cdots,\ u_f(t)]^T. \tag{5.30}$$

Now let the platoon dynamics in (5.19) be expressed by

$$\dot{\xi}_1(t) = A_H \xi_1(t) + B_H v_{des}(t), \tag{5.31}$$

where state vector $\xi_1(t)$ is thus defined as

$$\xi_1(t) = [X(t),\ U(t),\ u_0(t),\ p_0(t)]^T, \tag{5.32}$$

and matrix A_H and vector B_H are defined as in (5.19). Let a second state vector $\xi_2(t)$ being defined as

$$\xi_2(t) = [\chi(t),\ U(t),\ u_0(t),\ p_0(t)]^T. \tag{5.33}$$

Since the platoon dynamics (5.19) represent a linear time-invariant system, it is known that there exists a similarity transformation matrix T_f, such that

$$\xi_2(t) = T_f \xi_1(t). \tag{5.34}$$

This similarity transformation matrix T_f can be found in (B.15) in Appendix B (for $f = 3$). Applying this similarity transformation to (5.31) results in

$$\dot{\xi}_2(t) = T_f A_H T_f^{-1} \xi_2(t) + T_f B_H v_{des}(t). \tag{5.35}$$

As was mentioned above, it is known that the acceleration $a_f(t)$ and desired acceleration velocity $u_f(t)$ of vehicle $i = f$ are both equal to zero. Furthermore, it is known that the velocity $v_f(t) = v_{max}$ is constant, and as a result, the inter-vehicle distance error dynamics of vehicle $i = f$ is given by

$$\dot{e}_f(t) = v_{f-1}(t) - v_{max}. \tag{5.36}$$

The states $v_f(t)$, $a_f(t)$ and $u_f(t)$ are removed from the state space in (5.35), such that the state vector of the platoon dynamics is defined as

$$\xi_3(t) = [\chi_1^T(t),\ \cdots,\ \chi_{f-1}^T(t),\ e_f(t),\ U_r^T(t),\ u_0(t),\ p_0^T(t)]^T, \tag{5.37}$$

where $U_r(t) = [u_1(t),\ \cdots,\ u_{f-1}(t)]^T$. Thus the order of the entire platoon dynamics (5.35) is reduced with order three. Given this, the platoon dynamics can be represented by

$$\dot{\xi}_3(t) = A_R \xi_3(t) + B_{R,1} v_{max} + B_{R,2} v_{des}(t), \tag{5.38}$$

where system matrix A_R, vector $B_{R,1}$ and vector $B_{R,2}$ have a complex structure. And, therefore, are not given here, but can be found in Appendix B. As can be seen in (5.38), the maximum velocity v_{max} and the desired platoon velocity $v_{des}(t)$ are now both written as external inputs to the platoon.

By setting all the time-derivatives equal to zero (except for $\dot{q}_0(t)$), it can be found that the steady state of the dynamics in (5.38) is given by

$$\bar{\xi}_3 = \begin{bmatrix} Q_3 \otimes [\frac{k_v}{k_p}(v_{des} - v_{max}),\ v_{max},\ 0]^T \\ \frac{k_v}{k_p}(v_{des} - v_{max}) \\ O_{(f-1)\times 1} \\ 0 \\ [\bar{q}_0(t),\ v_{max},\ 0]^T \end{bmatrix}, \tag{5.39}$$

with vector $Q_3 \in \mathbb{R}^{(f-1)\times 1}$ being defined as

$$Q_3 = [1, \ \cdots \ , \ 1]^T, \tag{5.40}$$

and where $\bar{q}_0(t)$ is the position of the virtual reference vehicle in steady state. Now suppose that the steady-state solution in (5.39) is asymptotically stable. Whether the solution is indeed asymptotically stable will be treated below. From the steady-state solution in (5.39), it can be seen that all vehicles in the platoon have adapted their velocity to the maximum velocity v_{max} of vehicle $i = f$ and all inter-vehicle distance errors have a steady-state offset being defined as

$$\bar{e}_i = lim_{t\to\infty} e_i(t) = \frac{k_v}{k_p}(v_{des} - v_{max}) \quad \forall i \in \{i \in S_n | i \leq f\}. \tag{5.41}$$

As was given in (5.12), if the length of the platoon n is larger than the index of the saturated vehicle $i = f$, i.e., $n > f$, the steady-state error is zero for the vehicles $i \in \{i \in S_n | i > f\}$.
Note that this steady-state solution implies that the inter-vehicle distance error $e_i(t)$ is not zero for all vehicles in the platoon, but has a positive offset for some vehicles. This means that in *Mode 2* the platoon performance in terms of traffic throughput is a little less, but since this steady-state offset is positive, it does not compromise on safety.

The inter-vehicle distance errors $e_i(t)$ in steady state thus depend on the difference between the desired velocity and maximum velocity of the saturated vehicle $(v_{des} - v_{max})$ and the value of the control gains k_v and k_p. Thus it can be concluded that the ratio k_v/k_p should be small to reduce the inter-vehicle distance error in steady state.
When the desired velocity of the leading vehicle is much higher than the maximum velocity of the slowest vehicle $i = f$ in the platoon, i.e., $v_{des} \gg v_{max}$, this can lead to large steady-state inter-vehicle distance errors $\bar{e}_i$. However, this is scalable by the ratio k_v/k_p.

Next, asymptotic stability of this steady state is evaluated. Due to the complex structure of the dynamics in (5.38), the system matrix A_R cannot be broken into smaller subsystems to evaluate asymptotic stability, as was the case for the lumped error state vector $X(t)$ in the dynamics in (5.19). Therefore, asymptotic stability of the steady state of the platoon dynamics (5.38) can only be assessed by evaluation of the poles of the system matrix A_R.

5.4.2 Analysis of closed-loop poles depending on platoon length

Suppose that the poles of the entire platoon dynamics in (5.38) are stacked in a vector $\sigma = [\sigma_i] \in \mathbb{R}^{(4(f-1)+5)\times 1}$. The poles σ are shown in Figure 5.4, again for different platoon lengths, namely $n = f \in \{4, 9, 12\}$ vehicles. The first notion regarding the eigenvalues is the fact that now only one pole is fixed and thus does not change with changing platoon length, compared to $n + 4$ fixed poles for the dynamics in *Mode 1*, which where shown in Figure 5.3.
This one pole is the pole at zero, associated with the position $q_0(t)$ of the virtual reference vehicle. All other poles of the dynamics (5.38) change (or shift) as a result of a change in the platoon length $n = f$. The entire eigenvalue plot, shown in Figure 5.4a, shows two circles on which conjugate pairs of eigenvalues are positioned. For increasing platoon length, more complex conjugate pairs of eigenvalues appear on these circles. As a result, for an increased platoon length n, at some point, eigenvalues appear on the right hand-side of the imaginary axis. This can be observed in Figure 5.4b, which shows an enlargement of the dashed region of the entire eigenvalue plot in Figure 5.4a. For the platoon lengths $n = 9$ and $n = 12$, it can be seen that a complex conjugate pair appears in the right half-plane. It is found that, for these particular controller gains for k, k_v and k_0^T, the platoon dynamics (5.38) contains unstable modes for a platoon length $n = f > 7$. Of course, the threshold for platoon length n, resulting in an unstable platoon, can be larger when the controller gains are designed differently. For example, decreasing the proportional control gain k_p results in this threshold to increase. However, decreasing the proportional control gain k_p results in a larger steady-state error, as was shown in (5.41). Therefore, increasing the damping control gain k_d is a more convenient solution, since this

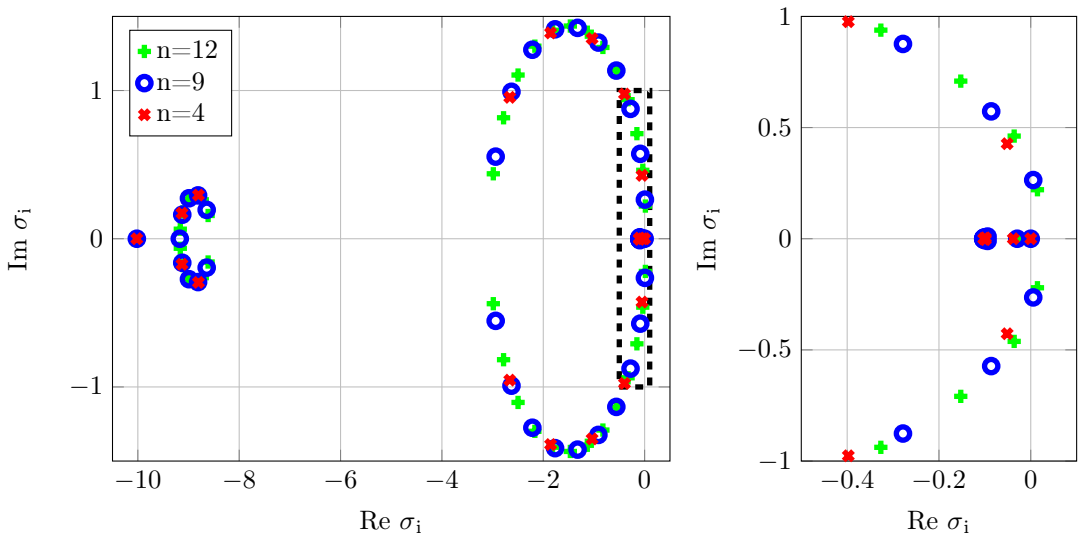

(a) all eigenvalues

(b) zoomed dashed box of eigenvalue plot

Figure 5.4: The poles of platoon dynamics (5.38), with matrix $\hat{L}$ being defined as in (5.5), for three different platoon lengths, namely $n = 4$, $n = 9$, and $n = 12$ vehicles. The controller gain vector is designed to be $k^T = [0.2,\ 1.0,\ 0]$, $k_v = 0.1$ and $k_0^T = [0.05,\ 1.0,\ 0]$. The desired time gap $h = 0.6$ s.

also leads to this threshold for the platoon length to increase and does not influence the steady-state offset, as was shown in (5.41).

Apparently, the introduction of a vehicle having a certain maximum velocity v_{max} has a major influence on the closed-loop stability of the entire platoon dynamics. In *Mode 1*, when vehicle f is not in saturation, asymptotic stability of the platoon is not influenced by the (finite) platoon length $n = f$. But in *Mode 2*, when vehicle f is in saturation, asymptotic stability of the platoon dynamics depends in the platoon length $n = f$.

5.5 Simulation results

A simulation is executed to verify the results as derived above. A platoon consisting of $n = 10$ vehicles, modeled as in Section 2.3, with actuator delay $\phi = 0$ s, is simulated. The desired standstill distance and time gap are $r = 2$ m and $h = 0.6$ s, respectively. The distributed controller applied to the vehicles in the platoon uses *Topology 2* and is thus defined as in (5.4), with controller gain vector $k^T = [0.2,\ 1.0,\ 0]$. The controller applied to the virtual reference vehicle is as in (5.17), with $k_v = 0.05$, $k_0^T = [0.08,\ 0.4,\ 0]$ and the desired platoon velocity is constant and equal to $v_{des} = 22$ m/s.
Initially, at $t = 0$ s, vehicle $i = f = 5$ in the platoon has a maximum velocity $v_{max} = 20$ m/s. At $t = 100$ s, this saturation on the velocity of the fifth vehicle is removed such that its dynamics are similar to the dynamics of all other unconstrained vehicles for $t > 100$ s.

The platoon response can be observed in Figure 5.5. The platoon is subjected to an initial conditions perturbation. At $t = 0$ s, all vehicles in the platoon have a velocity around 17 m/s and all vehicles have a slightly different nonzero initial acceleration. Also, one can observe that the initial inter-vehicle distance error $e_i(0)$ is non-zero for all vehicles i.
As can be observed from the platoon response, first the platoon starts to accelerate as a result of the

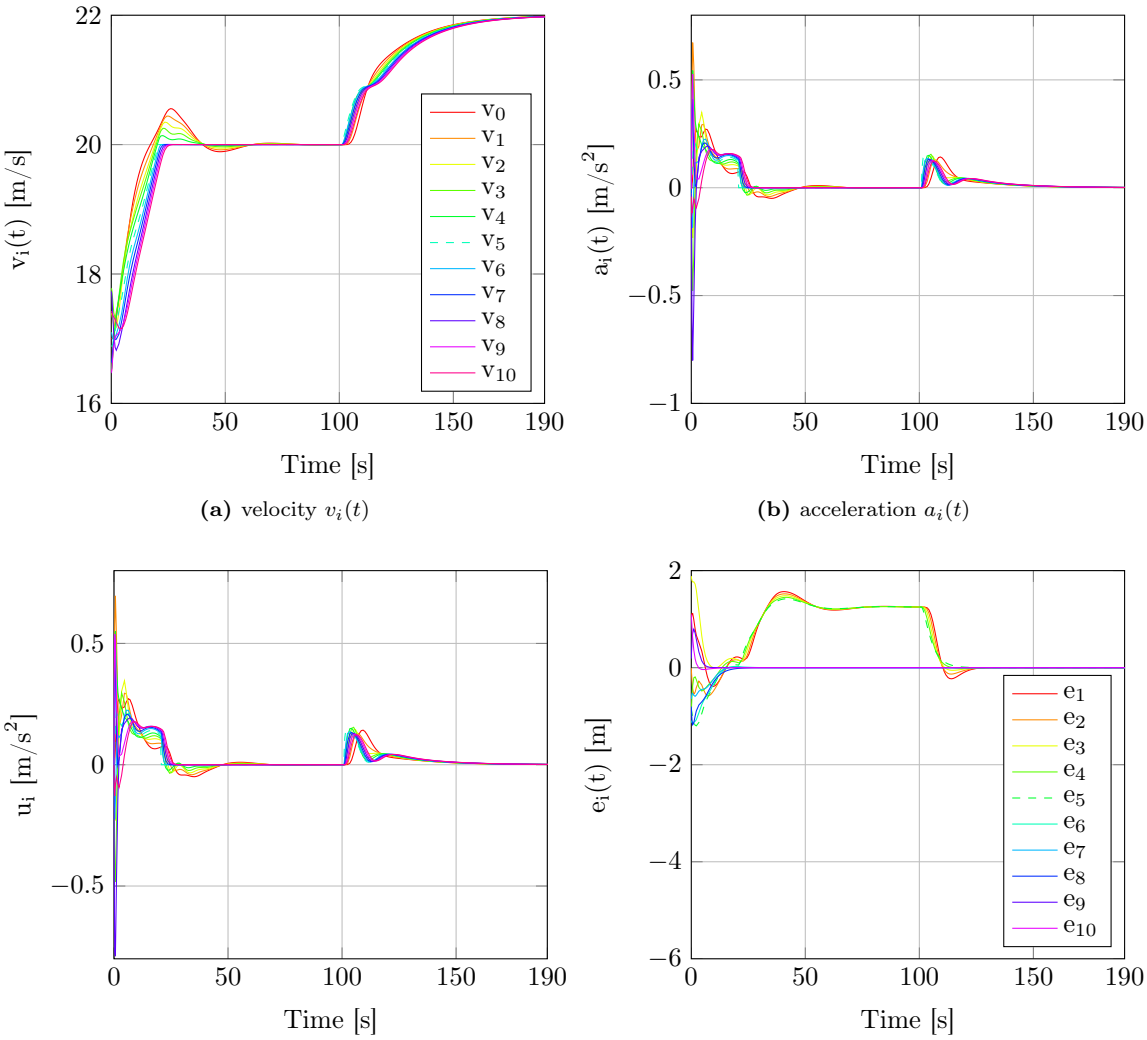

(a) velocity $v_i(t)$

(b) acceleration $a_i(t)$

(c) desired acceleration $u_i(t)$

(d) inter-vehicle distance error $e_i(t)$

Figure 5.5: The velocity $v_i(t)$, acceleration $a_i(t)$, desired acceleration $u_i(t)$ and inter-vehicle longitudinal distance error $e_i(t)$ of each vehicle i versus time. The legend shown in the velocity plot also applies for the acceleration $a_i(t)$ and desired acceleration $u_i(t)$. The response regarding vehicle $i = f = 5$ is indicated by a dashed line.

desired velocity imposed by the virtual reference vehicle being $v_{des} = 22$ m/s. It can be seen that the inter-vehicle distance error $e_i(t)$ tends to go to zero during this acceleration phase. Then, at $t \approx 20$ s, vehicle $i = 5$ reaches its maximum velocity v_{max}, i.e., the platoon dynamics switches from *Mode 1* to *Mode 2*. The velocities of all vehicles behind the fifth vehicle, i.e., vehicles $i \in \{i \in S_n | i > f\}$, converge to this maximum velocity v_{max} and also the inter-vehicle distance errors $e_i(t)$ quickly converge to zero for these vehicles. For the vehicles in front of the fifth vehicle, i.e., vehicles $i \in \{i \in S_n | i < f\}$, some overshoot is visible for the velocity. This can be understood as follows. The virtual reference vehicle first tries to drive the platoon velocity to the desired velocity. Due to an increase in the inter-vehicle distance $e_1(t)$ of the first vehicle, after some seconds, the virtual reference vehicle decelerates until its velocity converges to the maximum velocity of the fifth vehicle v_{max}. At $t \approx 60$ s, the entire platoon is cruising at this maximum velocity v_{max}. Furthermore, for the inter-vehicle distance errors $e_i(t)$ of the vehicles in front of the fifth vehicle, it can be seen that these converge to $\bar{e}_i = 1.25$ m. This steady-state

value corresponds to the analytically derived equilibrium given in (5.41). At $t = 100$ s, the saturation constraint is removed from vehicle $i = f = 5$, i.e., the platoon dynamics switches from *Mode 2* to *Mode 1* and the entire platoon starts to speed up to the desired velocity $v_{des} = 22$ m/s. Furthermore, it can be observed that the inter-vehicle distance errors $e_i(t)$ also rapidly converge to zero after $t = 100$ s.

5.6 Steady state for *Topology 1*

Above, a steady-state analysis is described for the distributed consensus control approach by use of *Topology 2* for the distributed controller. For *Topology 2*, it is shown that when the velocity of a vehicle $i = f$ saturates, the steady state of the platoon is defined by (5.12) for vehicles $i \in \{i \in S_n | i > f\}$ and (5.39) for vehicles $i \in \{i \in S_n | i \leq f\}$. Thus only the vehicles in front of the saturated vehicle will have a positive steady-state error, whereas the vehicles behind the saturated vehicle will have a steady-state error equal to zero.
In this section, a similar steady-state analysis is described, but for communication *Topology 1* with, in addition, the pinning constraint applied to the last vehicle. An elaborate pole analysis as described above for *Topology 2* is not described here, but it is analysed which parameters influence stability of the platoon dynamics. *Topology 1* is described by the Laplacian matrix L_1 in (4.47), such that the neighbouring sets for the distributed controller are defined as

$$\mathcal{N}_1 = \{2\}\,, \quad \mathcal{N}_i = \{i-1, i+1\}\ \forall i \in \{i \in S_n | 1 < i < n\} \quad \text{and} \quad \mathcal{N}_n = \{n-1\}\,. \tag{5.42}$$

Now the last vehicle is subjected to the pinning constraint, i.e., the pinning constraint is defined as

$$\begin{cases} p_{ii} = 0 & \forall i \in \{i \in S_n | i \neq n\} \\ p_{nn} = 1. \end{cases} \tag{5.43}$$

Given this, the platoon dynamics are described by (5.19) with matrix $\hat{L} = L_1 + P$ being defined as

$$\hat{L} = \begin{bmatrix} 1 & -1 & 0 & \dots & 0 \\ -1 & 2 & -1 & \ddots & \vdots \\ 0 & \ddots & \ddots & \ddots & 0 \\ \vdots & \ddots & -1 & 2 & -1 \\ 0 & \dots & 0 & -1 & 2 \end{bmatrix}. \tag{5.44}$$

Again suppose that there is a vehicle $i = f$, having a maximum velocity v_{max}, but this is not necessarily the last vehicle, i.e., $i = f$ is not per se equal to the platoon length n. The platoon must again have a asymptotically stable steady state in *Mode 1* and in *Mode 2*. Asymptotic stability in *Mode 1* is ensured when the conditions (4.36) in ***Theorem 4.1*** and condition (5.24) for the virtual reference vehicle are satisfied. Next, stability of the steady state in *Mode 2* is analysed.

Let $U_{n-1}(t)$ be a vector, containing the desired acceleration $u_i(t)\ \forall i \in S_n$, except for $u_f(t)$, being defined as

$$U_{n-1}(t) = [u_1(t),\ \cdots,\ u_{f-1}(t),\ u_{f+1}(t),\ \cdots,\ u_n(t)]^T. \tag{5.45}$$

For now, again suppose that the dynamics has an asymptotically stable steady-state solution. This will be evaluated below. For this topology, this steady state in *Mode 2*, which is the mode when vehicle

$i = f$ in in saturation, is defined as

$$lim_{t\to\infty}\left[\begin{array}{c}\chi_1(t)\\ \vdots\\ \chi_{f-1}(t)\\ \hline e_f(t)\\ \hline \chi_i(t)\\ \hline U_{n-1}(t)\\ \hline u_0(t)\\ \hline p_0(t)\end{array}\right] = \left[\begin{array}{c} Q_3 \otimes [\frac{k_v}{k_p}(v_{des}-v_{max}),\ v_{max},\ 0]^T \\ \hline \frac{k_v}{k_p}(v_{des}-v_{max}) \\ \hline \left[\left(\frac{n+1-i}{n+1-f}\right)\frac{k_v}{k_p}(v_{des}-v_{max}),\ v_{max},\ 0\right]^T \\ \hline O_{(n-1)\times 1} \\ \hline 0 \\ \hline [\bar{q}_0(t),\ v_{max},\ 0]^T \end{array}\right] \forall i \in \{i \in S_n | f < i \leq n\},$$

(5.46)

where vector $Q_3 \in \mathbb{R}^{(f-1)\times 1}$ is defined as in (5.40). It can be seen, that all vehicles have a velocity equal to v_{max} in steady state. Furthermore, it can be observed that for the vehicles in front of the vehicle $i = f$, the steady state is same as for *Topology 2*, which was shown in (5.41). The vehicles behind vehicle $i = f$, however, have a different steady-state solution in comparison with *Topology 2*. It was shown that, the inter-vehicle distance errors $e_i(t)$ where equal to zero for those vehicles, when using communication *Topology 2*. For *Topology 1* with the pinning constraint on the last vehicle, as treated in this section, the steady-state offset for the inter-vehicle distance error for these vehicles is defined as

$$\bar{e}_i = lim_{t\to\infty} e_i(t) = \left(\frac{n+1-i}{n+1-f}\right)\frac{k_v}{k_p}(v_{des}-v_{max}), \quad \forall i \in \{i \in S_n | f < i \leq n\}. \tag{5.47}$$

From this expression, it can be seen that this steady-state offset is a fraction

$$\left(\frac{n+1-i}{n+1-f}\right) \quad (<1), \quad \forall i \in \{i \in S_n | f < i \leq n\} \tag{5.48}$$

of the steady-state offset for the vehicles in front of vehicle $i = f$. Thus it is known that the steady-state offset for the vehicles $i \in \{i \in S_n | f < i \leq n\}$ is always smaller than the steady-state offset for the vehicles $i \in \{i \in S_n | i < f\}$, which was given in (5.41). Similar as for *Topology 2*, stability of the steady state depends on the position of the saturated vehicle in the platoon. There exists a threshold index f_{max}, such that, if $f > f_{max}$, the platoon dynamics becomes unstable. The value for this threshold again depends on the designed controller gains. It is found that, stability does not depend on the platoon length n, but only on the index of the saturated vehicle $i = f$. Thus the amount of vehicles in between the virtual reference vehicle $i = 0$ and the saturated vehicle $i = f$, together with the designed controller gain vector k, determines platoon stability in *Mode 2*.

5.7 Summary

To summarize, a vehicle (temporarily) having a lower maximum velocity v_{max} is introduced. The platoon dynamics, given this maximum velocity, are analysed analytically and by using time simulations. It is observed that, both communication *Topology 1* and *Topology 2* seem to offer opportunities to be able to automatically adapt the platoon velocity to a (temporary) slower vehicle. In communication *Topology 1*, the error state vector of the preceding and following vehicle is used in the controller. In communication *Topology 2*, the error state vector of only the following vehicle is used in the controller. An additional control law, applied to the virtual reference vehicle, is designed and additional conditions for stability are derived.
During operation, two modes can be distinguished. *Mode 1* is the normal operation mode and *Mode 2* is the mode where vehicle $i = f$ is in saturation. Given the additional control law for the virtual reference vehicle, the platoon dynamics in *Mode 1* is asymptotically stable regardless of the position

of the saturated (or faulty) vehicle in the platoon. However, in *Mode 2*, the position of the saturated vehicle in the platoon affects asymptotic stability of the closed-loop platoon dynamics. For a fixed designed controller, there is a limit f_{max} on the allowable index position of the saturated vehicle in the platoon.

When comparing the steady state in *Mode 2* for *Topology 1* and *Topology 2*, both with the pinning constraint on the last vehicle $i = n$, it seems that the steady state of *Topology 2* is more desirable, since the inter-vehicle distance error $e_i(t)$ equals zero in steady state for all vehicles behind vehicle $i = f$, i.e., the vehicles $i \in \{i \in S_n | i > f\}$. In contrast, for *Topology 1* this steady-state error is nonzero, namely a fraction of the steady-state offset of the vehicle in front of vehicle $i = f$, as in (5.47). However, when the value of this steady-state offset for the vehicles in front of vehicle $i = f$ is within an allowable margin, it is known that the steady-state offset for the vehicles behind vehicle $i = f$ will also be within this allowable margin. In addition, *Topology 1* seems to offer better behavior in terms of string stability, but this will be treated in detail in Chapter 6.

Chapter 6

String Stability

As was mentioned before, another desired property in vehicle platooning is string stability. In addition to the normal (asymptotic) stability property of interconnected systems, string stability can be interpreted as a performance criterion regarding disturbance attenuation in a string of interconnected systems. There are various definitions of string stability in literature, however in this analysis the definition of Ploeg et al. (2014a) is considered.
In this chapter, first a definition of string stability is given in Section 6.1. In Section 6.2, string stability of a platoon controlled using the distributed consensus framework as described in the previous chapters is assessed.

6.1 Definition of string stability

Suppose that the entire closed-loop dynamics of interconnected systems, i.e., a platoon of vehicles, is given by

$$\begin{aligned} \dot{\rho}(t) &= \mathcal{A}\rho(t) + \mathcal{B}\nu(t) \\ \eta_i(t) &= \mathcal{C}_i\rho(t) \qquad \forall i \in S_n, \end{aligned} \tag{6.1}$$

with $\rho(t) \in \mathbb{R}^a$ containing all the states of the interconnected systems, $\nu(t) \in \mathbb{R}^b$ being the external input and $\eta_i(t) \in \mathbb{R}$ being an output corresponding to states of vehicle i with output vector $\mathcal{C}_i$ defined accordingly. The model in (6.1) can be seen as a general form of the closed-loop platoon dynamics in (5.19) with $a = 4(n+1)$ and $b = 1$, but extended with an output function $\eta_i(t)$.
The following is a definition for so-called $\mathcal{L}_2$ *string stability* of an interconnected string of systems.

Definition 6.1 ($\mathcal{L}_2$ string stability) (Ploeg et al., 2014a): *The system in (6.1), with a constant equilibrium solution $\bar{\rho}$ for $\nu(t) \equiv 0$ without loss of generality, is $\mathcal{L}_2$ string stable if there exist class $\mathcal{K}$ functions [1] α and β, such that, for any initial state $\rho(0) \in \mathbb{R}^b$ and any $\nu(t) \in \mathcal{L}_2$, it holds that*

$$||\eta_i(t) - \mathcal{C}_i\bar{\rho}||_{\mathcal{L}_2} \leq \alpha(||\nu(t)||_{\mathcal{L}_2}) + \beta(||\rho(0) - \bar{\rho}||) \quad \forall i \in S_n \text{ and } n \in \mathbb{N}. \tag{6.2}$$

If, in addition to (6.2), with $\rho(0) = \bar{\rho}$ it also holds that

$$||\eta_i(t) - \mathcal{C}_i\bar{\rho}||_{\mathcal{L}_2} \leq ||\nu(t)||_{\mathcal{L}_2} \quad \forall i \in S_n \text{ and } n \in \mathbb{N} \tag{6.3}$$

the system (6.1) is *semi-strictly $\mathcal{L}_2$ string stable* with respect to its input $\nu(t)$.

[1] A continuous function $\alpha : [0,a) \to [0,\infty)$ is said to belong to class $\mathcal{K}$ if it is strictly increasing and $\alpha(0) = 0$.

Note that $||\cdot||$ denotes any vector norm and $||\cdot||_{\mathcal{L}_2}$ denotes the signal 2-norm (Zhou et al., 1996).

Remark: *Note that this definition of semi-strict $\mathcal{L}_2$ string stability is slightly different then the definition of semi-strict $\mathcal{L}_2$ string stability as is given Ploeg et al. (2014a). The definition is altered to be able to assess semi-strict $\mathcal{L}_2$ string stability for the bidirectionally coupled platoon, as described above. This is due to the fact that the frequency-domain relation between the output of the first vehicle $i = 1$ and the output of another vehicle $i \in \{i \in S_n | i \neq 1\}$ is not a meaningful transfer function, because of the bidirectional nature of the distributed consensus control framework.*

As one can see in (6.2) and (6.3), both conditions regarding *(semi-strict) $\mathcal{L}_2$ string stability* are defined such that these should hold for each vehicle i in the platoon and for all possible platoon lengths $n \in \mathbb{N}$.

The model (6.1) can be formulated in the Laplace-domain as follows:

$$\hat{\eta}_i(s) = \mathcal{P}_i(s)\hat{\nu}(s) + \mathcal{O}_i(s)\rho(0) \quad i \in S_n \tag{6.4}$$

with $s \in \mathbb{C}$, $\rho(0) \in \mathbb{R}^b$ denotes the initial condition and $\mathcal{P}_i(s) = \mathcal{C}_i(sI - \mathcal{A})^{-1}\mathcal{B}$ and $\mathcal{O}_i(s) = \mathcal{C}_i(sI - \mathcal{A})^{-1}$.
Now suppose that system (6.1) represents system (5.19). Thus state vector $\rho(t)$ and input $\nu(t)$ are defined as

$$\rho(t) \equiv [X^T(t),\ U^T(t),\ u_0(t),\ p_0^T(t)]^T, \quad \nu(t) \equiv v_{des}(t). \tag{6.5}$$

For this particular system, with a proper design of the controller gains and the communication topology described by the Laplacian matrix L and a pinning constraint, the eigenmodes are typically asymptotically stable, with the exception for one marginally stable eigenmode associated with $p_0(t)$. Thus system matrix $\mathcal{A}$ is not Hurwitz. In the remainder of this chapter, it is assumed that the pair $(\mathcal{C}_i, \mathcal{B})$ is such that unstable and marginally stable modes are unobservable. This is verified for each designed output vector $\mathcal{C}_i$. Consequently, it holds that, for linear time-invariant systems, if the function α in (6.2) exists, then also the function β exists. For assessment of string stability, it therefore suffices to only analyse the input-output behavior, characterized by $\mathcal{P}_i(s)$. This is equivalent to assuming that the system is initially in equilibrium, i.e., $\rho(0) = \bar{\rho}$ in (6.4). To simplify the synthesis of string stability conditions, $\bar{\rho} = 0$ is chosen without loss of generality. This can be chosen since there always exists a coordination transformation yielding the origin as the equilibrium.

In the following, the condition for *$\mathcal{L}_2$ string stability* in ***Definition 6.1*** and the condition for *semi-strict $\mathcal{L}_2$ string stability* will be reformulated such that these can be easily verified in our specific application.

The derivation of the conditions given below is mainly based on the results presented in Ploeg et al. (2014a), however, slightly altered to cover the bidirectional interconnection structure which is considered in this master thesis.
It can be shown (Zhou et al., 1996, p. 101) that $||\mathcal{P}_i(s)||_{\mathcal{H}_\infty}$ equals the $\mathcal{L}_2$ induced norm related to the input $\nu(t)$ and the output $\eta_i(t)$, i.e.,

$$||\mathcal{P}_i(s)||_{\mathcal{H}_\infty} = \sup_{\nu(t)\neq 0} \frac{||\eta_i(t)||_{\mathcal{L}_2}}{||\nu(t)||_{\mathcal{L}_2}}, \tag{6.6}$$

where the $\mathcal{L}_2$ norm is defined on the interval $t \in [0, \infty)$. Given this, it can be stated that

$$\begin{aligned} ||\eta_i(t)||_{\mathcal{L}_2} &\leq ||\mathcal{P}_i(s)||_{\mathcal{H}_\infty} ||\nu(t)||_{\mathcal{L}_2} \\ &\leq \max_{i\in S_n} ||\mathcal{P}_i(s)||_{\mathcal{H}_\infty} ||\nu(t)||_{\mathcal{L}_2}. \end{aligned} \tag{6.7}$$

As a result of (6.6), it is known that (6.7) is not conservative, in the sense that there always exists a subsystem $i \in S_n$ and specific signal $\nu(t)$ for which the equality holds. Now, according to ***Definition 6.1*** and the assumption that marginally stable and unstable modes are unobservable, the existence of $\max_{i\in S_n} ||\mathcal{P}_i(s)||_{\mathcal{H}_\infty}$, for all possible platoon lengths $n \in \mathbb{N}$, is a necessary and sufficient condition for $\mathcal{L}_2$

string stability of the closed-loop interconnected system in (6.1).

Proposition 6.1: *The closed-loop interconnected platoon* (6.1) *is $\mathcal{L}_2$ string stable, under the condition that marginally and unstable modes are unobservable, if and only if*

$$\sup_{i \in S_n} ||\mathcal{P}_i(s)||_{\mathcal{H}_\infty} < \infty \quad \forall n \in \mathbb{N}. \tag{6.8}$$

Proposition 6.2: *The closed-loop interconnected platoon* (6.1) *is semi-strictly $\mathcal{L}_2$ string stable with respect to its input $\nu(t)$, under the condition that marginally and unstable modes are unobservable, if and only if*

$$\max_{i \in S_n} ||\mathcal{P}_i(s)||_{\mathcal{H}_\infty} \leq |\mathcal{P}_1(0)| \quad \forall n \in \mathbb{N}. \tag{6.9}$$

Remark: *In Ploeg et al. (2014a), an additional condition for semi-strict $\mathcal{L}_2$ string stability is given, namely*

$$||\mathcal{P}_1(s)||_{\mathcal{H}_\infty} < \infty. \tag{6.10}$$

However, this condition is trivial since marginally and unstable modes are assumed to be unobservable.

Note that $|\mathcal{P}_1(0)|$ in (6.9) is equal to one, i.e., $\mathcal{P}_1(s)$ has a static gain of 1, if the input $\nu(t)$ and the output $\eta_i(t)$ have the same units, for example, when the units of the input and output is both expressed in meter per second.
The platoon dynamics satisfying the condition in (6.9) means that input disturbances through $\nu(t)$ are not amplified to any vehicle i in the platoon, i.e., $i \in S_n$, for any platoon length $n \in \mathbb{N}$.

In Ploeg et al. (2014a), a condition for *strict $\mathcal{L}_2$ string stability* is formulated, however, this condition is based on the unidirectional (and single vehicle look-ahead) nature of the interaction topology which is considered there. It requires the existence of a transfer function between the output of vehicle $i-1$ and the output of vehicle i. Due to the bidirectional coupling between the interconnected vehicles in the platoon, as considered here, such a transfer function is not meaningful and thus a condition for assessment of *strict $\mathcal{L}_2$ string stability* cannot be stated for the distributed control approach designed in this master thesis.

6.2 String stability analysis

In this section, by using ***Proposition 6.2***, *semi-strict $\mathcal{L}_2$ string stability* of the distributed consensus control approach described in Chapter 4 and Chapter 5 is assessed. The following platoon dynamics, i.e., platoon dynamics during *Mode 1*, are analysed, since these are the platoon dynamics in normal operation.

$$\begin{bmatrix} \dot{X}(t) \\ \hline \dot{U}(t) \\ \hline \dot{u}_0(t) \\ \hline \dot{p}_0(t) \end{bmatrix} = \left[\begin{array}{c|c|c|c} I_n \otimes A - \hat{L} \otimes Bk^T & O_{3n\times n} & O_{3n\times 1} & O_{3n\times 3} \\ \hline \hat{L} \otimes \frac{k^T}{h} & \frac{1}{h}(I_{(-1),n} - I_n) & B_u & O_{n\times 3} \\ \hline B_u^T \otimes -k_0^T & O_{1\times n} & -\frac{1}{h} & [0,\ -\frac{k_v}{h},\ 0] \\ \hline O_{3\times 3n} & O_{3\times n} & B & A \end{array}\right] \begin{bmatrix} X(t) \\ \hline U(t) \\ \hline u_0(t) \\ \hline p_0(t) \end{bmatrix} + \cdots$$

$$\begin{bmatrix} O_{3n\times 1} \\ \hline O_{n\times 1} \\ \hline \frac{k_v}{h} \\ \hline O_{3\times 1} \end{bmatrix} v_{des}(t). \tag{6.11}$$

Note that these platoon dynamics where also given in (5.19), where the variables are explained in more detail. The state vector $\rho(t)$ and input $\nu(t)$ of the interconnected system dynamics (6.1) are then defined as in (6.5).

First, the actuator delay ϕ and communication delay θ are ignored, i.e., both ϕ and θ are assumed to be equal to zero, such that the dynamics are actually represented by (6.11). As was mentioned above, the input signal $\nu(t)$ is defined to be equivalent to the desired platoon velocity $v_{des}(t)$. Therefore, it is desired to define the vehicle velocity $v_i(t)$ as the output signal $\eta_i(t)$.
The state vector $\rho(t)$, as defined in (6.5), only contains the inter-vehicle distance error state vector $x_i(t)$ and the desired acceleration $u_i(t)$ of all n vehicles, and the states of the virtual reference vehicle. The output vector $\mathcal{C}_i \in \mathbb{R}^{4(n+1)}$ is designed as

$$\mathcal{C}_i = [O_{1\times(3n+i-1)},\ 1,\ O_{1\times(n-i+4)}], \tag{6.12}$$

where vector $O_{1\times q} \in \mathbb{R}^{1\times q}$ is a zero vector, such that the output signal $\eta_i(t)$ is equivalent to the desired acceleration $u_i(t)$, i.e.,

$$\mathcal{P}_i(s) = \frac{\hat{\eta}_i(s)}{\hat{\nu}(s)} = \frac{\hat{u}_i(s)}{\hat{v}_{des}(s)}. \tag{6.13}$$

With the output designed as such, the input and the output signal are not of the same type yet, since the input $v_{des}(t)$ is a velocity and the output is the desired acceleration $u_i(t)$ of vehicle i. The relation between the Laplace transform $\hat{u}_i(s)$ of the desired acceleration and the Laplace transform $\hat{v}_i(s)$ of the velocity of each vehicle i can be derived from (2.11) and is given by

$$\hat{v}_i(s) = \mathcal{G}(s)\hat{u}_i(s) = \frac{1}{s(\tau s+1)}\hat{u}_i(s) \quad \forall i \in S_n. \tag{6.14}$$

Using this relation, the transfer function from the platoon input $v_{des}(t)$ to the vehicle velocity $v_i(t)$ can be obtained, which is defined as

$$\bar{\mathcal{P}}_i(s) = \frac{\hat{v}_i(s)}{\hat{v}_{des}(s)} = \mathcal{G}(s)\mathcal{P}_i(s) \quad \forall i \in S_n. \tag{6.15}$$

Now if the magnitude of the transfer function $\bar{\mathcal{P}}_i(s)$ is smaller than $|\bar{\mathcal{P}}_1(0)|$ for all frequencies, i.e., $\bar{\mathcal{P}}_i(s)$ satisfies (6.9), the closed-loop interconnected platoon (6.11) is *semi-strictly $\mathcal{L}_2$ string stable* with respect to the input $v_{des}(t)$,

Let the neighbouring sets $\mathcal{N}_i$ for the distributed controller be described by *Topology 2*, i.e., the neighbouring sets are defined as

$$\mathcal{N}_i = \{i+1\}\ \forall i \in \{i \in S_n | 1 \leq i < n\} \quad \text{and} \quad \mathcal{N}_n = \emptyset, \tag{6.16}$$

and in addition the pinning constraint on the last vehicle $i = n$ as in (4.55), such that the entire platoon dynamics are described by (6.11) with matrix $\hat{L}$ being defined as

$$\hat{L} = \begin{bmatrix} 1 & -1 & 0 & \cdots & 0 \\ 0 & 1 & -1 & \ddots & \vdots \\ \vdots & \ddots & \ddots & \ddots & 0 \\ \vdots & \ddots & \ddots & 1 & -1 \\ 0 & \cdots & \cdots & 0 & 1 \end{bmatrix}. \tag{6.17}$$

Furthermore, let the desired time gap be defined as $h = 0.6$ s, whereas the controller gains are defined as $k^T = [0.2,\ 1.0,\ 0]$, $k_0^T = [0.05,\ 0.2,\ 0]$, and $k_v = 0.05$. For this configuration of the controller gains and communication topology, the magnitude of the frequency response functions $\bar{\mathcal{P}}_i(j\omega)$ for two different platoon lengths, namely $n = 10$ vehicles and $n = 50$ vehicles, are shown in Figure 6.1.

When observing Figure 6.1a, one can see that all transfer functions $\bar{\mathcal{P}}_i(s)$ satisfy the condition in (6.9) for a platoon of length $n = 10$. Note that some transfer functions $\bar{\mathcal{P}}_i(s)$, namely for vehicle $i = 6$

until vehicle $i = 9$, are not shown for the sake of readability of the plot. The transfer functions for all vehicles, look like a complementary sensitivity. All transfer functions $\bar{\mathcal{P}}_i(s)$ have a static gain of one, i.e., $\mathcal{P}_i(0) = 1$. After the "cut-off" frequency, the slope of the transfer function $\bar{\mathcal{P}}_1(s)$ of the first vehicle goes to -80 Db per decade. For all following vehicles, this slope decreases with 1, i.e., a slope of -100 Db per decade for vehicle $i = 2$, a slope of -120 Db per decade for vehicle $i = 3$, etc.
When observing the magnitude of the frequency response functions $\bar{\mathcal{P}}_i(j\omega)$ for a platoon of length $n = 50$ vehicles in Figure 6.1b, it can be seen that the frequency response functions for the vehicles $i \in \{1, 2, 3, 4, 5, 10\}$ are the same as depicted in Figure 6.1a for a platoon of length $n = 10$ vehicles and the slope decrease with 1 also still applies, i.e., -20 Db per decade extra for each consecutive (following) vehicle.
This seemingly desired behavior is obtained because the actuator delay ϕ and the communication delay θ are ignored. Especially the absence of a communication delay, which leads to a perfect feed-forward, influences the shape of the transfer function. In fact, with these delays being equal to zero, the transfer function $\bar{\mathcal{P}}_i(s)$ can be expressed as

$$\bar{\mathcal{P}}_i(s) = \frac{\hat{v}_i(s)}{\hat{v}_{des}(s)} = \frac{k_v}{(hs+1)^i\left((hs+1)(\tau s+1)s + k_v\right)} \quad \forall i \in S_n, \tag{6.18}$$

which are thus the transfer functions as shown in Figure 6.1. The derivation of (6.18) is given in Appendix C.
As can be seen in the entire platoon dynamics (6.11), the inter-vehicle distance error dynamics does not depend on the states $U(t)$, $u_0(t)$ and $p_0(t)$ nor on the input $v_{des}(t)$. Therefore, in the case of zero delay, the inter-vehicle distance error states and its time-derivatives in $X(t)$ do not play a role in the transfer function $\mathcal{P}_i(s)$ from the input $v_{des}(t)$ to the desired acceleration $u_i(t)$, which similarly applies to the transfer function $\bar{\mathcal{P}}_i(s)$ from the input $v_{des}(t)$ to velocity $v_i(t)$. The inter-vehicle distance error states and its time-derivatives in $X(t)$ only play a role in the platoon dynamics through the frequency-domain relation $\mathcal{O}_i(s)$ regarding the initial conditions, as in (6.4).
Given the transfer function in (6.18), and according to the plots in Figure 6.1, it is known that condition (6.9) is satisfied and thus the closed-loop interconnected platoon (6.11) is *semi-strictly $\mathcal{L}_2$ string stable* with respect to the input $v_{des}(t)$. However, this perfect feed-forward due to zero communication delay is of course unfeasible in practice.

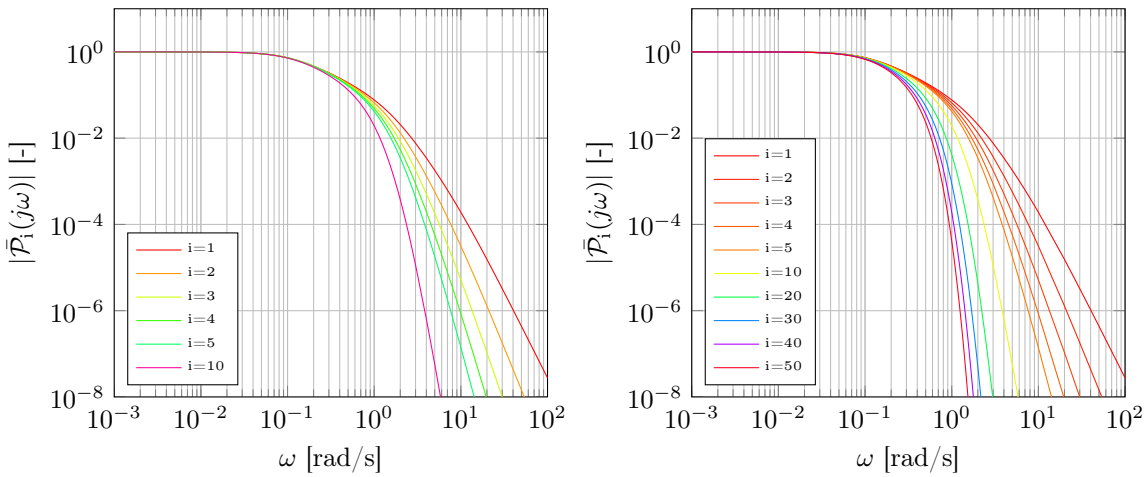

(a) $n = 10$ vehicles **(b)** $n = 50$ vehicles

Figure 6.1: The magnitude of the frequency response functions $\bar{\mathcal{P}}_i(j\omega)$ for $i \in S_n$, for two different platoon lengths n. The communication topology is of *Topology 2* and the pinning constraint is defined by (4.55).

Next, the effect of the actuator delay ϕ and the effect of the communication delay θ is investigated. First, the influence of the actuator delay ϕ is examined, while assuming that the communication delay θ is equal to zero. It is known that the actuator delay ϕ, for a Toyota Prius, is approximately equal to $\phi = 0.2$ seconds. It is found that the magnitude plots, as shown in Figure 6.1, do not change much due to this actuator delay $\phi = 0.2$ seconds.
Hereafter, the influence of the communication delay $\theta = 0.02$ seconds, in addition to the actuator delay $\phi = 0.2$ seconds, on the transfer functions $\bar{\mathcal{P}}_i(s)$ is analysed. Both the desired acceleration of the preceding vehicle $u_{i-1}(t)$ as well as the error state vector used in the distributed controller $x_j(t)\ \forall j \in \mathcal{N}_i$ are subjected to this communication delay θ, resulting in the control law for the desired acceleration $u_i(t)$ of vehicle i to be as defined in (4.59).

The magnitude plots of the frequency response functions $\bar{\mathcal{P}}_i(j\omega)$, for similar control configuration but including both delays ϕ and θ, are shown in Figure 6.2, again for a platoon of length $n = 10$ vehicles and $n = 50$ vehicles. For a platoon of length $n = 10$ vehicles, the influence of this communication delay $\theta = 0.02$ seconds on magnitude plot of the transfer function $\bar{\mathcal{P}}_i(s)$ is minor or even unnoticeable, as can be seen by comparing Figure 6.2a and Figure 6.1a.
When increasing the platoon length n, an increasing amount of resonance peaks start to appear in the magnitude plot of $\bar{\mathcal{P}}_i(s)$. Also, the height of these resonance peaks increases with increasing the platoon length n. The magnitude of $\bar{\mathcal{P}}_i(s)$ for a platoon of length $n = 50$ is shown in Figure 6.2b. For this platoon length, it can be observed that peaks above 1 appear, such that condition (6.9) is not satisfied for a platoon of length $n = 50$ vehicles. For this particular control gain configuration and for the delays being $\phi = 0.2$ s and $\theta = 0.02$ s, it is found that the condition in (6.9) is satisfied for a platoon length $n \leq n_{max} = 35$.
In contrast with the result without both the delays ϕ and θ, as was depicted in Figure 6.1, now the transfer functions $\bar{\mathcal{P}}_i(s)$ are influenced by the platoon length n. This can be explained as follows. As a result of the inclusion of the actuator delay ϕ and the communication delay θ in the platoon dynamics in (6.11), the transfer function $\bar{\mathcal{P}}_i(s)$ cannot be expressed by the ideal transfer function in (6.18) anymore. In fact, the transfer functions $\bar{\mathcal{P}}_i(s)$ now do depend on the dynamics of the inter-vehicle distance error states and its derivatives in $X(t)$.

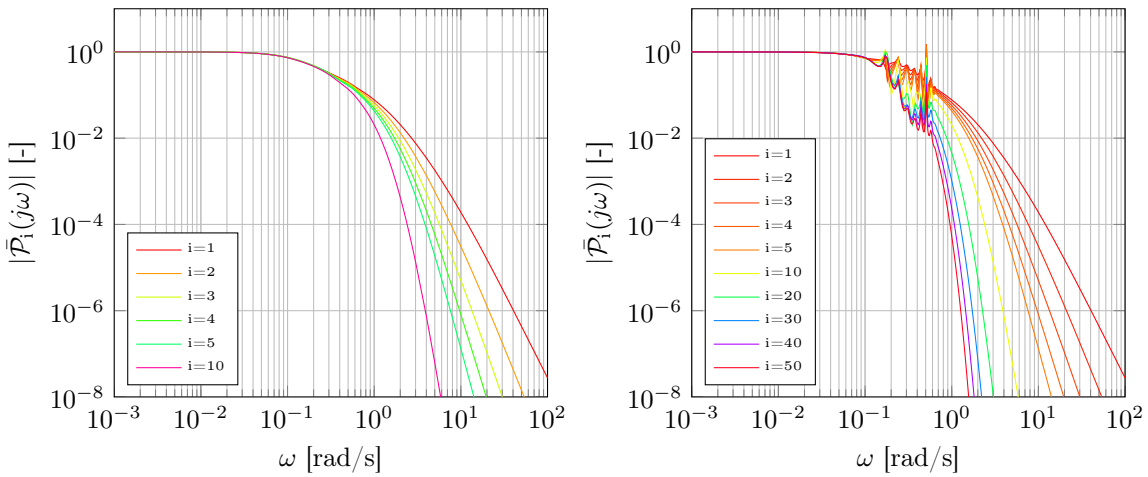

(a) $n = 10$ vehicles **(b)** $n = 50$ vehicles

Figure 6.2: The magnitude of the frequency response functions $\bar{\mathcal{P}}_i(j\omega)$ (including actuator delay $\phi = 0.2$ s and communication delay $\theta = 0.02$ s) for $i \in S_n$, for two different platoon lengths n. The communication topology is of *Topology 2* and the pinning constraint is defined by (4.55).

The result as shown in Figure 6.2 means that the closed-loop interconnected platoon, including the actuator delay $\phi = 0.2$ s and the communication delay $\theta = 0.02$ s, cannot be said to be *semi-strictly* $\mathcal{L}_2$ *string stable* with respect to the input $v_{des}(t)$, since for this, condition (6.9) should be satisfied for all platoon lengths $n \in \mathbb{N}$. The condition in (6.9) is only satisfied for a finite platoon length n, meaning that disturbances through input $v_{des}(t)$ are only being suppressed to each vehicle $i \in S_n$ for a certain maximum platoon length n.
For the same controller as used above and for an actuator delay $\phi = 0.2$ s, Figure 6.3 shows the maximum communication delay θ_{max} that yields

$$\max_{i \in S_n} ||\bar{\mathcal{P}}_i(s)||_{\mathcal{H}_\infty} \leq |\bar{\mathcal{P}}_1(0)|, \tag{6.19}$$

as a function of the platoon length n. Again note that $|\bar{\mathcal{P}}_1(0)| = 1$ when the input and the output have the same units, e.g., meter per second. The curve is obtained by numerically checking whether the condition in (6.19) is satisfied. For a small platoon length, i.e., $n \leq 16$ vehicles, the upper-bound in Figure 6.3 is determined by asymptotic stability of the platoon dynamics. If the communication delay θ is above the dotted blue line, an unstable eigenmode occurs in the platoon dynamics. When the platoon dynamics are unstable, the condition in (6.19) is by definition violated. For a larger platoon length, i.e., $n > 16$ vehicles, this upper-bound on the communication delay θ in Figure 6.3 (indicated by the red dots) is determined by violation of (6.19), however the platoon dynamics does not become unstable when violating this bound.

Next, the influence of the chosen communication topology is investigated. Suppose the communication topology for the distributed controller is as *Topology 1*, such that the neighbouring sets are defined as

$$\mathcal{N}_1 = \{2\}, \quad \mathcal{N}_i = \{i-1, i+1\} \ \forall i \in \{i \in S_n | 1 < i < n\} \quad \text{and} \quad \mathcal{N}_n = \{n-1\}. \tag{6.20}$$

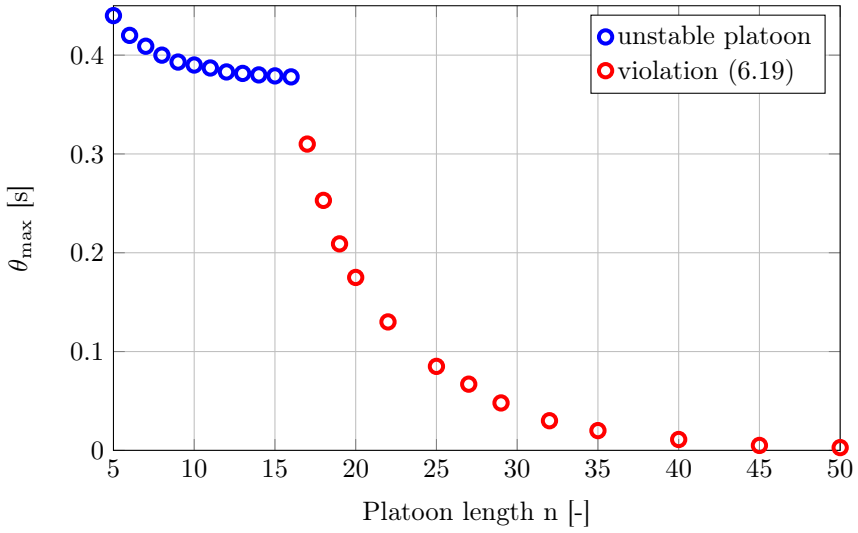

Figure 6.3: Maximum communication delay θ, as a function of the platoon length n (and for actuator delay $\phi = 0.2$ s). The blue dotted part of the upper-bound originates from platoon dynamics instability and the red dotted part of the upper-bound originates from violation of condition (6.19). The communication topology is of *Topology 2* and the pinning constraint is defined by (4.55).

Furthermore, the pinning constraint is on the last vehicle, as in (5.42). Given this, matrix $\hat{L}$ in the platoon dynamics in (6.11), is defined as

$$\hat{L} = \begin{bmatrix} 1 & -1 & 0 & \dots & 0 \\ -1 & 2 & -1 & \ddots & \vdots \\ 0 & \ddots & \ddots & \ddots & 0 \\ \vdots & \ddots & -1 & 2 & -1 \\ 0 & \dots & 0 & -1 & 2 \end{bmatrix}. \tag{6.21}$$

For this *Topology 1*, but with the same controller gains k, k_0 and k_v as used before, the magnitude of the frequency response functions $\bar{\mathcal{P}}_i(j\omega)$ are shown in Figure 6.4. It can be observed that for this topology, the magnitude of the frequency response functions $\bar{\mathcal{P}}_i(j\omega)$ satisfies the condition in (6.19), even for a platoon of length $n = 50$ vehicles. Also, when comparing Figure 6.4a and Figure 6.4b, the figures do not show a trend of an increase in magnitude for increasing n, indicating that the condition in (6.19) is satisfied for any platoon length $n \in \mathbb{N}$, i.e., thus indicating *semi-strict $\mathcal{L}_2$ string stability*.

By comparing the magnitude plot of $\bar{\mathcal{P}}_i(s)$ for various communication topologies defined by a Laplacian matrix L, plus in addition of a pinning constraint through matrix P, it is found that, when there exists an eigenvalue of matrix $\hat{L} = L + P$ having a large geometric multiplicity, the peaks in the magnitude plot of $\bar{\mathcal{P}}_i(s)$ appear/increase for increasing platoon length n, as was clearly visible in Figure 6.2b. Matrix $\hat{L} = L + P$ as given in (6.17) has only one eigenvalue equal to 1, which has a geometric multiplicity equal to n. Matrix $\hat{L} = L + P$ as in (6.21) has n distinct eigenvalues.
Thus, in relation to the actuator and communication delay, for a platoon being *semi-strictly $\mathcal{L}_2$ string stable*, i.e., disturbance rejection of input $v_{des}(t)$ for any platoon length n, eigenvalues of matrix $\hat{L}$ having a large geometric multiplicity should be avoided.

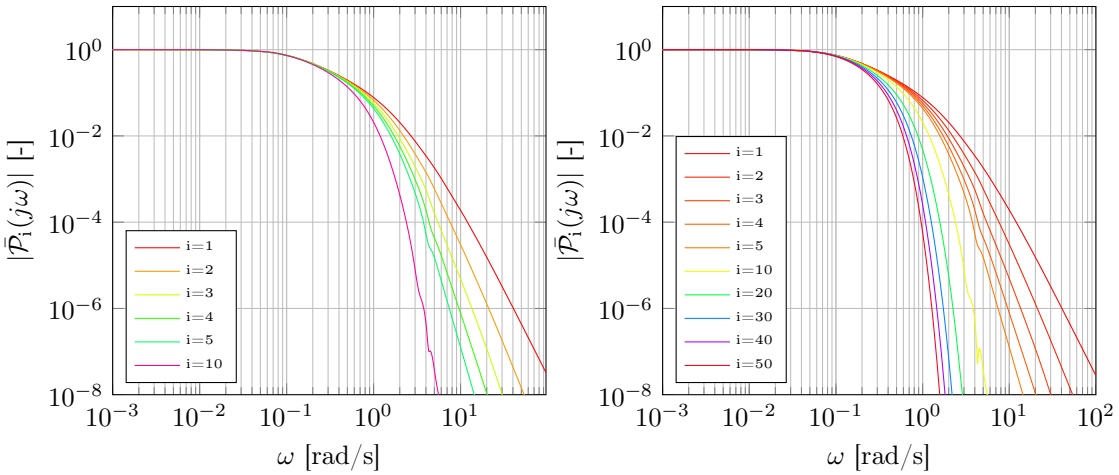

(a) $n = 10$ vehicles **(b)** $n = 50$ vehicles

Figure 6.4: The magnitude of the frequency response functions $\bar{\mathcal{P}}_i(j\omega)$ (including actuator delay $\phi = 0.2$ s and communication delay $\theta = 0.02$ s) for $i \in S_n$, for two different platoon lengths n. The communication topology in combination with the pinning constraint is described by matrix $\hat{L}$ as in (6.21).

6.3 Summary

In this chapter, a condition for *semi-strict $\mathcal{L}_2$ string stability*, i.e., disturbance rejection of input $v_{des}(t)$, based on results in Ploeg et al. (2014a) is defined. This condition is used in evaluation of the string stability properties of the distributed consensus control approach as designed in Chapter 4 and Chapter 5. It is found that, when neglecting the actuator delay ϕ and the communication delay θ, the closed-loop interconnected platoon is *semi-strictly $\mathcal{L}_2$ string stable* with respect to its input $v_{des}(t)$.
In practice, these delays are never equal to zero. Therefore, a nonzero actuator delay ϕ and communication delay θ are introduced. Various communication topologies in combination with a pinning constraint, described by a Laplacian matrix L and a pinning matrix P, are analysed. In particular, the frequency response functions $\bar{\mathcal{P}}_i(j\omega)$ for *Topology 1* and *Topology 2* are discussed. It is found that, for communication topologies of which the Laplacian matrix L has no eigenvalues having a large geometric multiplicity, the distributed controlled platoon is *semi-strictly $\mathcal{L}_2$ string stability* with respect to its input $v_{des}(t)$. Which means that disturbances through the only exogenous platoon input $v_{des}(t)$ are attenuated for any platoon length n.
Furthermore, it is found that, for communication topologies of which the Laplacian matrix L has an eigenvalue having a large geometric multiplicity, the distributed controlled platoon is cannot be said *semi-strictly $\mathcal{L}_2$ string stability* with respect to its input $v_{des}(t)$. For those communication topologies, disturbances through input $v_{des}(t)$ are only attenuated for a finite platoon length $n \leq n_{max}$, depending on the designed controller gains and the value for the actuator- and communication delays. Thus for such communication topologies, for a given actuator delay ϕ and communication delay θ, there is an upper-bound n_{max} on the maximum allowable platoon length n.

Chapter 7

Conclusions and recommendations

In this chapter, first conclusions regarding the results as presented in this master thesis are given. Thereafter, recommendations for future work are suggested.

7.1 Conclusions

The objective of this master thesis was to find a distributed consensus control framework which covers many of the desired properties in vehicle platooning, as was discussed in the problem statement in the introduction of this thesis. To this end, the existing literature regarding distributed consensus and formation control, also in application to vehicle platooning, is reviewed extensively. At first glance, it seems that the existing literature covers the properties desired in vehicle platooning, e.g., use of a realistic model of the vehicle's longitudinal dynamics, a velocity-dependent spacing-policy, only local information availability, string stability. However, non of the existing developed approaches covers all of these desired properties at once.
A distributed consensus control approach for vehicle platooning was presented and, within this approach, the longitudinal vehicle dynamics are modeled as a third-order linear system. Furthermore, a velocity-dependent spacing-policy, which is desired in vehicle platooning, is realised between consecutive vehicles. Within the proposed framework, the communication topology of the distributed controller can be arbitrary, as long as the given conditions for asymptotically stable platoon dynamics are satisfied. Depending on the chosen communication topology for the distributed controller, the interaction between the vehicles in the platoon can be of bidirectional nature. In addition, feed-forward control is included in the controller to improve string stability properties of the distributed controlled platoon.
Bidirectional interaction between the vehicles in the platoon can improve the platoon's coherence in the sense that the platoon does not break up when there is a limitation on a vehicles's velocity or acceleration. A control law for a virtual reference vehicle is introduced and the platoon dynamical behavior, subject to this control law, is analysed. It is found that the controlled platoon is able to adapt its cruising velocity when, at some moment, a saturation occurs on a (faulty) vehicle's velocity. Moreover, the platoon velocity will return to the desired cruise velocity when this saturation (or fault) is resolved. This property only holds when the amount of vehicles in between the vehicle subjected to this saturation and the leading vehicle is below some threshold value. The value of this threshold also depends on the designed controller gains.
Finally, string stability properties of the resulting closed-loop dynamics are evaluated. String stability is only evaluated for the situation when the platoon is in normal operation, i.e., when no fault occurs. It is observed that, the distributed controlled platoon is *semi-strictly $\mathcal{L}_2$ string stable* with respect to the platoon exogenous input $v_{des}(t)$ when the Laplacian matrix L, describing the communication topology, does not have an eigenvalue having a large geometric multiplicity.

7.2 Recommendations

The control approach as designed in this master thesis seems to offer opportunities for various applications. However, more research is required. For example, the influence of the choice of the communication topology is investigated, but it is worthwhile to be explored more into depth. More specifically, it is useful to investigate the influence of the geometric multiplicity of the eigenvalues of the Laplacian L describing the communication topology on string stability properties.
Also, in the stability analysis for the vehicle velocity saturation, it is assumed that back and forth switching between *Mode 1* and *Mode 2*, i.e., saturation mode and normal mode, does not occur. In future work, this stability analysis may be expanded by taking into account the switching between the two modes.
Furthermore, string stability is an important property of a vehicle platoon because it allows for scalability of the platoon with respect to its length. *Semi-strict $\mathcal{L}_2$ string stability* with respect to the platoon's only input $v_{des}(t)$ is investigated. However, for a more thorough investigation regarding string stability properties of a bidirectionally coupled vehicle platoon, the influence of additive disturbances should be investigated. For example, additive disturbances $\delta_{v_i}(t)$ can be added to the velocity $v_i(t)$ of each vehicle i and *semi-strict $\mathcal{L}_2$ string stability* with respect to this disturbances $\delta_{v_i}(t)$ can be evaluated.
In addition to distributed consensus control applied to longitudinal dynamics, an extension to lateral dynamics can be made as to include tasks like splitting from or merging into a platoon. In many lateral control techniques, constant longitudinal velocity is assumed, such that a linearised model for lateral dynamics suffices. However, when combining both longitudinal and lateral dynamics, using nonlinear dynamical models seems unavoidable, which makes stability (and string stability) analysis more complex.

Bibliography

Bernardo, M. di, Salvi, A., and Santini, S. (2014). Distributed consensus strategy for platooning of vehicles in the presence of time-varying heterogeneous communication delays. *IEEE Transactions on Intelligent Transportation Systems*.

Bondy, J.A. and Murty, U.S.R. (2008). Graph theory, volume 244 of Graduate Texts in Mathematics. 2008.

Cao, Y., Yu, W., Ren, W., and Chen, G. (2013). An overview of recent progress in the study of distributed multi-agent coordination. *IEEE Transactions on Industrial Informatics*, 9(1), p. 427–438.

Fax, J.A. and Murray, R.M. (2004). Information flow and cooperative control of vehicle formations. *IEEE Transactions on Automatic Control*, 49(9), p. 1465–1476.

Godsil, C.D. and Royle, G. (2001). *Algebraic graph theory*. **207**. Springer New York.

Gouvea, J.A., Lizarralde, F., and Hsu, L. (2013). Formation control of dynamic nonholonomic mobile robots with curvature constraints via potential functions. In *American Control Conference (ACC)*, 2013. p. 3039–3044, IEEE.

Gowal, S., Falconi, R, and Martinoli, A. (2010). Local Graph-based Distributed Control for Safe Highway Platooning. In *Proceedings of the IEEE/RSJ International Conference on Intelligent Robots and Systems*, 2010. p. 6070–6076.

Horn, R.A. and Johnson, C.R. (1988). *Matrix analysis*. Cambridge university press.

Hurwitz, A. (1964). On the conditions under which an equation has only roots with negative real parts. *Selected papers on mathematical trends in control theory*, 65, p. 273–284.

Iftekhar, L. and Olfati-Saber, R. (2012). Autonomous driving for vehicular networks with nonlinear dynamics. In *Intelligent Vehicles Symposium (IV), IEEE*, 2012. p. 723–729, IEEE.

Le, Y.W., Ali, S., Yin, G., Pandya, A., and Zhang, H. (2012). Coordinated vehicle platoon control: weighted and constrained consensus and communication network topologies. *Proceedings of CDC*.

Lin, Z., Broucke, M., and Francis, B. (2004). Local control strategies for groups of mobile autonomous agents. *IEEE Transactions on Automatic Control*, 49(4), p. 622–629.

Middleton, R.H. and Braslavsky, J.H. (2010). String instability in classes of linear time invariant formation control with limited communication range. *IEEE Transactions on Automatic Control*, 55(7), p. 1519–1530.

Montanaro, U., Tufo, M., Fiengo, G., di Bernardo, M., Salvi, A., and Santini, S. (2014). Extended cooperative adaptive cruise control. In *Intelligent Vehicles Symposium Proceedings*, 2014. p. 605–610, IEEE.

Naus, G.J.L., Vugts, R.P.A., Ploeg, J., Van de Molengraft, M.J.G., and Steinbuch, M. (2010). String-stable CACC design and experimental validation: A frequency-domain approach. *IEEE Transactions on Vehicular Technology*, 59(9), p. 4268–4279.

Neudecker, H. (1969). A note on Kronecker matrix products and matrix equation systems. *SIAM Journal on Applied Mathematics*, 17(3), p. 603–606.

Olfati-Saber, R. (2006). Flocking for multi-agent dynamic systems: Algorithms and theory. *IEEE Transactions on Automatic Control*, 51(3), p. 401–420.

Olfati-Saber, R. and Murray, R.M. (2004). Consensus problems in networks of agents with switching topology and time-delays. *IEEE Transactions on Automatic Control*, 49(9), p. 1520–1533.

Ploeg, J., Shukla, D.P., van de Wouw, N., and Nijmeijer, H. (2014a). Controller synthesis for string stability of vehicle platoons. *IEEE Transactions on Intelligent Transportation Systems*, 15(2), p. 854–865.

Ploeg, J., van de Wouw, N., and Nijmeijer, H. (2014b). Lp string stability of cascaded systems: Application to vehicle platooning. *IEEE Transactions on Control Systems Technology*, 22(2), p. 786–793.

Qu, Z., Wang, J., and Hull, R.A. (2008). Cooperative control of dynamical systems with application to autonomous vehicles. *IEEE Transactions on Automatic Control*, 53(4), p. 894–911.

Ramakers, R., Henning, K., Gies, S., Abel, D., and Max, H. (2009). Electronically coupled truck platoons on German highways. In *Systems, Man and Cybernetics. IEEE International Conference on*, 2009. p. 2409–2414, IEEE.

Ren, W. (2007). Consensus seeking in multi-vehicle systems with a time-varying reference state. In *American Control Conference*, 2007. p. 717–722, IEEE.

Ren, W. and Atkins, E. (2007). Distributed multi-vehicle coordinated control via local information exchange. *International Journal of Robust and Nonlinear Control*, 17(10-11), p. 1002–1033.

Ren, W. and Beard, R.W. (2008). *Distributed consensus in multi-vehicle cooperative control*. Springer.

Ren, W., Moore, K., and Chen, Y.Q. (2006). High-order consensus algorithms in cooperative vehicle systems. In *Networking, Sensing and Control, 2006. ICNSC. Proceedings of the IEEE International Conference on*, 2006. p. 457–462, IEEE.

Saboori, I., Nayyeri, H., and Khorasani, K. (2013). A distributed control strategy for connectivity preservation of multi-agent systems subject to actuator saturation. In *American Control Conference (ACC)*, 2013. p. 4044–4049, IEEE.

Semsar-Kazerooni, E. and Khorasani, K. (2007). Optimal performance of a modified leader-follower team of agents with partial availability of leader command and presence of team faults. In *Proc. IEEE Conference on Decision and Control, December12–14*, 2007. p. 2491–2497.

Swaroop, D. and Hedrick, J.K. (1999). Constant spacing strategies for platooning in automated highway systems. *Journal of dynamic systems, measurement, and control*, 121(3), p. 462–470.

Wang, X., Li, X., and Lu, J. (2010). Control and flocking of networked systems via pinning. *IEEE Circuits and Systems Magazine*, 10(3), p. 83–91.

Xie, G. and Wang, L. (2007). Consensus control for a class of networks of dynamic agents. *International Journal of Robust and Nonlinear Control*, 17(10-11), p. 941–959.

Yang, Z., Liu, Z., Chen, Z., and Yuan, Z. (2008). Tracking control for multi-agent consensus with an active leader and directed topology. In *Intelligent Control and Automation, WCICA 7th World Congress on*, 2008. p. 1037–1041, IEEE.

Zheng, Y., Li, S.E., Wang, J., Wang, L.Y., and Li, K. (2014). Influence of information flow topology on closed-loop stability of vehicle platoon with rigid formation. In *Intelligent Transportation Systems (ITSC), IEEE 17th International Conference on*, 2014. p. 2094–2100, IEEE.

Zhou, K., Doyle, J.C., and Glover, K. (1996). *Robust and optimal control*. Prentice Hall, NJ, USA.

Appendix A

Proof of Lemma 4.1

In this appendix, the following lemma will be used in the proof of ***Lemma 4.1***.

Lemma A.1 (Neudecker, 1969): The mixed-product property of a Kronecker product: If E, F, G and H are matrices of such size that one can form the matrix products EG and FH, then

$$(EG) \otimes (FH) = (E \otimes F)(G \otimes H). \tag{A.1}$$

The inverse of a Kronecker product is given by

$$(E \otimes G)^{-1} = E^{-1} \otimes G^{-1}. \tag{A.2}$$

Lemma 4.1: *The origin is an asymptotically stable equilibrium of the dynamics in* (4.34) *if and only if all matrices*

$$A - \lambda_i B k^T \,, \quad \forall i \in S_n \tag{A.3}$$

are Hurwitz, where λ_i *is the* i^{th} *eigenvalue of the square* $n \times n$ *matrix* $\hat{L}$.

Proof of Lemma 4.1:
The Schur decomposition (Horn and Johnson, 1988) of an $n \times n$ matrix $\tilde{L}$ is defined as

$$\tilde{L} = V D V^{-1} \tag{A.4}$$

with matrix D being an upper triangular matrix having the eigenvalues of matrix $\tilde{L}$ on its diagonal and matrix V being an unitary matrix, thus satisfying

$$V I_n V^{-1} = I_n. \tag{A.5}$$

By using the relation in $(A.4)$ and by using the property in $(A.5)$, the system dynamics (4.34) can be rewritten as

$$\dot{X}(t) = \left((V I_n V^{-1} \otimes A) - (V D V^{-1} \otimes B k^T) \right) X(t). \tag{A.6}$$

By using the mixed-product property of **Lemma A.1**, the first term on the righthand-side of $(A.6)$ can be rewritten as follows

$$\begin{aligned} V I_n V^{-1} \otimes A &= V I_n V^{-1} \otimes I_m A = (V \otimes I_m)(I_n V^{-1} \otimes A) \\ &= (V \otimes I_m)(I_n V^{-1} \otimes A I_m) = (V \otimes I_m)(I_n \otimes A)(V^{-1} \otimes I_m). \end{aligned} \tag{A.7}$$

Similarly, the second term of $(A.6)$ can be rewritten:

$$\begin{aligned} V D V^{-1} \otimes B k^T &= V D V^{-1} \otimes I_m B k^T = (V \otimes I_m)(D V^{-1} \otimes B k^T) \\ &= (V \otimes I_m)(D V^{-1} \otimes B k^T I_m) = (V \otimes I_m)(D \otimes B k^T)(V^{-1} \otimes I_m). \end{aligned} \tag{A.8}$$

Using the relations (A.7) and (A.8), the platoon error dynamics (A.6) can be written as

$$\dot{X}(t) := A_d X = \{(V \otimes I_m)(\underbrace{I_n \otimes A - D \otimes Bk^T}_{\tilde{A}})(V^{-1} \otimes I_m)\}X(t) \quad . \tag{A.9}$$

Let us define the matrix $\tilde{V}$ as

$$\tilde{V} = V \otimes I_m. \tag{A.10}$$

Using the inverse property of **Lemma A.1**, matrix A_d in (A.9) can be written as

$$A_d = \tilde{V}\tilde{A}\tilde{V}^{-1}. \tag{A.11}$$

Let the eigenvalues of matrix A_d being defined as $\mu_i \; \forall i \in \{1, 2, .., mn\}$, and the corresponding eigenvectors being defined as $n_i \; \forall i \in \{1, 2, .., mn\}$. The eigenvectors n_i have dimensions $mn \times 1$.
These eigenvalues and -vectors thus satisfy

$$\tilde{V}\tilde{A}\tilde{V}^{-1}n_i = \mu_i n_i, \quad i \in \{1, 2, .., mn\}\,. \tag{A.12}$$

Pre-multiplication of (A.12) with $\tilde{V}^{-1}$ results in

$$\tilde{A}\tilde{V}^{-1}n_i = \mu_i \tilde{V}^{-1}n_i, \quad i \in \{1, 2, .., mn\}\,. \tag{A.13}$$

From (A.13), it can be observed that the eigenvalues of matrix $\tilde{A}$ are equal to the eigenvalues μ_i of matrix A_d, with the corresponding eigenvector for matrix $\tilde{A}$ being defined as $\tilde{V}^{-1}n_i$. Matrix $\tilde{A}$ is an upper-triangular block matrix of the following structure:

$$\tilde{A} = \begin{bmatrix} A - \lambda_1 Bk^T & \tilde{A}_{12} & \cdots & \tilde{A}_{nn} \\ 0_{m\times m} & A - \lambda_2 Bk^T & & \vdots \\ \vdots & & \ddots & \tilde{A}_{(n-1)n} \\ 0_{m\times m} & \cdots & 0_{m\times m} & A - \lambda_n Bk^T \end{bmatrix}. \tag{A.14}$$

Due to the upper-triangular structure, matrix $\tilde{A}$ is Hurwitz if all matrices $A - \lambda_i Bk^T \; \forall i \in S_n$ are Hurwitz (Horn and Johnson, 1988). The eigenvalues of matrix $\tilde{A}$ are equivalent to the eigenvalues of matrix A_d. Consequently, the origin is an asymptotically stable equilibrium of (4.34) if all matrices $A - \lambda_i Bk^T \; \forall i \in S_n$ are Hurwitz.

Note that according to the proof, the opposite also holds: if matrix A_d is Hurwitz, then all matrices $A - \lambda_i Bk^T \; \forall i \in S_n$ are Hurwitz. Hence, **Lemma 4.1** is proven.

Appendix B

Platoon dynamics state transformation and reduction

In this appendix, a similarity transformation of the platoon dynamics is given. Also, given that one vehicle $i = f$ has a fixed velocity v_{max}, the platoon dynamics are reduced with order three, i.e., three states are removed. Let the index $i = f$ of the faulty (or saturated) vehicle be equal to the platoon length n, i.e., $f = n$. Let $x_i(t)$ be defined as

$$x_i(t) = [e_i(t),\ \dot{e}_i(t),\ \ddot{e}_i(t)]^T \tag{B.1}$$

and let $\chi_i(t)$ be defined as

$$\chi_i(t) = [e_i(t),\ v_i(t),\ a_i(t)]^T. \tag{B.2}$$

Matrix T_f describes the transformation from the platoon state vector

$$\xi_1(t) = \begin{bmatrix} X(t) \\ U(t) \\ u_0(t) \\ p_0(t) \end{bmatrix} = \begin{bmatrix} x_1(t) \\ \vdots \\ x_f(t) \\ U(t) \\ u_0(t) \\ p_0(t) \end{bmatrix} \tag{B.3}$$

to the platoon state vector

$$\xi_2(t) = \begin{bmatrix} \chi(t) \\ U(t) \\ u_0(t) \\ p_0(t) \end{bmatrix} = \begin{bmatrix} \chi_1(t) \\ \vdots \\ \chi_f(t) \\ U(t) \\ u_0(t) \\ p_0(t) \end{bmatrix}, \tag{B.4}$$

such that

$$\xi_2(t) = T_f \xi_1(t). \tag{B.5}$$

For a platoon length $n = f = 3$, this similarity transformation matrix T_f is defined as given in (B.15) below. There is a repeating structure in this similarity transformation matrix T_3, but a general expression for T_f for any platoon length is not given here.

Let the platoon dynamics in (5.19) be expressed by

$$\dot{\xi}_1(t) = A_H \xi_1(t) + B_H v_{des}(t). \tag{B.6}$$

Applying the similarity transformation results in

$$\dot{\xi}_2(t) = T_f A_H T_f^{-1} \xi_2(t) + T_f B_H v_{des}(t). \tag{B.7}$$

As defined in Section 5.4, when the platoon is in *Mode 2*, it is known that the acceleration $a_f(t)$ and desired acceleration velocity $u_f(t)$ of vehicle $i = f$ are both equal to zero. Furthermore, it is known that the velocity $v_f(t) = v_{max}$ is constant. Therefore, the states $v_f(t)$, $a_f(t)$ and $u_f(t)$ are removed from the state space in (B.7), such that the state vector of the platoon dynamics is defined as

$$\xi_3(t) = \left[\begin{array}{c} \chi_1(t) \\ \vdots \\ \hline \chi_{f-1}(t) \\ \hline e_f(t) \\ \hline U_r(t) \\ \hline u_0(t) \\ \hline p_0(t) \end{array}\right], \tag{B.8}$$

where $U_r = [u_1(t),\ \cdots,\ u_{f-1}(t)]^T$. Given this, the platoon dynamics can be represented by

$$\dot{\xi}_3(t) = A_R \xi_3(t) + B_{R,1} v_{max} + B_{R,2} v_{des}(t), \tag{B.9}$$

where system matrix A_R, vector $B_{R,1}$ and vector $B_{R,2}$ are defined as follows. Note that the structure, especially of matrix A_R, is complex, but this cannot be avoided. Also, the following expression for A_R, $B_{R,1}$ and $B_{R,2}$ only holds for matrix $\hat{L}$ being defined as $\hat{L} = L_2 + P$ as in (5.5), thus not hold for any $\hat{L}$ in general. System matrix A_R is defined as

$$A_R = \left[\begin{array}{c|c|c|c|c} I_{(f-1)} \otimes A_1 + I_{(-1),(f-1)} \otimes A_2 & O_{3(f-1)\times 1} & I_{(f-1)} \otimes B & O_{3(f-1)\times 1} & Q_1 \otimes A_2 \\ \hline Q_2^T \otimes [0,\ 1,\ 0] & 0 & O_{1\times(f-1)} & 0 & O_{1\times 3} \\ \hline V_1 & -\frac{k_1}{h} Q_2 & L_u & \frac{1}{h} Q_1 & Q_1 \otimes [0,\ \frac{k_2}{h},\ \frac{k_3}{h}] \\ \hline Q_1^T \otimes [-\frac{k_p}{h},\ \frac{k_d}{h},\ k_d] & 0 & O_{1\times(f-1)} & -\frac{1}{h} & [0,\ -\left(\frac{k_d+k_v}{h}\right),\ 0] \\ \hline O_{3\times 3(f-1)} & O_{3\times 1} & O_{3\times(f-1)} & B & A \end{array}\right], \tag{B.10}$$

where matrices A, A_1, A_2, and vector B are as in (4.18) and (5.29), $I_{(f-1)} \in \mathbb{R}^{(f-1)\times(f-1)}$ being the identity matrix, $I_{(-1),(f-1)} \in \mathbb{R}^{(f-1)\times(f-1)}$ being a matrix defined as in (4.24), vectors $Q_1 \in \mathbb{R}^{(f-1)\times 1}$ and $Q_2 \in \mathbb{R}^{(f-1)\times 1}$ are defined as

$$Q_1 = [1,\ 0,\ \cdots,\ 0]^T, \quad Q_2 = [0,\ \cdots,\ 0,\ 1]^T. \tag{B.11}$$

Matrix $V_1 \in \mathbb{R}^{(f-1)\times 3(f-1)}$ is defined as

$$V_1 = L_e \otimes [\frac{k_1}{h},\ 0,\ 0] + L_v \otimes [0,\ -\frac{k_2}{h},\ 0] + L_a \otimes [0,\ 0,\ 1], \tag{B.12}$$

where matrices $L_e \in \mathbb{R}^{(f-1)\times(f-1)}$, $L_v \in \mathbb{R}^{(f-1)\times(f-1)}$ and $L_a \in \mathbb{R}^{(f-1)\times(f-1)}$ are defined as

$$\begin{aligned} L_e &= I_{(f-1)} - I_{(1),(f-1)} \\ L_v &= 2I_{(f-1)} - I_{(-1),(f-1)} - I_{(1),(f-1)} \\ L_a &= \left(-k_2 + \frac{k_3(h-2\tau)}{\tau}\right) I_{(f-1)} + \left(k_2 - \frac{k_3(h-\tau)}{\tau}\right) I_{(1),(f-1)} + \frac{k_3}{h} I_{(-1),(f-1)}, \end{aligned}$$

with matrix $I_{(1),(f-1)} \in \mathbb{R}^{(f-1)\times(f-1)}$ being a matrix having ones on all entries of the first upper off-diagonal and zeros elsewhere, and matrix $L_u \in \mathbb{R}^{(f-1)\times(f-1)}$ in (B.10) is defined as

$$L_u = \left(-\frac{1}{h} - \frac{k_3}{\tau}\right) I_{(f-1)} + \frac{k_3}{h} I_{(1),(f-1)} + \frac{1}{h} I_{(-1),(f-1)}. \tag{B.13}$$

Vectors $B_{R,1}$ and $B_{R,2}$ are defined as

$$B_{R,1} = \left[\begin{array}{c} O_{3(f-1)\times 1} \\ \hline -1 \\ \hline \frac{k_2}{h} Q_2 \\ \hline 0 \\ \hline O_{3\times 1} \end{array}\right], \quad B_{R,2} = \left[\begin{array}{c} O_{3(f-1)\times 1} \\ \hline 0 \\ \hline O_{(f-1)\times 1} \\ \hline \frac{k_v}{h} \\ \hline O_{3\times 1} \end{array}\right]. \tag{B.14}$$

$$
\begin{bmatrix} e_1 \\ v_1 \\ a_1 \\ e_2 \\ v_2 \\ a_2 \\ e_3 \\ v_3 \\ a_3 \\ u_1 \\ u_2 \\ u_3 \\ u_0 \\ q_0 \\ v_0 \\ a_0 \end{bmatrix} = \left[\begin{array}{cc|c|cc|c|ccc|c|c|ccccc} 1 & 0 & 0 & 0 & 0 & 0 & 0 & 0 & 0 & 0 & 0 & 0 & 0 & 0 & 0 \\ 0 & -1 & -h\tau\epsilon & 0 & 0 & 0 & 0 & 0 & 0 & -h^2\epsilon & 0 & 0 & 0 & 0 & 1 & h\tau\epsilon \\ 0 & 0 & \tau\epsilon & 0 & 0 & 0 & 0 & 0 & 0 & h\epsilon & 0 & 0 & 0 & 0 & 0 & -\tau\epsilon \\ 0 & 0 & 0 & 1 & 0 & 0 & 0 & 0 & 0 & 0 & 0 & 0 & 0 & 0 & 0 & 0 \\ 0 & -1 & -h(\tau\epsilon - \tau^2\epsilon^2) & 0 & -1 & -h\tau\epsilon & 0 & 0 & 0 & -h^2(\epsilon - \tau\epsilon^2) & -h^2\epsilon & 0 & 0 & 0 & 0 & 1 & h(\tau\epsilon - \tau^2\epsilon^2) \\ 0 & 0 & -\tau^2\epsilon^2 & 0 & 0 & \tau\epsilon & 0 & 0 & 0 & -h\tau\epsilon & h\epsilon & 0 & 0 & 0 & 0 & \tau^2\epsilon^2 \\ 0 & 0 & 0 & 0 & 0 & 0 & 1 & 0 & 0 & 0 & 0 & 0 & 0 & 0 & 0 & 0 \\ 0 & -1 & -h(\tau\epsilon - \tau^2\epsilon^2 + \tau^3\epsilon^3) & 0 & -1 & -h(\tau\epsilon - \tau^2\epsilon^2) & 0 & -1 & -h\tau\epsilon & -h^2(\epsilon - \tau\epsilon^2 + \tau^2\epsilon^3) & -h^2(\epsilon - \tau\epsilon^2) & -h^2\epsilon & 0 & 0 & 1 & h(\tau\epsilon - \tau^2\epsilon^2 + \tau^3\epsilon^3) \\ 0 & 0 & \tau^3\epsilon^3 & 0 & 0 & -\tau^2\epsilon^2 & 0 & 0 & \tau\epsilon & h\tau^2\epsilon^3 & -h\tau\epsilon^2 & h\epsilon & 0 & 0 & 0 & -\tau^3\epsilon^3 \\ 0 & 0 & 0 & 0 & 0 & 0 & 0 & 0 & 0 & 1 & 0 & 0 & 0 & 0 & 0 & 0 \\ 0 & 0 & 0 & 0 & 0 & 0 & 0 & 0 & 0 & 0 & 1 & 0 & 0 & 0 & 0 & 0 \\ 0 & 0 & 0 & 0 & 0 & 0 & 0 & 0 & 0 & 0 & 0 & 1 & 0 & 0 & 0 & 0 \\ 0 & 0 & 0 & 0 & 0 & 0 & 0 & 0 & 0 & 0 & 0 & 0 & 1 & 0 & 0 & 0 \\ 0 & 0 & 0 & 0 & 0 & 0 & 0 & 0 & 0 & 0 & 0 & 0 & 0 & 1 & 0 & 0 \\ 0 & 0 & 0 & 0 & 0 & 0 & 0 & 0 & 0 & 0 & 0 & 0 & 0 & 0 & 1 & 0 \\ 0 & 0 & 0 & 0 & 0 & 0 & 0 & 0 & 0 & 0 & 0 & 0 & 0 & 0 & 0 & 1 \end{array}\right] \begin{bmatrix} e_1 \\ \dot{e}_1 \\ \ddot{e}_1 \\ e_2 \\ \dot{e}_2 \\ \ddot{e}_2 \\ e_3 \\ \dot{e}_3 \\ \ddot{e}_3 \\ u_1 \\ u_2 \\ u_3 \\ u_0 \\ q_0 \\ v_0 \\ a_0 \end{bmatrix}
$$

$$
= T_3 \begin{bmatrix} e_1 \\ \dot{e}_1 \\ \ddot{e}_1 \\ e_2 \\ \dot{e}_2 \\ \ddot{e}_2 \\ e_3 \\ \dot{e}_3 \\ \ddot{e}_3 \\ u_1 \\ u_2 \\ u_3 \\ u_0 \\ q_0 \\ v_0 \\ a_0 \end{bmatrix}, \quad \text{with } \epsilon = \frac{1}{h - \tau}. \tag{B.15}
$$

Appendix C

Transfer function $\bar{\mathcal{P}}_i(s)$ for zero delay

In this appendix, the origin of the transfer function in (6.18) is explained. As was presented in (5.19), the entire platoon dynamics are given by

$$\begin{aligned}
\left[\begin{array}{c} \dot{X}(t) \\ \hline \dot{U}(t) \\ \hline \dot{u}_0(t) \\ \hline \dot{p}_0(t) \end{array}\right] &= \mathcal{A}\left[\begin{array}{c} X(t) \\ \hline U(t) \\ \hline u_0(t) \\ \hline p_0(t) \end{array}\right] + \mathcal{B}v_{des}(t) \\
&= \left[\begin{array}{c|c|c|c} I_n \otimes A - \hat{L} \otimes Bk^T & O_{3n\times n} & O_{3n\times 1} & O_{3n\times 3} \\ \hline \hat{L} \otimes \frac{k^T}{h} & \frac{1}{h}(I_{(-1),n} - I_n) & B_u & O_{n\times 3} \\ \hline B_u^T \otimes -k_0^T & O_{1\times n} & -\frac{1}{h} & [0,\ -\frac{k_v}{h},\ 0] \\ \hline O_{3\times 3n} & O_{3\times n} & B & A \end{array}\right]\left[\begin{array}{c} X(t) \\ \hline U(t) \\ \hline u_0(t) \\ \hline p_0(t) \end{array}\right] + \cdots \\
&\quad \left[\begin{array}{c} O_{3n\times 1} \\ \hline O_{n\times 1} \\ \hline \frac{k_v}{h} \\ \hline O_{3\times 1} \end{array}\right] v_{des}(t),
\end{aligned} \tag{C.1}$$

where the definition of all variables can be found in the main text. The system in (C.1) can be written as a partitioned system as follows

$$\left[\begin{array}{c} \dot{X}(t) \\ \hline \dot{U}(t) \\ \dot{u}_0(t) \\ \dot{p}_0(t) \end{array}\right] = \left[\begin{array}{c|c} \mathcal{A}_{11} & \mathcal{A}_{12} \\ \hline \mathcal{A}_{21} & \mathcal{A}_{22} \end{array}\right]\left[\begin{array}{c} X(t) \\ \hline U(t) \\ u_0(t) \\ p_0(t) \end{array}\right] + \left[\begin{array}{c} \mathcal{B}_1 \\ \hline \mathcal{B}_2 \end{array}\right] v_{des}(t). \tag{C.2}$$

The transfer function $\mathcal{P}_i(s)$ from input $v_{des}(t)$ to the desired acceleration $u_i(t)$ of vehicle i in the Laplace-domain is defined as

$$\mathcal{P}_i(s) = \mathcal{C}_i\left(sI_a - \left[\begin{array}{c|c} \mathcal{A}_{11} & \mathcal{A}_{12} \\ \hline \mathcal{A}_{21} & \mathcal{A}_{22} \end{array}\right]\right)^{-1}\left[\begin{array}{c} \mathcal{B}_1 \\ \hline \mathcal{B}_2 \end{array}\right], \tag{C.3}$$

where output vector $\mathcal{C}_i$ is defined as

$$\mathcal{C}_i = [O_{1\times(3n+i-1)},\ 1,\ O_{1\times(n-i+4)}], \tag{C.4}$$

$I_a \in \mathbb{R}^{4(n+1)\times 4(n+1)}$ is the identity matrix and $s \in \mathbb{C}$. It can be seen in (C.1), that matrix $\mathcal{A}_{12}$ is a zero matrix. Using this result, transfer function $\mathcal{P}_i(s)$ can be written as (Horn and Johnson, 1988)

$$\mathcal{P}_i(s) = \mathcal{C}_i \left[\begin{array}{c|c} (sI_b - \mathcal{A}_{11})^{-1} & O_{3n\times(n+4)} \\ \hline (sI_c - \mathcal{A}_{22})^{-1}\mathcal{A}_{21}(sI_b - \mathcal{A}_{11})^{-1} & (sI_c - \mathcal{A}_{22})^{-1} \end{array}\right] \left[\begin{array}{c} \mathcal{B}_1 \\ \hline \mathcal{B}_2 \end{array}\right], \tag{C.5}$$

where $I_b \in \mathbb{R}^{3n\times 3n}$ and $I_c \in \mathbb{R}^{(n+4)\times(n+4)}$ are both identity matrices.
Suppose that the output vector $\mathcal{C}_i$ is also partitioned, such that $\mathcal{C}_i = [\mathcal{C}_{i1}\,|\mathcal{C}_{i2}]$, where $\mathcal{C}_{i1} \in \mathbb{R}^{3n}$ and $\mathcal{C}_{i2} \in \mathbb{R}^{n+4}$. From (C.1), it is known that all elements in $\mathcal{B}_1$ are equal to zero. Therefore, it is known that the transfer function $\mathcal{P}_i(s)$ from $v_{des}(t)$ to $u_i(t)$ in the Laplace-domain is given by

$$\frac{\hat{u}_i(s)}{\hat{v}_{des}(s)} = \mathcal{C}_{i2}(sI_c - \mathcal{A}_{22})^{-1}\mathcal{B}_2. \tag{C.6}$$

By using

$$\hat{v}_i(s) = \mathcal{G}(s)\hat{u}_i(s) = \frac{1}{s(\tau s+1)}\hat{u}_i(s), \tag{C.7}$$

matrix $\mathcal{A}_{22}$, vector $\mathcal{B}_2$ and vector $\mathcal{C}_{i2}$, this results in

$$\bar{\mathcal{P}}_i(s) = \frac{\hat{v}_i(s)}{\hat{v}_{des}(s)} = \frac{k_v}{(hs+1)^i\left((hs+1)(\tau s+1)s + k_v\right)}. \tag{C.8}$$